

TALLINN UNIVERSITY OF TECHNOLOGY  
DOCTORAL THESIS  
42/2018

# **The Contribution of Cavity Insulations to the Load-Bearing Capacity of Timber Frame Assemblies Exposed to Fire**

MATTIA TISO



TALLINN UNIVERSITY OF TECHNOLOGY

School of Engineering

Department of Civil Engineering and Architecture

This dissertation was accepted for the defence of the degree 17/07/2018

**Supervisor:** Prof. Alar Just  
School of Engineering  
Tallinn University of Technology  
Tallinn, Estonia

**Co-supervisor:** Prof. Massimo Fragiaco  
Civil, Construction-Architectural and Environmental Engineering  
Department  
University of L'Aquila, Italy

**Opponents:** Prof. Andrea Frangi  
Department of Civil, Environmental and Geomatic Engineering  
Institute of Structural Engineering  
Eidgenössische Technische Hochschule Zürich, Switzerland

Dr. Norman Werther  
Department of Civil, Geo and Environmental Engineering  
Chair of Timber Structures and Building Construction  
Technical University of Munich, Germany

**Defence of the thesis:** 17/08/2018, Tallinn

**Declaration:**

Hereby I declare that this doctoral thesis, my original investigation and achievement, submitted for the doctoral degree at Tallinn University of Technology, has not been previously submitted for doctoral or equivalent academic degree.

Mattia Tiso

-----  
signature



European Union  
European Social Fund



Investing in your future

Copyright: Mattia Tiso, 2018

ISSN 2585-6898 (publication)

ISBN 978-9949-83-297-2 (publication)

ISSN 2585-6901 (PDF)

ISBN 978-9949-83-298-9 (PDF)

TALLINNA TEHNIKAÜLIKOOL  
DOKTORITÖÖ  
42/2018

**Isolatsioonimaterjalide mõju  
puitkarkass-seinte ja -vahelagede  
kandevõimele tules**

MATTIA TISO



# Contents

List of Publications .....	7
Author's Contribution to the Publications .....	8
Preface .....	9
Abbreviations .....	10
Symbols .....	11
Latin capital letters.....	11
Latin lower-case letters.....	11
Greek letters .....	12
1 Introduction .....	13
1.1 Aims.....	13
1.2 Research significance .....	13
1.3 Organisation .....	14
1.4 Limitations.....	14
2 State-of-the-art .....	15
2.1 Timber frame assemblies .....	15
2.1.1 Insulation materials in timber frame assemblies .....	16
2.2 Fire resistance .....	16
2.2.1 Standard temperature-time fire exposure.....	17
2.3 Load-bearing capacity of timber frame assemblies exposed to fire .....	17
2.3.1 Evaluation by fire-testing .....	18
2.3.2 Evaluation by analytical models.....	18
2.3.3 Evaluation by numerical simulations .....	20
2.4 Standardising insulation materials.....	24
2.5 An existing design model for assemblies insulated with stone wool.....	25
2.6 An existing design model for assemblies insulated with glass wool .....	30
3 Evaluation of the fire protection provided by cavity insulations .....	32
3.1 Selection of insulation materials.....	32
3.2 Cubic metre furnace tests .....	34
3.2.1 Mounting of the specimens .....	36
3.2.2 Test results and discussions .....	40
3.3 Protection levels for cavity insulations .....	42
3.3.1 Criteria for protection levels .....	44
3.3.2 Earlier fall-off of the cladding.....	44
3.3.3 Validity of the methodology used for loose-fill cavity insulations .....	45
4 Improved charring model.....	48
4.1 Unloaded cubic metre furnace tests.....	48
4.2 Determination of the cross-section and corner rounding factors .....	49
4.2.1 Cross-section factor .....	49
4.2.2 Corner rounding factor .....	50
4.3 The charring scenario in the improved design model.....	51
4.4 Protection factors .....	54
4.4.1 Charring on the lateral sides .....	56
4.4.2 Verification of the notional section modulus.....	58
4.5 Protection factors evaluated by means of heat-transfer analysis .....	59

4.6 Charring of TFA with cavities partially filled.....	61
4.6.1 Heat-transfer analysis .....	62
4.6.2 The results of the heat-transfer analysis.....	64
4.6.3 Design prescriptions for TFA with cavities partially filled .....	65
4.7 Validation of the heat-transfer analysis .....	65
5 Improved design model .....	68
5.1 The mechanical properties of uncharred timber members.....	68
5.1.1 Heat-transfer analysis .....	69
5.1.2 Mechanical analysis .....	70
5.1.3 Simulation programme .....	70
5.1.4 Evaluation of zero-strength layer depths for bending members.....	72
5.1.5 An evaluation of zero-strength layer depths for compression members.....	74
5.1.6 A simplified approach to determine zero-strength layer depths.....	75
5.1.7 Members with an imperfection which are subjected to axial compression and bending..	77
5.1.8 An optimised approach for determining zero-strength layer depths .....	79
5.1.9 Loaded cubic metre furnace tests.....	82
5.2 Validation of the design model by means of full-scale tests.....	84
5.2.1 Performed full-scale tests .....	84
5.2.2 An evaluation of existing test reports .....	87
5.3 Load-bearing capacity according to EN 1995-1-2:2004 versus improved design model....	91
6 Cavity insulation remaining in place during fire situations .....	95
6.1 Prescriptions for the existing design models .....	95
6.2 An evaluation of the fall-off times of insulation to fall off based upon existing test reports..	95
6.3 A survey of the existing fixation systems for cavity insulation in timber frame assemblies.....	97
6.3.1 Fixing systems used for batt-type insulations being applied to floor elements ....	98
6.3.2 Fixing systems for batt-type insulation which is applied in wall elements .....	100
6.3.3 Fixing systems for loose-fill insulation being applied to floor elements.....	102
6.3.4 Fixing systems for loose-fill insulations applied in wall elements.....	103
6.4 Investigation needs to study the fall-off of the cavity insulations .....	104
6.5 Limitations of the contribution of insulation materials in the I-criterion .....	104
7 Conclusions and outlook .....	107
7.1 Conclusions .....	107
7.2 Outlook.....	109
List of Figures .....	110
List of Tables .....	114
References .....	115
Acknowledgements.....	122
Lühikokkuvõte.....	123
Abstract.....	124
Abstract.....	125
Appendix .....	127
Curriculum vitae.....	140
Elulookirjeldus.....	141

## List of Publications

This thesis is mainly based on the data presented in the following peer-reviewed papers:

- I Tiso, M., Just, A. 2017. Fire Protection Provided by Insulation Materials – A New Design Approach for Timber Frame Assemblies. *Structural Engineering International* 27(2), pp. 231–237. DOI: 10.2749/101686617X14881932435899.
- II Tiso, M., Just, A. 2017. Design criteria for insulation materials applied in timber frame assemblies. *Journal of Structural Fire Engineering*. Available at: <http://www.emeraldinsight.com/doi/10.1108/JSFE-01-2017-0015>
- III Tiso, M., Just A., Schmid, J., Mäger, K. N., Klippel, M., Izzi, M., Fragiaco, M. Evaluation of zero-strength layer depths for timber members of floor assemblies with heat resistant cavity insulations. *Fire Safety Journal* (submitted).
- IV Tiso, M., Just, A., Schmid, J., Klippel, M. 2018. Effective cross-sectional method for timber frame assemblies – definition of coefficients and zero-strength layers. *Fire and Materials* 1-17. DOI: 10.1002/fam.2645
- V Tiso, M., Just, A. 2018. Fire resistance of timber frame assemblies with cavities partially filled by insulation materials. *Structures in Fire conference: Proceedings of the 9<sup>th</sup> international conference, 6-8.6.2018*, Belfast, UK, pp 233–240.

### Other published works:

- VI Tiso, M., Just, A. 2018. Design of timber frame assemblies under standard fire conditions – A proposal for the next revision of EN 1995-1-2. *WCTE 2018 - World Conference on Timber Engineering*, Seoul, South Korea.
- VII Tiso, M., Just, A. Klippel, M., Schmid, J., Brandon, D. 2017. Zero-Strength Layers for Timber Frame Assemblies in a Standard Fire *Proceeding of INTER, meeting 50, August 28-31, Kyoto, Japan*.
- VIII Just, A., Tiso, M. 2016. Improved fire design model for timber frame assemblies *Proceeding of INTER, meeting 49, August 16-19, Graz, Austria*.
- IX Tiso, M., Just A. 2016. Parameters influencing the behaviour of timber frame assemblies exposed to fire, development of new design criteria for insulation materials. *Structures in Fire (Proceedings of Ninth International Conference)*, Princeton University, 8-10 June 2016, pp 659–666.
- X Tiso, M., Just A., Mäger, K. N. 2016. Behavior of Wooden Based Insulations at High Temperatures. *Energy Procedia* 96, pp. 729–737. DOI: 10.1016/j.egypro.2016.09.135.
- XI Tiso, M. Just, A. 2016. Behaviour of insulation materials in timber frame assemblies exposed to fire. *WCTE 2016 - World Conference on Timber Engineering*, Vienna, Austria.
- XII Tiso, M. Just, A. 2015. Protective effect of insulation materials on charring of timber elements. *Proceeding of INTER, meeting 48, August 24-27, Šibenik, Croatia*.

## **Author's Contribution to the Publications**

Contributions to the papers in this thesis are as follows:

- I Tiso prepared the specimens, carried out the experimental part of the work, analysed the results, proposed the qualification methodology, and was the corresponding author. Just contributed to carrying out the experimental part of the work, as well as contributing towards discussions and helping in writing the paper.
- II Tiso prepared the specimens, carried out the experimental part of the work, analysed the results, and was the corresponding author. Just contributed to planning and carrying out the experiments, as well as contributing towards discussions and helping in writing the paper.
- III Tiso carried out the experimental and numerical parts of the work, analysed the results, and was the corresponding author. Mäger calculated the effective thermal properties of the insulation material. Just, Schmid, and Klippel contributed to the discussions and gave advice on writing the paper. Izzi and Fragiacomio gave advice on the numerical model.
- IV Tiso planned and carried out the numerical simulations, wrote the code which extrapolated and analysed the results, and was the corresponding author. Tiso also planned and carried out the full-scale tests. Just, Schmid, and Klippel contributed to the discussions, and gave advice on carrying out the simulations and on writing the paper.
- V Tiso carried out numerical simulations, analysed the results, and was the corresponding author. Just contributed towards the discussions.

## Preface

This work is the result of research which has been carried out by myself during the period between October 2014 and June 2018 at Tallinn University of Technology and RISE Research Institutes of Sweden.

The research which is described in this thesis was supervised by Professor Alar Just of Tallinn University of Technology.

My first experience with timber structures took place in 2011 when, during an internship at a design office, I was asked to design a residential building with a load-bearing structure that was made with cross-laminated timber. That project became my bachelor thesis at University of Padova, my home town.

After completion of my bachelor's degree, I continued the study of structural engineering at University of Trieste. As a recipient of the Erasmus Placement grant, thanks to Professor Massimo Fragiacomio, I had the opportunity of carrying out experimental work at SP Technical Research Institute of Sweden.

At SP Technical Research Institute of Sweden, I had my first experience in the field of timber structure fire resistance, with Joachim Schmid and Alar Just as teachers.

This experience was concluded with an invitation by Alar Just to join his team at Tallinn University of Technology and continue my studies in the field of timber structures. Very happy to be able to accept this interesting and challenging proposal, I started my doctoral studies on the topic of timber frame assemblies under fire-related conditions. In this new 'adventure', I had the opportunity to be supported by the industry itself, as well as by colleagues both old and new.

This work comprises an extensive experimental and numerical investigation, which has resulted in this present PhD thesis and in proposals for the revision of the design criteria for the next generation of Eurocode 5 Part 1-2.

## Abbreviations

CEN	-	European committee for standardisation
CF	-	Cellulose fibre
CSW	-	Compression side warm
DIN	-	Deutsches Institut für Normung (German standardisation institute)
DSC	-	Differential scanning calorimeter
ECSM	-	Effective cross-section method
GHP	-	Guarded hot plate
GP	-	Gypsum plasterboard
GtA	-	Gypsum plasterboard Type A
GtF	-	Gypsum plasterboard Type F
GW	-	Glass wool
HTE	-	High temperature extruded mineral wool
HW	-	Hot wire
I	-	Insulation criterion
E	-	Integrity criterion
EN	-	European norm
EPS	-	Extruded polystyrene
FE	-	Finite elements
FSITB	-	European guideline <i>Fire Safety in Timber Buildings</i>
ISO	-	International organisation for standardisation
N/A	-	Not applicable
OSB	-	Oriented strand board
PL	-	Protection level for cavity insulation products
PUR	-	Polyurethane
R	-	Load-bearing capacity criterion
RPM	-	Reduced properties method
SW	-	Stone wool
TC	-	Thermocouple
TFA	-	Timber frame assemblies
TGA	-	Thermogravimetric analysis
TPS	-	Transient plane source
TSW	-	Tension side warm
WF	-	Wood fibre

# Symbols

## Latin capital letters

$A$	-	area	$[\text{mm}^2]$
$A_{fi}$	-	area of residual cross-section	$[\text{mm}^2]$
$A_n$	-	notional area	$[\text{mm}^2]$
$E$	-	modulus of elasticity	$[\text{N}/\text{mm}^2]$
$E_c$	-	modulus of elasticity in compression	$[\text{N}/\text{mm}^2]$
$E_{fi}$	-	modulus of elasticity under fire conditions	$[\text{N}/\text{mm}^2]$
$E_t$	-	modulus of elasticity in tension	$[\text{N}/\text{mm}^2]$
$E_{20^\circ\text{C}}$	-	modulus of elasticity at ambient temperature	$[\text{N}/\text{mm}^2]$
$I$	-	moment of inertia	$[\text{mm}^4]$
$I_{fi}$	-	moment of inertia for the residual cross-section	$[\text{mm}^4]$
$I_n$	-	notional moment of inertia	$[\text{mm}^4]$
$I_{20^\circ\text{C}}$	-	initial moment of inertia at ambient temperature	$[\text{mm}^4]$
$M$	-	bending moment	$[\text{N m}]$
$M_e$	-	external bending moment	$[\text{N m}]$
$M_{fi}$	-	bending moment capacity under fire conditions	$[\text{N m}]$
$M_{20^\circ\text{C}}$	-	bending moment resistance at ambient temperature	$[\text{N m}]$
$N$	-	compression force	$[\text{N}]$
$N_e$	-	external compression force	$[\text{N}]$
$N_{cr}$	-	buckling resistance	$[\text{N}]$
$N_{cr,II}$	-	force causing buckling while considering second order effects	$[\text{N}]$
$T$	-	temperature	$[\text{°C}]$
$W$	-	section modulus	$[\text{mm}^3]$
$W_{ef}$	-	effective section modulus	$[\text{mm}^3]$
$W_{fi}$	-	section modulus for the residual cross-section	$[\text{mm}^3]$
$W_n$	-	notional section modulus	$[\text{mm}^3]$
$W_{20^\circ\text{C}}$	-	initial section modulus at ambient temperature	$[\text{mm}^3]$

## Latin lower-case letters

$a_0$	-	coefficient	
$a_1$	-	coefficient	
$b$	-	width of the member at ambient temperature	$[\text{mm}]$
$b_{ef}$	-	effective width of the member	$[\text{mm}]$
$b_n$	-	notional width of the member	$[\text{mm}]$
$c$	-	constant value	
$c_p$	-	specific heat	$[\text{kJ}/(\text{kg K})]$
$d$	-	depth	$[\text{mm}]$
$d_{char,n}$	-	notional charring depth	$[\text{mm}]$
$d_{char,1,n}$	-	notional charring depth from the fire-exposed side	$[\text{mm}]$
$d_{char,2,n}$	-	notional charring depth from the lateral sides	$[\text{mm}]$
$d_{char,2,n,unexp}$	-	notional charring depth from the lateral sides, top side	$[\text{mm}]$
$d_{char,fi}$	-	charring depth in the middle of the residual cross-section	$[\text{mm}]$
$d_{ef}$	-	effective charring depth	$[\text{mm}]$
$d_0$	-	zero-strength layer depth	$[\text{mm}]$
$d_{300,m}$	-	charring depth in the middle of the member cross-section	$[\text{mm}]$

$d_{300,s}$	- charring depth on the lateral side of the member	[mm]
$e_0$	- initial deformation of the member	[mm]
$e_1$	- eccentricity due to external loads	[mm]
$e_{11}$	- deformation due to P-delta effects	[mm]
$f$	- strength	[N/mm <sup>2</sup> ]
$f_c$	- compression strength	[N/mm <sup>2</sup> ]
$f_{m,20^\circ C}$	- bending strength at ambient temperature	[N/mm <sup>2</sup> ]
$f_t$	- tension strength	[N/mm <sup>2</sup> ]
$h$	- depth of the member at ambient temperature	[mm]
$h_n$	- notional depth of the member	[mm]
$h_{ef}$	- effective depth of the member	[mm]
$h_{ins}$	- depth of the cavity insulation or insulation layer	[mm]
$h_p$	- cladding depth	[mm]
$k$	- modification factor	
$k_{mod,fm,fi}$	- modification factor for strength	
$k_n$	- modification factor for corner-rounding	
$k_{pr}$	- protection factor	
$k_s$	- cross-section factor	
$k_2$	- protection factor for the protection phase (Phase 2)	
$k_3$	- protection factor for the post-protection phase (Phase 3)	
$k_{3,1}$	- protection factor for the post-protection phase of the fire-exposed side (direction 1)	
$k_{3,2}$	- protection factor for the post-protection phase of the lateral sides (direction 2)	
$l$	- length	[mm]
$l_{cr}$	- effective buckling length	[mm]
$t$	- time	[min]
$t_{ch}$	- start time of charring on the fire-exposed side	[min]
$t_{ch,2}$	- start time for charring on the lateral sides	[min]
$t_f$	- fall-off time of the cladding	[min]
$t_{f,ins}$	- time for complete recession of insulation or fall-off time of the cladding	[min]
$t_{peak}$	- time at which the zero-strength layer depth peaks	[min]
$t_{prot,i}$	- protection time value	[min]
$V_{rec}$	- recession speed for the cavity insulation	[mm/min]

## Greek letters

$\beta_0$	- basic charring rate	[mm/min]
$\epsilon$	- strain	
$\kappa$	- curvature	[mm <sup>-1</sup> ]
$\kappa_{fi}$	- curvature under fire conditions	[mm <sup>-1</sup> ]
$\lambda$	- thermal conductivity	[W/(m K)]
$\pi$	- mathematical constant	
$\rho$	- density	[kg/m <sup>3</sup> ]
$\rho_{fi}$	- density under fire conditions	[kg/m <sup>3</sup> ]
$\rho_{20^\circ C}$	- density at ambient temperature	[kg/m <sup>3</sup> ]
$\sigma$	- stress	[N/mm <sup>2</sup> ]

# 1 Introduction

Insulation materials have the potential to contribute to the load-bearing capacity of timber frame assemblies under fire-related conditions by avoiding or slowing down the carbonisation of timber members. Within a building, the initial protection for a timber member is provided by the exterior cladding. After the cladding has fallen off, secondary protection is provided by insulation materials which are present within the structure.

At present there are two analytical models for the design of timber frame assemblies under fire-related conditions: one is inserted into Annex C of Eurocode 5 Part 1-2, the current standard for fire design of timber structures (CEN, European Committee for Standardization, 2004b), and the other is in the European technical guideline, *Fire Safety in Timber Buildings* (B. Östman et al., 2010). The design model for Eurocode 5 Part 1-2 takes into account the contribution provided by stone wool products and is extended to assemblies which are filled with glass wool until the cladding has fallen away. This design model is also limited to sixty minutes of fire resistance. The design model used in *Fire Safety in Timber Buildings* also considers the contribution provided by glass wool products after the cladding has fallen off. No information is available regarding the contribution provided by other insulation products. In the available design models, the different contributions provided by stone wool and glass wool products are clearly distinguished, while these two types of product are not distinguished in the European standard for factory-made mineral wools EN 13162 (CEN, European Committee for Standardization, 2013b). Furthermore, in the European standards for thermal insulation products, only the reaction performance has to be declared. A standardised European test method for the evaluation of fire resistance performance of insulation materials does not yet exist.

## 1.1 Aims

This thesis investigates the potential contribution under fire-related conditions which is being offered by the insulation materials to the load-bearing timber members in framing assemblies.

The main aim of this thesis is the development of a method to distinguish between different insulation products with respect to their ability to protect timber members from fire. It also aims to restructure the available design models for load-bearing capacity under fire-related conditions, providing clear input values for the design of timber structures which are insulated with any form of insulation material. The restructured design model should be open to being able to consider the contribution of insulation materials other than mineral wools.

The new procedure to distinguish between insulation products and the restructured design model for timber components should allow designers to use insulation materials with respect to the specific material characteristics rather than density and raw material.

## 1.2 Research significance

Existing design models for timber frame assemblies are linked to a specific category of insulation product and are limited in terms of fire resistance levels (in respect of the time in which such resistance can last). The influence of different insulation products on

the load-bearing capacity of timber frame assemblies is still uncertain. Within this thesis, an evolution is presented of the existing fire design criteria for insulation materials in timber buildings. The findings of this study will serve as input for the revision of the design criteria for timber frame assemblies in the next generation of Eurocode 5 Part 1-2.

### **1.3 Organisation**

Section 2 of this thesis summarises state-of-the-art timber frame assemblies under fire conditions. The first part of this section deals with existing methods when it comes to evaluating the load-bearing capacity of timber frame assemblies under fire-related conditions. Then an overview will be presented of the current situation regarding the requirements with respect to the fire resistance levels of insulation materials in the European standards. The last part of this section explains in detail the available design models for the evaluation of the load-bearing capacity of timber frame assemblies that are exposed to fire.

Section 3 deals with the methodology for distinguishing between different insulation materials with respect to the ability of the material in question to protect timber members from fire. The test methodology is explained in detail, along with the criteria that has been adopted to distinguish between the different insulation materials when they are exposed to fire.

In Sections 4 and 5 the improvements are explained that have been introduced to the available design models for load-bearing capacity under fire-related conditions. A summary is given of the experimental and numerical work that has been carried out. Proposed procedures are explained which will derive design values for the different factors that are included in the improved design model. A validation is included of the design models by means of full-scale fire tests.

The first part of Section 6 summarises the existing proposals to prevent insulation materials from falling off under fire-related conditions. Then inputs are suggested for a future investigation of measures to prevent cavity insulation from falling off.

The conclusions and the outlook for this thesis are given in Section 7.

### **1.4 Limitations**

The present thesis focuses on the load-bearing capacity of timber frame assemblies which are exposed to a fire-related standard temperature time curve.

Despite the purpose being to develop a method that is open to any form of insulation materials, in this thesis the design values for various factors are proposed only for a limited number of insulation products. However, the procedures to derive the design values are explained.

To investigate the influence of the insulation materials on the load-bearing capacity of timber members, the assumption was made that the insulation material remains in place after the cladding has fallen off. Design proposals are required to ensure the validity of this assumption. Suggestions are given in the thesis in relation to an investigation in regard to insulation materials falling off under fire conditions.

## 2 State-of-the-art

Since antiquity, solid wood has been utilised to realise load-bearing structures in the form of roofs and floors. Further uses of solid wood are found in column foundations of buildings, in elevated structures such as walls and columns, and in domes and false ceilings.

### 2.1 Timber frame assemblies

One of the systems used to realise buildings with a load-bearing structure that is made of solid wood is one that is known as the timber frame system. A timber frame system is composed of straight members of solid wood which are connected to each other in order to form the building's load-bearing structure. Depending on static, thermal, acoustic, or aesthetic factors, several layers may be applied to the straight members. Normally, the straight members are braced by boards. These boards may constitute wood-based products (such as, for example, particle board, plywood, or Oriented Strand Board), or mineral-based boards (such as, for example, gypsum plasterboard or fibre reinforced cement board). With this system, walls and floors are composed of parallel wooden members which are covered by boards. The space delimited by two consecutive straight members as covered by boards on opposite sides is defined as a cavity.

In order to improve thermal and acoustic comfort levels, the cavities of wall and floor elements could be filled with an insulation material. Wall and floor elements which are composed of parallel solid wood members, and which are covered by boards with cavities that are filled with an insulation material, are commonly known as timber frame assemblies (TFA).

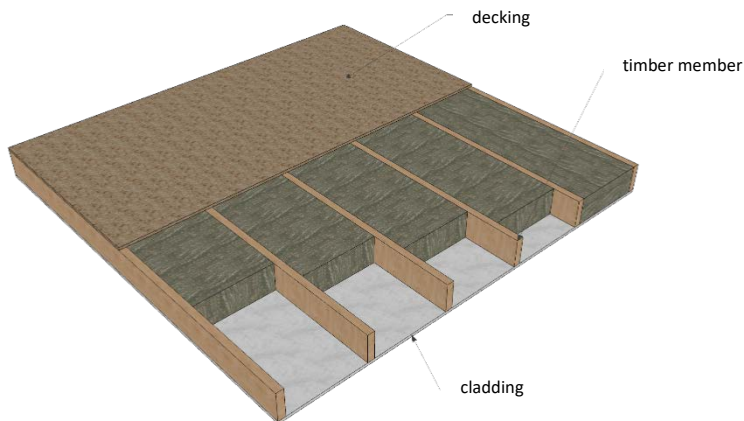


Figure 2-1. Timber frame assembly (TFA) in floor position.

Timber frame assemblies are normally composed of timber members with relatively small cross-sections. Cavities can be completely filled with an insulation material as well as partially filled or also void.

Timber frame assemblies could be created directly on-site or in a factory as single wall and floor elements which are subsequently transported to the building site and assembled there.

### **2.1.1 Insulation materials in timber frame assemblies**

The main functions of insulation materials which are applied to building elements are (i) the conservation of energy by reducing the transmission of heat through building elements, and (ii) the control of inside surface temperatures where these affect the comfort of occupants and where they also deter condensation. Physical properties and envelope design may also allow insulation materials to perform additional functions (Bynum, 2001). These include:

- providing support for a surface finish,
- impeding water vapour transmission
- preventing or reducing damage to equipment and structure from exposure to fire or freezing conditions
- reducing noise and vibration

Insulation materials which are inserted into the cavities of timber frame assemblies are often known as cavity insulation. There are many different types of cavity insulation being used with timber framed buildings. Insulation products which are used as cavity insulation may depend upon the location and period of construction of the building as this can reflect regional styles, the materials that are locally available, and the social status of the building (Westergaard, 2010). Cavity insulation products can come in the form of batt or loose-fill products.

## **2.2 Fire resistance**

The aims of fire safety regulations in buildings are (i) the safety of the life of the occupants and rescue teams; (ii) damage prevention to the structures, contents, and public image, and from interrupted operations; and (iii) the prevention of the release of hazardous substances. To fulfil these aims, various principles are taken into consideration by the fire safety regulations.

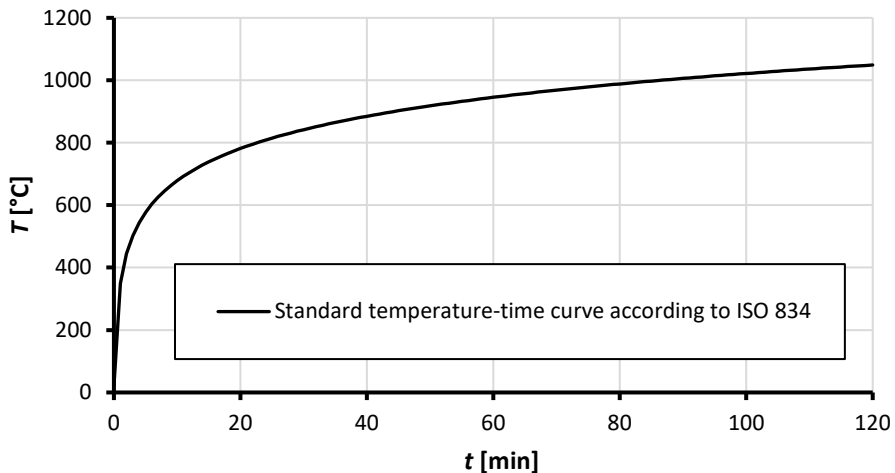
Among these principles are included two that are of particular importance: ensuring a load-bearing structure which is able to resist fire for a required minimum duration of time; and ensuring a structure which limits the spread of fire to adjacent buildings. The aims of fire safety regulations in buildings can be met by adopting comprehensive structural fire protection measures, technical fire protection measures, or organisational fire protection measures.

Structural fire protection measures are building elements which are designed and constructed to maintain their load-bearing function and which limit the spread of fire to adjacent buildings for a required minimum duration of exposure to fire (B. Östman et al., 2010).

Fire resistance means that structural elements must withstand a fully-developed fire and fulfil certain performance requirements. If any exposure to fire is in accordance with a standard temperature-time fire curve, the performance requirements are as follows: load-bearing capacity (also known as the R criterion), integrity (also known as the E criterion), and insulation (also known as the I criterion). The fire resistance of a building element can be evaluated by testing, by using simplified calculation methods, or by advance numerical simulations (B. Östman et al., 2010).

### 2.2.1 Standard temperature-time fire exposure

The temperature development of a fire in a room depends upon several factors such as the combustible materials present in the room and the available ventilation (Walton, Thomas, and Ohmiya, 2016). To simplify the description of the fire's action, codes have included nominal and parametric fire curves. Nominal curves are a simple description of the fire's temperature in a compartment as a function of time. One nominal curve is known as the standard temperature ( $T$ ) time ( $t$ ) curve that is given in ISO 834 (ISO International Organization for Standardization, 1999). The European Standard on fire resistance tests, EN 1363-1 (CEN, European Committee for Standardization, 2012), has adopted the nominal curve that is prescribed in ISO 834. Additionally, EN 1363-1 prescribes the means of control for the temperature-time curve in fire-resistance test equipment: this involves what is known as plate-thermometers (Wickström, 2016). Fire resistance requirements which are of a load-bearing capacity, integrity, and insulation are referred to as the standard temperature-time fire exposure as given in EN 1363-1.



KEY:  $T$  – temperature;  $t$  – time.

Figure 2-2. Standard temperature-time curve as given in ISO 834, and also adopted in EN 1363-1.

### 2.3 Load-bearing capacity of timber frame assemblies exposed to fire

The load-bearing capacity of structural timber members which are exposed to fire is influenced by the properties of the materials, geometrical characteristics, protection and thermal boundary conditions. When timber is exposed at elevated temperatures, an evaporation of moisture, pyrolysis, and the charring and cracking of the charred material takes place (Buchanan and Abu, 2017).

The evaporation of moisture starts when the temperature reaches 100°C. The thermal degradation (pyrolysis) of wood starts between temperatures of 160°C and 180°C. When the surface temperature reaches the range of 350-360°C the combustion of timber takes place. At this stage, a char layer with fissures is formed (Mikkola, 1991). Previously, Schaffer (1967) found that charring is formed at a temperature of 550°F which corresponds to 288°C. The charring depth which is defined as the position of the 300°C isotherm is widely accepted as a rounded value (Hadvig, 1981). In addition, the European Standard for the structural fire design of timber structures, Eurocode 5 Part 1-2,

assumes the position of the char line as the position of the 300°C isotherm (CEN, European Committee for Standardization, 2004b).

The charred layer is considered to have no strength. In the area of wood that has been heated but which has not combusted, a decrease exists in strength and stiffness (Kollmann, 1951).

In timber members that have been fully exposed to the temperature-time standard fire conditions, the reduction of the original cross-section by charring has a larger influence on load-bearing capacity in the form of a reduction in the mechanical properties within the uncharred cross-section (Just, Schmid, Werther, and Frangi, 2014). The behaviour of load-bearing timber members in framing assemblies that have been exposed to fire is influenced by the protective properties of both the cladding and the cavity insulations (Just, 2010b; König and Walleij, 2000).

In general, the load-bearing capacity of timber members that have been exposed to fire can be evaluated by means of (i) fire tests, (ii) simplified design models, and (iii) advanced calculations.

### **2.3.1 Evaluation by fire-testing**

In order to be able to fulfil the requirements of building regulations, fire-resistance building elements can be assessed by testing. Those European standards which regulate the testing methodology of load-bearing walls and floors are respectively EN 1365-1 and EN 1365-2 (CEN, European Committee for Standardization, 1999, 2000).

The load-bearing capacity of timber frame assemblies exposed to fire is a subject that has been the focus of a large body of research. Fire resistance times for thirteen different set-ups involving TFA being used in wall assemblies were assessed by Richardson and McPhee (1996). Later, Richardson also studied the effect of gypsum plasterboard as a form of cladding and stone wool and glass wool products as cavity insulation (Richardson, McPhee, and Batista, 2000).

An extensive experimental programme on loaded TFA exposed to fire has been conducted in Canada (Sultan et al., 2005; Sultan, Seguin, and Leroux, 1998; Sultan and Lougheed, 2002). From this testing programme, the effects have been investigated of several design parameters on the fire resistance performance of assemblies, including: the effects of the spacing of gypsum board screws from board edges, insulation installation, insulation type, timber member spacing, timber member depth, resilient channel installation, resilient channel spacing, and load level (Sultan, 2008).

In all of the studies before above, thermal exposure was set according to the standard temperature-time curve, ISO 834 (ISO International Organization for Standardization, 1999). Regarding non-standard fire exposure, a full-scale compartment fire test in a timber-framed building with gypsum plasterboard as cladding and stone wool cavities insulation has recently been carried out (Kolaitis, Asimakopoulou, and Founti, 2014).

### **2.3.2 Evaluation by analytical models**

In general, analytical design models consider the effects of fire on load-bearing timber members by (i) reducing the cross-section with a notional charring depth, and then (ii) considering a reduction in the strength and stiffness properties of the uncharred timber. A reduction in strength and stiffness may be taken into account by using modification factors (Lie, 1977). This procedure is known as the reduced properties method (RPM), and it can be compared to fire design for steel structures. Another approach takes into account the reduction of mechanical properties serving to

decrease the cross-section by the addition of a fictive layer which is known as a 'zero-strength layer' (Schaffer, Marx, Bender, and Woeste, 1986). This method is referred to as the effective cross-section method (ECSM). This is also known as the reduced cross-section method. The area of the cross-section that is reduced by the char layer and the zero-strength layer is defined as the effective cross-section, in which the material properties are considered as being at the ambient temperature. The ECSM was initially developed for glued-laminated timber beams as a simplified method for designers (Schaffer et al., 1986).

The Canadian testing programme has also provided the basis for a model to calculate the structural response of timber members in TFA that has been exposed to fire and where it has been installed as part of a wall (Bénichou and Sultan, 2003, 2004, 2005a; Bénichou, Sultan, and Kodur, 2003), or as a floor (Bénichou, 2006). The model for wall elements takes the temperature distribution from WALL2D software package, a two-dimensional numerical model for predicting heat-transfer through timber members that are protected by gypsum plasterboard with void cavities, which was developed by Takeda and Mehaffey (1998). In the floor model, the thermal conditions being used as an input are taken from temperature profiles that were measured during fire tests.

Collier (2002) has developed a model to predict the time required for the structural collapse of TFA that has been used in a wall. In this proposal, the effects of a fire are taken into account as a loss of timber cross-section due to charring and a calculation of the residual load-bearing capacity. The charring is evaluated depending upon the incident's radiating effect upon the timber member, with the result that the maximum stress on the timber element can be predicted. The prediction of the maximum stress is based upon a modification of what is known as the 'secant formula' (Young and Budynas, 2002) for eccentrically-loaded columns. This model has been verified by means of TFA fire tests with void cavities that have been subjected both to standard and non-standard levels of fire exposure.

A simple analytical model which can be used in the structural fire design of timber frame assemblies has been developed based upon the results of an extensive experimental programme (König, 1995; König, Norén, Olesen, and Hansen, 1997; König and Walleij, 2000). This design of model can predict the load-bearing capacity of TFA with stone wool (SW) products being used as cavity insulation, whether it is being used as a wall or a floor, which is exposed to a standard temperature-time fire exposure. The fire protection provided by stone wool cavity insulation can be taken into account before and after any cladding has potentially fallen off in a fire-related situation. The same model can be used for TFA with cavities that are insulated with glass wool (GW) products if the cladding does not fall-off. A design model that considers the contribution to the load-bearing capacity of the timber members where this is provided by glass wool cavity insulation after the cladding has fallen-off was proposed by Just (2010b, 2010a). Frangi et al. (2008) developed a design model to predict the load-bearing capacity of TFA with void cavities exposed to standard temperature-time fire exposure.

The design proposed by König and Walleij (2000) is included in Annex C of the current Eurocode 5 Part 1-2 (CEN, European Committee for Standardization, 2004b) while the design models proposed by Just (2010b) and Frangi et al. (2008) are included in the European Guideline Fire Safety in Timber Buildings (FSITB) (Östman et al., 2010).

A detailed description of the design models proposed by König and Just is included in the following sections.

A study of how applicable was König's model to TFA that has been insulated with a different form of heat-resistant insulation has been carried-out by Just (2012).

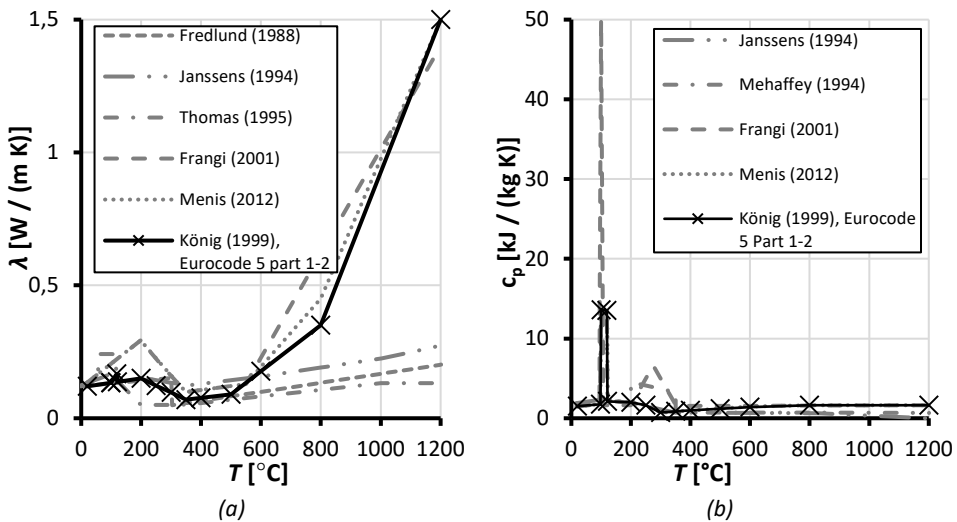
### **2.3.3 Evaluation by numerical simulations**

By using numerical models, it is possible to predict the temperature and stress distributions of TFA exposed to fire. A first attempt of a heat transfer simulation for TFA under fire conditions was carried out by Gammon (1988). Mehaffey et al. (1994) tried to predicted temperature profiles for TFA exposed to fire by means of a self-written code. In this code, Mehaffey et al. tried to implement the effect of the shrinkage of gypsum plasterboard and the effect of smokes. König (2006) has proved that the temperature scenario for an element exposed to fire can be successfully described by means of heat-transfer simulations using effective conductivity ( $\lambda$ ), specific heat ( $c_p$ ), and a loss in mass of the materials that compose the element. For this purpose, several Finite Element (FE) software packages can be used (such as, for example, ABAQUS, ANSYS, SAFIR, and TASEF) (Wickström, 1979; Franssen, 2005; Madenci and Guven, 2015; Dassault Systèmes Simulia, 2012).

Several testing techniques are available when it comes to measuring conductivity, specific heat and loss in mass of materials at different temperatures. For example, the widely used techniques to measure thermal conductivity are the hot-wire method (HW) (Healy, De Groot, and Kestin, 1976), the guarded hot plate method (GHP) (ISO International Organization for Standardization, 1991; Salmon, 2001) and the transient plane source method (TPS) (Gustafsson, 1991). In general, measurements of thermal conductivity which are made using these techniques are found to be in steady-state conditions (in the case of the HW and GHP methods), or present a linear temperature-time relationship (in the case of the TPS method). The TPS method is also capable of measuring the thermal diffusivity of a material where, when knowing the thermal conductivity and thermal diffusivity, it is possible to calculate the specific heat. Another technique which can be used to measure the specific heat as a function of the temperature is the differential scanning calorimeter (DSC) (Höhne, Hemminger, and Flammersheim, 1996). Loss in mass as a function of temperature can be evaluated experimentally by means of thermogravimetric analysis (TGA) (Coats and Redfern, 1963). Using testing techniques, it is possible to measure real values. However, for structural engineering purposes the use of real values are not considered in the numerical simulation of complex phenomena such as the moisture evaporation of wood and the cracking of charred materials. Complex phenomena can be taken into account implicitly by using effective values. A first approach was presented for a more complex model that is capable of predicting the formation of cracks, the opening of joints, and changes to material properties which are caused by moisture transportation in wood (Winter and Meyn, 2009).

Information about the effective conductivity, specific heat and loss in mass (the text which follows this section will refer to these three physical quantities as effective thermal properties) of wood at elevated temperatures can be found in various studies. The thermal properties of softwood that has been exposed to elevated temperatures have been investigated both experimentally (Cachim and Franssen, 2009; Frangi, 2001; Mehaffey et al., 1994; Menis, Fragiaco, and Clemente, 2012; Moss, Buchanan, and Fragiaco, 2009) and numerically (Fredlund, 1988; Hadvig, 1981; Janssens, 1994; König, 1999; Thomas, Buchanan, Carr, Fleischmann, and Moss, 1995). The effective

thermal properties which have been proposed by König are a result of calibrations from test results and a discussion of values that have been proposed by other authors. In this set of properties, the conductivity function presents a rise for temperatures above 500°C to take into account the cracking of the char layer (König, 1999). This set of effective thermal properties has also been adopted in the current Eurocode 5 Part 1-2 (CEN, European Committee for Standardization, 2004b). Effective thermal properties which have been adopted by the Eurocode 5 Part 1-2 should only be applied to the standard temperature-time fire exposure (König, 2005). A modification of these effective thermal properties for non-standard fire exposures has also been proposed (Hopkin, El-Rimawi, Silberschmidt, and Lennon, 2011). Two improved material models have recently been presented that can be used in numerical simulations for additionally calculating the temperature distribution under non-standard fire conditions (Werther, 2016).

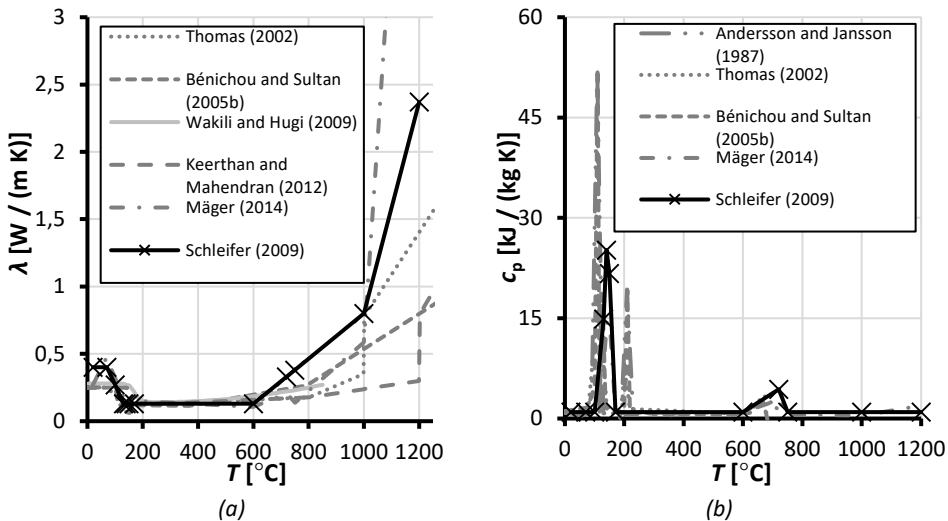


KEY:  $\lambda$  – conductivity;  $c_p$  – specific heat;  $T$  – temperature.

Figure 2-3. (a) thermal conductivity and (b) specific heat of wood as a function of the temperature.

The variation of thermal properties in terms of temperatures for gypsum plasterboard (GP) has also been the focus of a large body of research. A model was proposed to predict heat transfer through non-insulated steel-stud gypsum board wall assemblies that have been exposed to fire (Sultan, 1996). A search was presented in relation to the physical and chemical phenomena that occur at different temperatures and the relative effective thermal properties (Wakili and Hugi, 2009). The effect of moisture transfer on the specific heat levels of gypsum plasterboard at high temperatures has also been studied (Ang and Wang, 2009). It has been proved that the thermal properties of gypsum plasterboard given as a default in some software programs presents some limitations (Thomas, 2010). It has also been shown that the thermal properties of gypsum plasterboard which have been derived from standard fire tests, in some cases, can lead to significant levels of inaccuracy when used in non-standard fire conditions (Hopkin, Lennon, El-Rimawi, and Silberschmidt, 2012). Thermal properties have also been proposed for various types of gypsum plasterboard and products which have been derived from standard temperature-time fire exposure

(Andersson and Jansson, 1987; Bénichou and Sultan, 2005b; Keerthan and Mahendran, 2012; Mäger, 2016; Schleifer, 2009; Thomas, 2002, 2010). Effective thermal properties of other boards that are commonly applied with TFA, such as gypsum fibreboard and Oriented Strand Board, can be found in the available literature (Schleifer, 2009).



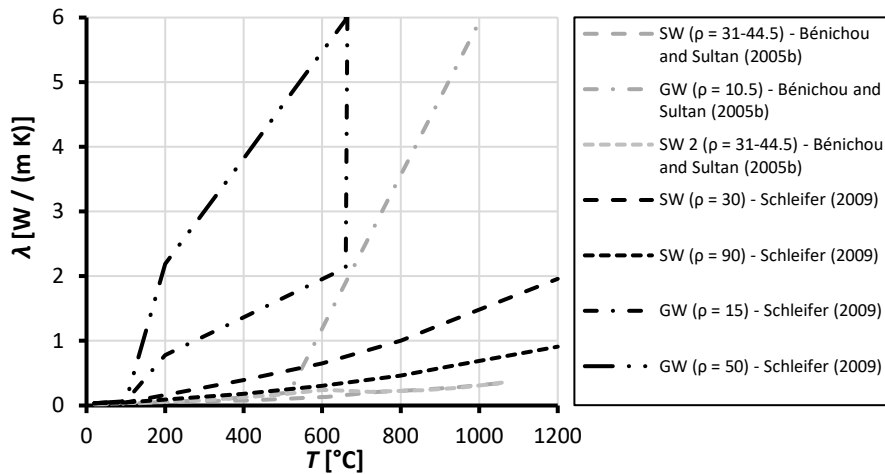
KEY:  $\lambda$  – conductivity;  $c_p$  – specific heat;  $T$  – temperature.

Figure 2-4. (a) thermal conductivity and (b) specific heat of gypsum plasterboard as a function of the temperature.

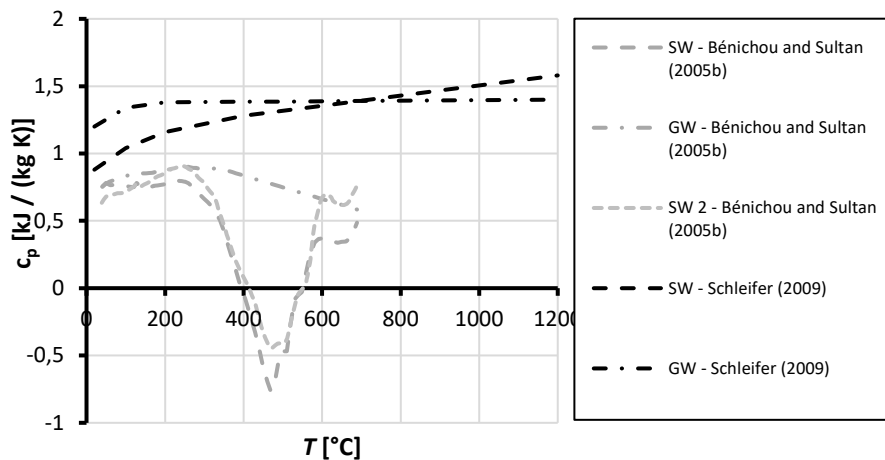
Thermal conductivity and specific heat were published as a function of the temperature for stone wool and glass wool (GW) products which are to be used in numerical simulations (Bénichou and Sultan, 2005b). These properties were directly measured by using the HW method and the DSC method respectively for thermal conductivity and specific heat.

Effective thermal properties which have been backwards-calculated from temperatures which were recorded during standard fire resistance tests for a limited number of insulation products such as SW and GW are also available in the available literature (Schleifer, 2009). In these set of thermal properties, the variation in thermal conductivity with the temperature is also given as a function of the initial density ( $\rho$ , expressed in  $\text{kg}/\text{m}^3$ ) for temperatures above  $100^\circ\text{C}$ . The thermal properties of gypsum plasterboard, stone wool, and glass wool insulation materials which have been proposed by Schleifer are also included in the FSITB guideline.

Wood presents a different mechanical behaviour when it is subjected to compression or tension parallel to the grain. Timber members which are subjected to compression that is parallel to the grain presents an elastic-plastic behaviour whilst, when subjected to tension, they present an elastic-brittle behaviour. This difference in behaviour can be described by a bilinear elastic-plastic stress ( $\sigma$ ) - strain ( $\epsilon$ ) relationship (Neely, 1898). After the evaluation of the temperature distribution has been carried out, stress distribution on load-bearing timber members can be evaluated numerically by adopting the temperature-dependent mechanical properties of wood (König and Walleij, 2000; Schmid, König, and Köhler, 2010; Menis et al., 2012; Klippel, 2014).



(a)



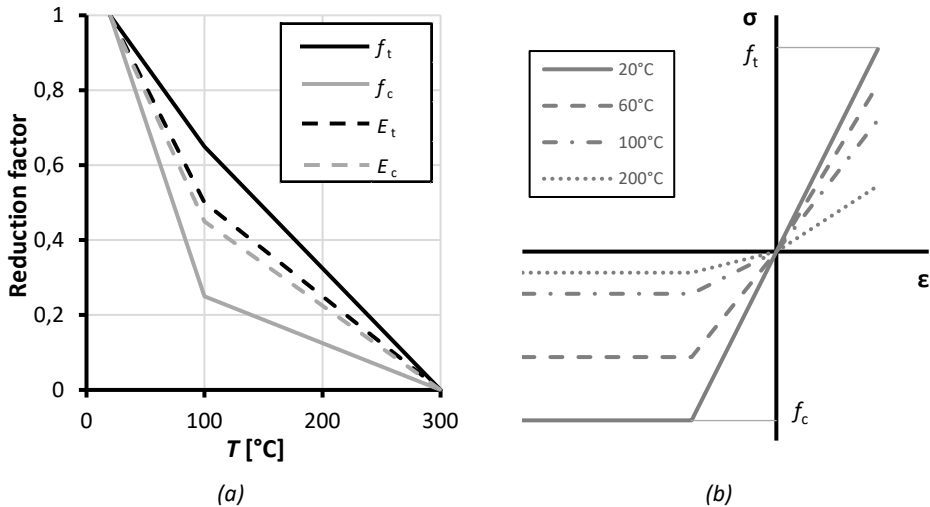
(b)

KEY:  $\lambda$  – conductivity;  $c_p$  – specific heat;  $T$  – temperature;  $\rho$  – density (expressed in  $\text{kg}/\text{m}^3$ ).

Figure 2-5. (a) thermal conductivity and (b) specific heat of stone wool (SW) and glass wool (GW) products as a function of the temperature.

Different research projects have focused on the impact of temperature on the strength and stiffness behaviour of timber. The modulus of elasticity for softwood in compression decreased between 20°C and 100°C by approximately 33% (Kollmann, 1951). It was pointed out that in the range between 20°C and 180°C under compression, tension, or bending conditions, the effect of temperature on the modulus of elasticity is approximately 12%, whilst from 180°C the modulus of elasticity decreased linearly until it reach a value that was equal to zero at 300°C (Schaffer et al., 1986). Tests results on structural timber which is subject to bending, compression, and tension have shown that at 100°C the modulus of elasticity has decreased to 88% for tension, and to 75% for bending (Glos and Henrici, 1991). Other studies found similar values for the modulus of elasticity under tension (Gerhards, 1982; König et al., 1997; Östman, 1985). Strength as a function of the temperature functions that were investigated by various authors exhibited a large degree of range (Glos and Henrici,

1991; Kollmann, 1951; Schaffer et al., 1986). König and Walleij (2000) have summarised all of these results and have proposed strength and stiffness functions for compression and tension which depend upon the temperature. These functions have also been included in Annex B of the current Eurocode 5 Part 1-2.



KEY:  $T$  – temperature;  $f_t$  – tensile strength;  $f_c$  – compressive strength;  $E_t$  – modulus of elasticity in tension;  $E_c$  – modulus of elasticity in compression;  $\epsilon$  – strain;  $\sigma$  – stress.

Figure 2-6. (a) reduction factors for strength and stiffness properties in compression and tension according to Eurocode 5 Part 1-2 and (b) bilinear elastic–plastic stress–strain relationship (Neely, 1898) with reductions for different temperatures according to Eurocode 5 Part 1-2.

## 2.4 Standardising insulation materials

In Europe, factory-made thermal insulation products for buildings are regulated by a series of standards. See, for example, the standard for factory-made mineral wool products, EN 13162 (CEN, European Committee for Standardisation, 2013b). In this series of standards, only the performance in reaction to fire has to be declared by the producers. Furthermore, EN 13162 refers to mineral wool products in general, and therefore do not differentiate between glass wool and stone wool products. Vice versa, in the current Eurocode 5 Part 1-2, the different contributions to the fire resistance of TFA which are provided by stone wool and glass wool products can clearly be distinguished (CEN, European Committee for Standardization, 2004b). For this purpose, Just (2010b) asserted that there is a need to distinguish mineral wool products into heat-resistant and non-heat-resistant types.

In Germany, a test method already exists to evaluate the performance in a fully-developed fire (Deutsches Institut für Normung, 2016). This test method, which is also known as the ‘melting point test’, aims to verify whether or not a mineral wool product possesses a melting point above 1000°C. This test methodology requires the measurement of the thickness of mineral wool insulation before and after its exposure to fire. The verification process is accomplished, meaning that the melting point is above 1000°C, when the loss in thickness after ninety minutes of fire testing according to DIN 4102-2 (Deutsches Institut für Normung, 1977) is less than 50%. This test methodology is addressed in a limited category of insulation materials. In the case of

cavity insulation in TFA, the loss in thickness may not be the only crucial parameter when it comes to evaluating the levels of contribution towards fire protection that is provided by the insulation material. Other behaviours such as lateral shrinkage or an increase in thermal conductivity under high temperature may intensify the charring of the timber member.

Outside Europe the situation is different. In New Zealand, TFA-related fire regulations do not provide any statement about insulation materials. The national building regulations simply specify the length in time of fire resistance that is required for timber frame assemblies, so it is up to the supplier to provide an assembly that satisfies the requirement (Standards New Zealand, 2012).

The Australian building code requires timber assemblies that are used in buildings other than a dwelling and for which fire resistance must be proven to include only non-combustible insulation materials (Board, A. B. C., 2015).

## 2.5 An existing design model for assemblies insulated with stone wool

The design model for TFA with cavities which has been proposed by König and Walleij (2000) is based upon the reduced properties method (RPM). To describe the charring evolution of the timber member, König et al. (1997) have identified three phases. In the first phase (Phase 1), the cladding is already in place and prevents the formation (start) of charring in the timber member. Charring might start with the cladding still in place. The phase which lies between the start of charring and the fall-off of the cladding is defined as the protection phase (Phase 2). During the protection phase the timber member is not directly exposed to fire. The phase after the fall-off of the cladding is defined as the post-protection phase (Phase 3).

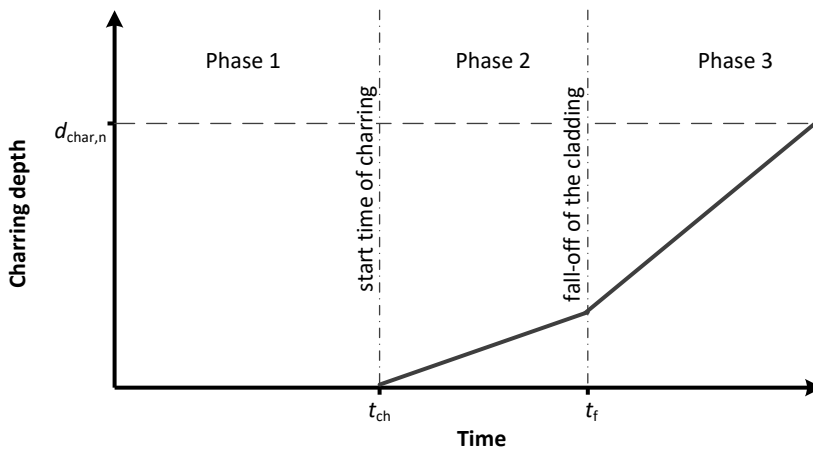


Figure 2-7. Different charring phases for the design model for TFA that has been insulated using stone wool (König and Walleij, 2000).

The time at which charring ( $t_{ch}$ ) starts in timber members depends upon the type of cladding that has been applied on the side of the timber members that has been exposed to fire. For example, the start time for charring behind one layer of gypsum plasterboard as proposed by König (1995) - and which is also included in the current Eurocode 5 Part 1-2 - can be calculated as follows:

$$t_{ch} = 2.8 h_p - 14 \quad (1)$$

where:  $t_{ch}$  is the start time of charring and  $h_p$  is the depth of the gypsum plasterboard.

Other expressions which serve to evaluate the start time of charring for timber members that are protected by various forms of cladding can be found in the currently available literature. For example, the start times of charring for timber members that are protected by clay-based materials were proposed by Liblik and Just (2017).

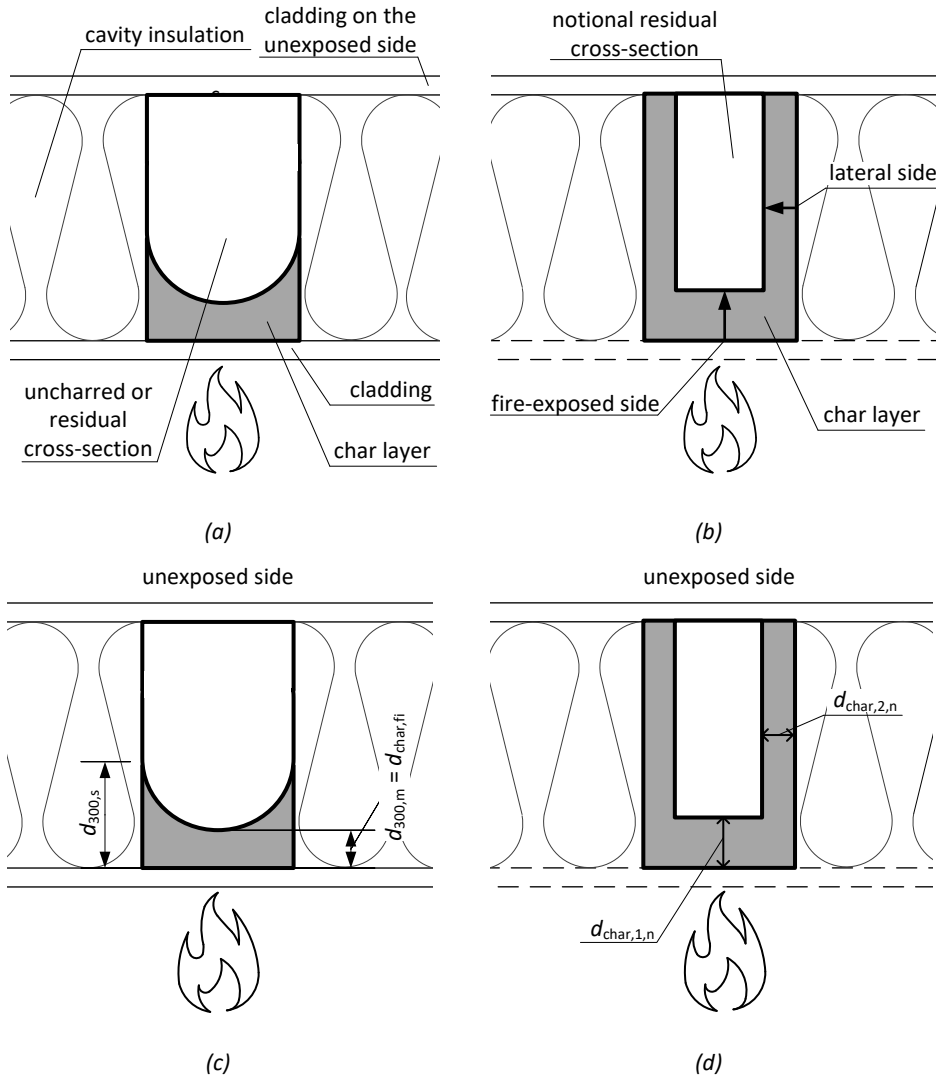


Figure 2-8. (a) cross-section of a timber frame assembly under fire conditions, (b) schematics for the charring directions used in analytical design models and (c) (d) a definition of charring depths.

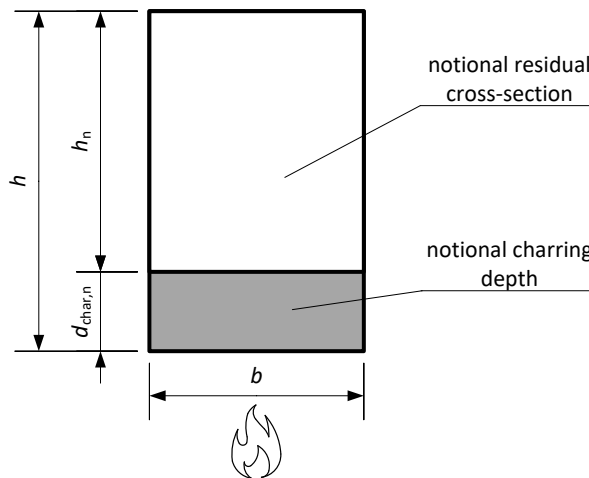
In order to obtain a simple expression which could be used by the designer, a linear relationships between charring depth and time can be assumed after the start of charring (König and Walleij, 2000). Charring on timber members can be divided into (i) one-dimensional or basic charring ( $\beta_0$ ) as physical properties for specific wood

species, densities, or strength class (Klippel and Schmid, 2017; König, 1999) and (ii) two-dimensional charring where the effects of cross-sectional dimensions or other effects are included.

The effects of corner-rounding are taken into account by multiplying the basic charring rate for the factor  $k_n$ . The width of the member has an influence on the charring rate as narrow members present a faster charring rate (Frangi and König, 2011). The influence of cross-sectional width is taken into account by the cross-section factor ( $k_s$ ).

Different charring rates in different protection phases are described using the protection factors ( $k_{pr}$ ). The protection factor for the protection phase (Phase 2) is referred to as  $k_2$  while the protection factor for the post-protection phase (Phase 3) is referred to as  $k_3$  (König and Walleij, 2000). The sub-indexes indicate the specific protection phase.

A charring depth for which the effects of cross-sectional dimensions or other effects are included, such as protection provided by cladding, is referred to as the notional charring depth ( $d_{char,n}$ ). In the design model for TFA which is insulated by using stone wool, the uncharred cross-section of the timber member is simplified as a rectangular residual cross-section.



KEY:  $h$  - initial depth of the member;  $b$  - initial width of the member;  $h_n$  - notional height of the member;  $d_{char,n}$  - notional charring depth.

Figure 2-9. Charring model for timber frame assemblies which are insulated with stone wool products (CEN, European Committee for Standardization, 2004b; König and Walleij, 2000).

The residual cross-section is evaluated by subtracting a notional charring depth from the fire-exposed side. The notional charring depth from the fire-exposed side can be calculated as follows:

$$d_{char,n} = \beta_0 k_n k_s k_2 (t_f - t_{ch}) + \beta_0 k_n k_s k_3 (t - t_f) \quad (2)$$

where  $d_{char,n}$  is the notional charring depth along the fire-exposed side;  $\beta_0$  is the basic design charring rate;  $k_n$  is the modification factor for corner-rounding,  $k_s$  is the cross-section factor;  $k_2$  and  $k_3$  are the protection factors in the protection and post-protection phases, respectively;  $t_{ch}$  is the start time of charring;  $t_f$  is the fall-off time of the cladding;  $t$  is the fire exposure time.

The notional charring depth can be evaluated by calculating the sum of two terms as shown in Equation (2): the first term describes the notional charring depth which occurs during the protection phase; the second term describes the notional charring depth during the post-protection phase.

The one-dimensional or basic charring rate for softwood solid timber products (pine or spruce) according to the current Eurocode 5 Part 1-2 (CEN, European Committee for Standardization, 2004b) is equal to 0.65 mm/min.

The modification factor for corner-rounding ( $k_n$ ) as proposed by Eurocode 5 Part 1-2 is equal to 1.5. In fact, König and Walleji (2000) discovered that this modification factor in the case of TFA with stone wool as a form of cavity insulation may vary between 1.3 and 1.5 and they proposed taking  $k_n = 1.5$  as a conservative value.

The cross-section factor  $k_s$  depends upon the width ( $b$ ) of the member (Frangi and König, 2011; König and Walleij, 2000). The current Eurocode 5 Part 1-2 provides values for  $k_s$  in different widths. The values given in Eurocode 5 Part 1-2 are derived for the following expression which has been proposed by König and Walleji (2000):

$$k_s = \begin{cases} 0.000167 b^2 - 0.029 b + 2.27 & \text{for } 38 \text{ mm} \leq b \leq 90 \text{ mm} \\ 1 & \text{for } b > 90 \text{ mm} \end{cases} \quad (3)$$

A research study has shown that a stone wool product may provide less fire protection for the sides of the timber member when  $d_{char,n}$  is deeper than 30 mm (Just, 2010c). In this case, Just (2010c) has proposed a different expression for the cross-section factor to apply only after  $d_{char,n}$  has reached 30 mm:

$$k_s = \begin{cases} 0.00023 b^2 - 0.045 b + 3.19 & \text{for } 38 \text{ mm} \leq b \leq 90 \text{ mm} \\ 1 & \text{for } b > 90 \text{ mm} \end{cases} \quad (4)$$

The protection factor for the protection phase ( $k_2$ ) depends upon the type of cladding that has been applied to the fire-exposed side. For example, in Eurocode 5 Part 1-2 the protection factor for gypsum plasterboard is given as a function of the depth of the board ( $h_p$ ):

$$k_2 = 1.05 - 0.0073 h_p \quad (5)$$

For other cladding materials, the protection factor for the protection phase can be determined according to EN 13381-7 (CEN, European Committee for Standardization, n.d.).

During the post-protection phase, a the secondary protection of the timber member is provided by the cavity insulation (Just, 2010b; König and Walleij, 2000). The protection factor for the post-protection phase ( $k_3$ ) other than the cavity insulation product itself, depends upon the fall-off time of the cladding ( $t_f$ ). The expression proposed by König and Walleji (2000) and which has also been adopted in Eurocode 5 Part 1-2 is as follows:

$$k_3 = 0.036 t_f + 1 \quad (6)$$

Standard gypsum plasterboard Type A (GtA), which is produced according prescription given in the European standard EN 520 (CEN, European Committee for Standardization, 2004c), would normally fall off shortly after that timber member has started to char (König and Walleij, 2000). Gypsum plasterboard Type F (GtF) presents an improved core cohesion which provides better performance under fire conditions. Therefore it remains in place during a period beyond the start of charring, dependent upon the material levels of resistance in the boards and/or the length of the fastening system.

According to Eurocode 5 Part 1-2, fall-off time ( $t_f$ ) for GtA can be taken as being equal to the start time of charring behind the cladding ( $t_{ch}$ ). König et al. (1997),

reported that GtF applied to horizontal elements (floors) had fell-off earlier than the corresponding vertical elements (walls). König et al. (1997) proposed the time at which temperatures of 600°C and 800°C are reached, in floors and walls respectively, on the unexposed side of the board as a design criterion to assess the fall-off time of GtF. Later, König and Walleji (2000) have developed an expression to predict the fall-off of GtF due to a pull-out failure of the fastening system. This expression is also inserted into the current Eurocode 5 Part 1-2.

Just (2010b) proposed expressions to predict the length of time it takes for different gypsum plasterboard products to fall off due to their material resistance. The fall-off times were studied on a database of full-scale test results which had been carried out across the world. Fall-off times depend upon the depth of the board and the type of gypsum plasterboard, on its application (whether it is being used in a wall or as part of a floor), and on the number of layers that have been applied. These expressions are also included in the guideline, FSITB (B. Östman et al., 2010). Later, Krauduk (2015) proposed revised expressions which were based upon an updated database of full-scale test results. The expression which was proposed by Krauduk (2015) predicted the 0.05 fractile of the fall-off time.

The design model for TFA which is insulated by using stone wool has been based upon the reduced properties method (RPM) (König and Walleij, 2000). After the subtraction of the notional charring depth, the mechanical properties have to be reduced by means of a modification factor. For example, the modification factor for the strength ( $k_{\text{mod, fm, fi}}$ ) is evaluated as:

$$k_{\text{mod, fm, fi}} = a_0 - a_1 \frac{d_{\text{char, n}}}{h} \quad (7)$$

where:  $d_{\text{char, n}}$  is the notional charring depth,  $h$  is the initial depth of the member, and  $a_0$  and  $a_1$  are tabulated coefficients which depend upon the load configuration.

Since  $k_{\text{mod, fm, fi}}$  is given as a function of the charring depth, the modification factor implicitly depends upon the fire exposure time.

In Eurocode 5 Part 1-2, the design model has been adopted for TFA which is insulated by using stone wool that is based upon the RPM. Furthermore, this design model has been limited to sixty minutes of fire exposure.

Later, König and Schmid (2010) have adapted this design model for the effective cross-section method (ECSM). Zero-strength layer depths ( $d_0$ ) for TFA which is insulated by using stone wool in different load configurations have been calculated using a thermo-mechanical analysis. Expressions have been proposed to evaluate zero-strength layer depths which depend upon the load configuration and the initial depth of the timber member. For example, zero-strength layer depths for TFA in bending with the tension side having been exposed to fire can be evaluated as:

$$d_0 = 13.5 + 0.1 h \quad (8)$$

where:  $d_0$  is the zero-strength layer depth, and  $h$  is the initial depth of the member.

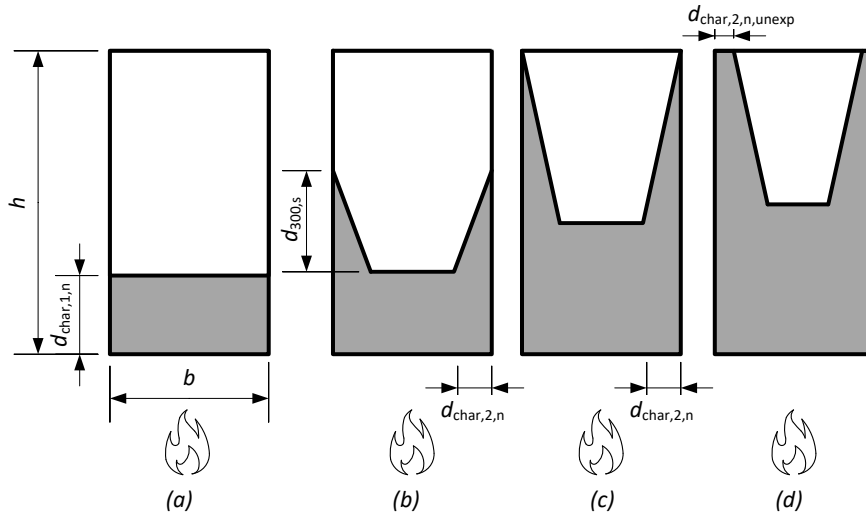
The design model for TFA which is insulated by using stone wool and which is based upon the ECSM has been inserted into the FSITB guideline.

Recent studies have demonstrated that the design model that has been included in Eurocode 5 Part 1-2 may be used to predict the notional charring depth of TFA with cavities that are completely filled with a heat-resistance insulation that is not stone wool using new values for the cross-section factor  $k_s$  (Just et al., 2012).

## 2.6 An existing design model for assemblies insulated with glass wool

Under fire conditions, glass wool products present a faster degree of degradation, or recession, than do stone wool products (Just, 2010b). Due to this faster rate of degradation, TFA timber members which have glass wool (GW) as cavity insulation exhibit a different charring scenario during the post-protection phase. To this purpose, a design model has been presented which can predict the load-bearing capacity of TFA with cavities that are insulated with glass wool (Just, 2010a, 2010b). In addition to charring from the fire-exposed side of the timber members (the fire-exposed side and the lateral sides are defined in Figure 2-8b), this design model also considers charring on the lateral sides, with differing starting times for the top and bottom sides, resulting in a trapezoidal residual cross-section (see Figure 2-10c and Figure 2-10d).

The design model for TFA with cavities that are filled with glass wool assumes the same charring phases as for the design model which uses stone wool-insulated TFA. More particularly, the notional charring depth during the protection phase (Phase 2) can be evaluated in the same way as it was evaluated for TFA which is insulated with stone wool.



**KEY:**  $h$  - initial depth of the member;  $b$  - initial width of the member;  $d_{char,1,n}$  - notional charring depth for the fire-exposed side;  $d_{char,2,n}$  - notional charring depth for the lateral sides on the bottom;  $d_{char,2,n,unexp}$  - notional charring depth for the lateral sides on the top;  $d_{300,s}$  - charring depth on the wood-insulation interface.

Figure 2-10. Charring phases according to the design model for timber frame assemblies which have been insulated with GW (Just, 2010a, 2010b): (a) protection phase; (b) post-protection phase before the complete recession of GW; (c) the completed recession of GW; and (d) after the complete recession of GW.

During the post-protection phase ( $t > t_f$ ) the notional charring depth from the fire-exposed side ( $d_{char,1,n}$  where sub-index 1 indicates the direction of the fire-exposed side) is calculated as follows:

$$d_{char,1,n} = \beta_0 k_n k_s k_2 (t_f - t_{ch}) + \beta_0 k_3 (t - t_f) \quad (9)$$

where  $d_{char,1,n}$  is the notional charring depth along the fire-exposed side;  $\beta_0$  is the basic design charring rate;  $k_n$  is the modification factor for corner-rounding,  $k_s$  is the

cross-section factor;  $k_2$  and  $k_3$  are the protection factors in the protection and post-protection phases respectively;  $t_{ch}$  is the start time of charring;  $t_f$  is the fall-off time of the cladding;  $t$  is the fire exposure time.

In this case, the protection factor for the post-protection phase ( $k_3$ ) is given as:

$$k_3 = \begin{cases} 1 + \frac{8}{75} t_f & \text{for } 0 \text{ min} \leq t_f \leq 15 \text{ min} \\ 1.9 + \frac{7}{150} t_f & \text{for } 15 \text{ min} < t_f \leq 60 \text{ min} \end{cases} \quad (10)$$

Once the cladding has fallen off, the recession (or thermal decomposition) of glass wool takes place and the lateral sides of the timber member are exposed to fire. When the thermal decomposition of the glass wool has reached the unexposed side of the insulation batt (the time being defined as the time in which the complete recession of the insulation  $t_{f,ins}$  takes place), the insulation does not provide any further protection against charring. From this moment onwards, the lateral sides are fully exposed to fire.

The time in which the complete recession of insulation ( $t_{f,ins}$ ) takes place can be calculated as:

$$t_{f,ins} = t_f + \frac{h}{v_{rec}} \quad (11)$$

where:  $t_f$  is the fall-off time of the cladding;  $h$  is the initial depth of the member and  $v_{rec}$  is the speed of recession of the insulation.

The speed of recession of any insulation being provided by glass wool products can be taken with a sufficient safety margin that is equal to 30 mm/min (Just, 2010a).

The notional charring depth from lateral sides on the bottom ( $d_{char,2,n}$ ) can be calculated as:

$$d_{char,2,n} = \beta_0 k_3 (t - t_f) \quad (12)$$

where  $d_{char,2,n}$  is the notional charring depth from the lateral sides;  $k_3$  is the protection factor in the post-protection phase.

As long as the insulation product provides protection against the charring process ( $t \leq t_{f,ins}$ ), the charring depth on the wood-insulation interface ( $d_{300,s}$ ) is calculated as:

$$d_{300,s} = v_{rec} (t - t_f) \quad (13)$$

When protection against the charring which is provided by the use of glass wool ( $t = t_{f,ins}$ ), the notional charring depth starts on the top of the lateral sides ( $d_{char,2,n,unexp}$ ); this charring can be calculated as:

$$d_{char,2,n,unexp} = \beta_0 k_3 (t - t_{f,ins}) \quad (14)$$

To calculate both notional charring depths on the top and bottom of the lateral sides, the post-protection factor has to be calculated according to Equation (10).

A reduction of the strength and stiffness of the timber member can be predicted as is done so for the stone wool model as long as the cladding is in place (for  $t < t_f$ ). After the fall-off of the cladding, any reduction in strength and stiffness can be taken into account according the ECSM by subtracting a zero-strength layer depth ( $d_0$ ) which is equal to 7 mm on each side which is affected by charring (Just, 2010b).

### **3 Evaluation of the fire protection provided by cavity insulations**

The previous section has shown that current EN standards regarding thermal insulation building products refer to their reaction to fire performance only and therefore do not distinguish any properties which may be related to fire resistance testing. The available design models predict the load-bearing capacity of TFA that has been exposed to fire, taking into account the contribution provided only by stone wool and glass wool products. All other types of insulation material that are available on the market are excluded from the models described above.

The lack of information available and limited investigation that has been carried out has imposed the necessity of developing a methodology that considers the contribution of a wide range of insulation materials in relation to the load-bearing capacity of TFA that has been exposed to fire. In this section, a criterion is presented to distinguish between different insulation materials based only upon their performance under fire-related conditions and their effect in terms of protecting a timber member.

#### **3.1 Selection of insulation materials**

A study which was conducted by Papadopoulos (2004) pointed out that the European market for insulation materials showed a predominant presence of stone wool and glass wool (contributing to 60% of the market), followed by organic foamy materials, expanded and extruded polystyrene and, to a lesser extent, polyurethane (all of which together account for 27% of the market). Although approximately 250 companies were present on the European market in 2003, nine of them accounted for more than 55% of the market share. In a later work (Papadopoulos, 2005), the most widely used insulation materials present on the European market have been grouped according to their chemical or physical structure.

One of the aims of this thesis is to develop a methodology which is able to evaluate the contribution of any kind of insulation product. Therefore the choice of tested products should comprise the widest possible range of products. However, the choice should also consider (i) the significant section of the market that is covered by a single category as it stands for mineral wools, and (ii) those products which, more than any other, are designed to be used with timber construction. In recent years the market has seen an increase in demand for organic and bio-based products as thermal insulation.

A summary of the selected batt-type insulation materials is shown in Table 3-1. The insulation materials that are involved in this study have been selected randomly to cover materials with very different raw sources and behaviour in a fire. Insulation materials of the same type but which are reported in Table 3-1 with a different frame of reference (such as, for example, different SW products), differ in their producer or density. The aim of this study was to determine a methodology and not to compare different products. For this reason, the product names and manufacturers are not being published. For each batt-type insulation product selected, the density ( $\rho$ ) has been evaluated in small samples. The thickness of the samples was measured according to EN 823 (CEN, European Committee for Standardization, 2013a). Table 3-1 also shows the declared thermal conductivity at 10°C according to the respective product standard and the reaction to fire class according to EN 13501-1 (CEN, European Committee for Standardization, 2007).

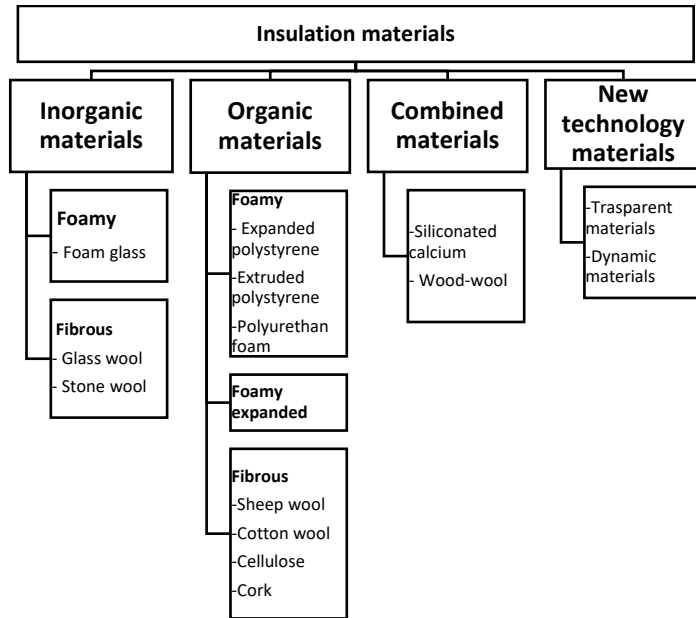


Figure 3-1. The most often-used insulation materials grouped according to their chemical or physical structure (Papadopoulos, 2005).

Table 3-1. Batt-type insulation materials which have been selected for this study.

Insulation material reference	Type	Declared thermal conductivity [W/(m K)]	Reaction to fire class	Measured density [kg/m <sup>3</sup> ]
SW 1	Stone wool	0.036	A1	32.56
SW 2	Stone wool	0.037	A1	37,71
SW 3	Stone wool	0.035	A1	34.10
SW 4	Stone wool	0.037	A1	40.90
SW 5	Stone wool	0.037	A1	42.50
HTE 1	High temperature extruded mineral wool	0.039	A1	15.96
HTE 2	High temperature extruded mineral wool	0.039	A1	19.32
GW 1	Glass wool	0.035	A1	17.77
GW 2	Glass wool	0.037	A1	18.24
CF	Cellulose fibre	0.038	E	41.37
PUR	Polyurethane	0.023	E	34.90
EPS	Extruded polystyrene	0.038	F	14.61

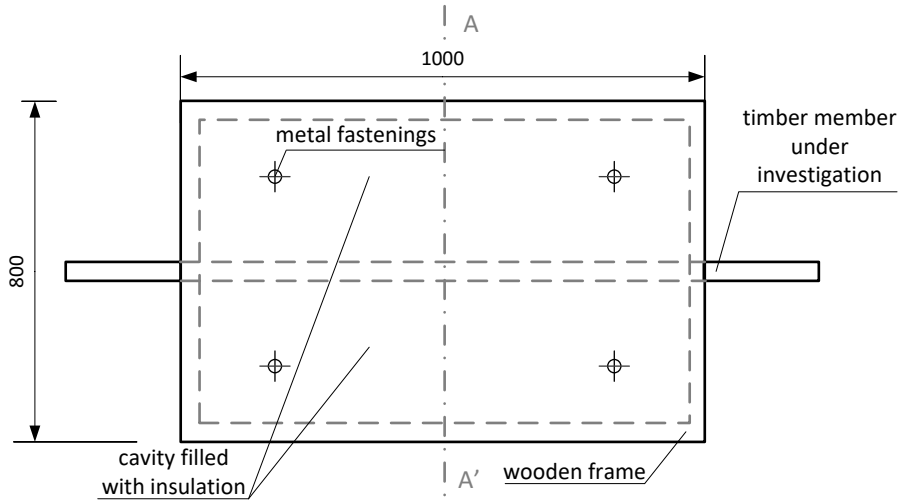
### 3.2 Cubic metre furnace tests

For this research project, a cubic gas-fired furnace was used to investigate the capability of different types of insulation to resist charring. The interior dimensions of the furnace were set at 1000 mm × 1000 mm × 1000 mm, with these measurements being referred to hereafter as a cubic metre furnace. In an initial test programme, a total of sixteen cubic metre furnace tests were carried out, whereby timber frame assemblies were tested in a horizontal position following the standard temperature-time fire exposure according to EN 1363-1 (CEN, European Committee for Standardization, 2012) (Table 3-2). The assemblies consisted of a wooden frame (with external dimensions of 800 × 1000 mm) with a timber member placed in the middle of the frame, parallel to the 1000 mm side (Figure 3-2a). The timber member in the frame (which was set at 45 mm wide, with a depth of 145 mm) allowed for two cavities at the sides of the member (with the dimensions at 333 × 910 mm) which could be filled with a selected form of insulation. If allowed by the flexibility of the insulation material, batts were oversized by 5 mm in both directions (with final dimensions of 338 × 915 mm).

The fire-exposed side of the tested specimens was protected by 15 mm-thick gypsum plasterboard Type F (GtF), according to EN 520 (CEN, European Committee for Standardization, 2004c) which was sourced from different providers. In order to avoid any joint, the board was installed in one piece of 800 × 1000 mm. The board was held in place by a metal fastening system. Four of these fastening system elements were applied to each specimen. A fastening system was composed of a metal bar which passed through the thickness of the specimen, metal washer, and a clip which was placed on both the exposed and unexposed sides of the specimen. These elements allowed the gypsum plasterboard to remain affixed to the wooden frame. It was possible to release the fastening and to impose the board's simulated falling off by means of hammering on the metal bars. On the unexposed side of the specimen, a particle board with a depth of 19 mm was applied in all of the specimens being tested.

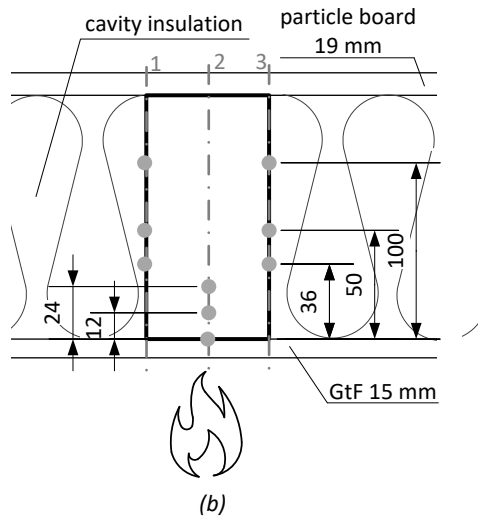
In order to guarantee that the insulation remained in place after the cladding had fallen off, the cavity insulation material was glued to the particle board using a sodium silicate-based glue. Thermal monitoring was achieved using Type K thermocouples (TC) which were embedded in the timber member in the middle of the cross-section and on the wood-insulation interface (Figure 3-2b).

PLAN



(a)

SECTION A-A'



(b)

KEY: GtF – gypsum plasterboard Type F.

Dimensions in millimetres

Figure 3-2. Test specimen for a cubic metre furnace: (a) overall plan; and (b) position of thermocouples on the timber member cross-section.

In order to obtain comparable results for the post-protection phase amongst the various insulation materials, the fall-off for the gypsum plasterboard was imposed at 45 minutes from the beginning of the test. The fall-off time of the cladding was taken as expected from the 15 mm thick gypsum plasterboard, Type F, in wall position (Just, 2010b). Tests 14, 15, and 16 presented an earlier fall-off of the cladding due to a failure of the fastening system; some of these tests are analysed separately in a later section of this research. The differing duration of charring phases due to various imposed

fall-off times of cladding are investigated in another test programme which is described as follows.

*Table 3-2. Overview of cubic metre tests carried out in the first test programme.*

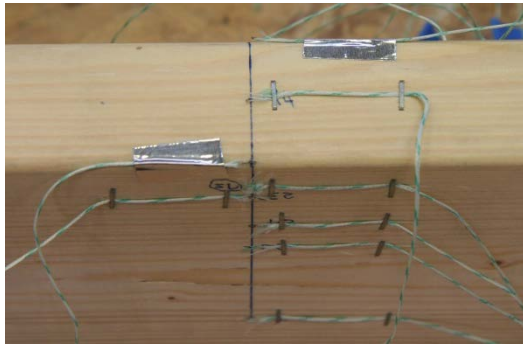
<b>Test number</b>	<b>Cavity insulation</b>	<b>Fall-off time of the cladding [min]</b>	<b>Duration of the test [min]</b>
Test 1	HTE 1	45	60
Test 2	HTE 2	45	60
Test 3	HTE 2	45	60
Test 4	HTE 2	45	60
Test 5	SW 1	45	60
Test 6	SW 2	45	60
Test 7	SW 2	45	60
Test 8	GW 1	45	52.2
Test 9	GW 2	45	60
Test 10	CF	45	60
Test 11	PUR	45	54.3
Test 12	EPS	45	45
Test 13	SW 3	45	60
Test 14	SW 4	33	60
Test 15	SW 4	35	60
Test 16	SW 5	42	60

The expected duration of the tests was sixty minutes, although in some tests the specimen was removed earlier due to the start of charring on the particle board. The start of charring on the particle board was monitored by means of a thermocouple placed on the insulation-particle board's interface.

### **3.2.1 Mounting of the specimens**

The quality of mounting in regard to the specimen can affect the measurement results. In order to be able to gain accurate results, the same mounting procedure was followed each time for all specimens:

1. Holes to allocate the thermocouple wires were drilled into the timber member using a drill press. A drill bit with a diameter of 1.5 mm was used.
2. Thermocouple wires with an external diameter equal to 1 mm were placed into the timber member which was to be subjected to investigated. The wires were positioned along a hypothetical isotherm for a length of at least 50 mm as prescribed in EN 1363-1 (CEN, European Committee for Standardization, 2012). Thermocouple wires were affixed by means of metal staples and aluminium foil tape respectively on the timber member and particle boards (Figure 3-3). Thermocouple wires were led out of the specimen from the side which was not to be exposed to fire.



(a)



(b)

Figure 3-3. Thermocouples positioned (a) on a timber member and (b) on the particle board.

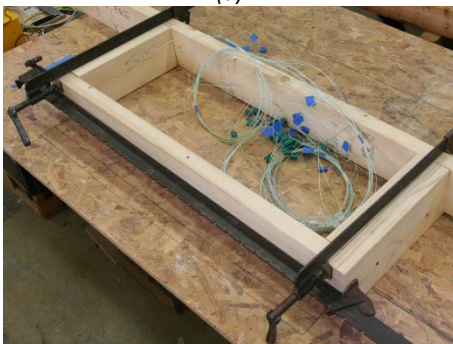
3. The timber components of the wooden frame and timber member which were under investigation were assembled together. To keep the timber components tight, clamps were used during the assembling procedure. To support the specimen on the furnace walls, addition planks were placed along the 800 mm-long side.



(a)



(b)



(c)



(d)

Figure 3-4. Mounting the wooden frame.

4. Particleboard was adjusted and affixed with screws on the top of the wooden frame. Then the specimen was rotated upside-down and all of the inner joints of the wooden frame were sealed with a sodium silicate-based glue.

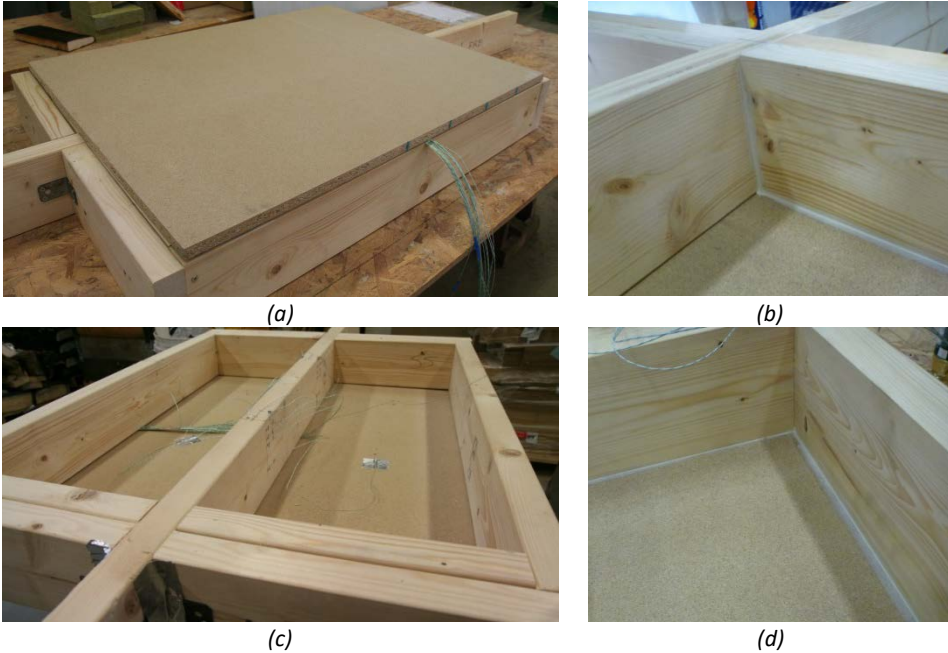


Figure 3-5. (a) positioning of the particle board, (c) specimen rotated upside-down and (b) (d) sealing the internal edges with a sodium silicate-based glue.

5. Insulation batts were cut which were 5 mm longer and wider with respect to the cavity dimensions (the dimensions of the insulation batts equalled  $915 \times 338$  mm); the glue was distributed along the inner side of the particleboard and the batts were positioned into the specimen.



Figure 3-6. A mineral wool product positioned in a wooden frame.

6. The gypsum plasterboard cladding (with dimensions of  $800 \times 1000$  mm) was placed into the wooden frame and was affixed with four screws on the four corners (with screws of a diameter of 3.9 mm and a length of 41 mm). Additional ribs of gypsum plasterboard (with dimensions of  $800 \times 200$  mm) were placed on the shorter side of the specimen. All of the visible joints were taped with aluminium foil tape.

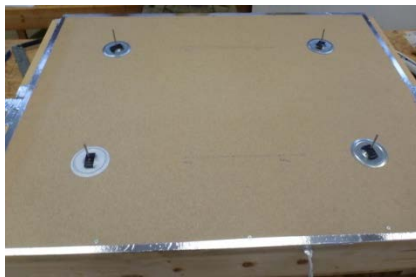


Figure 3-7. Gypsum plasterboard as fire protection mounted on a specimen.

7. The specimen was rotated with gypsum plasterboard facing downwards. All remaining joints were taped with aluminium foil tape. To allocate the metal bars of the fastening system, four holes (of a diameter of 4.5 mm) were drilled into the particle boards. Metal bars with a sharp tip (and a diameter of 4 mm) were inserted through the insulation batt and gypsum plasterboard. A washer and clip were placed on both extremities of the metal bars.



(a)



(b)

Figure 3-8. Placing the fastening systems to hold the gypsum plasterboard in place.

8. To monitor the temperature of the unexposed side of the specimen, copper disc thermometers with insulation pad. The insulation pads were affixed on the particle board by means of sodium silicate-based glue.

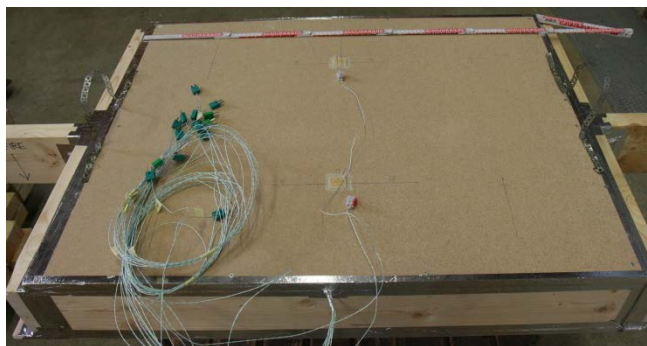


Figure 3-9. Top view of a specimen.

9. Prior to testing, the specimen was stored in a conditioned environment (at an air temperature of 20°C and 65% relative humidity).

### 3.2.2 Test results and discussions

At the end of the tests the char layer was removed from the timber members being investigated by means of a metal brush. Residual cross-sections were collected at different lengths along the investigated member: (i) at the points at which the thermocouples had been installed, and (ii) at the point at which the charring depth resulted deepest. These criteria were adopted for each member being investigated. Different residual cross-section shapes were observed for beams that were protected by different forms of insulation (Figure 3-10). For some specimens, the residual cross-sections were also analysed with the resistograph drilling along the depth of the member, from the unexposed side of the member towards its exposed side. The resistograph provides the resistance to the penetration versus the drilling depth.

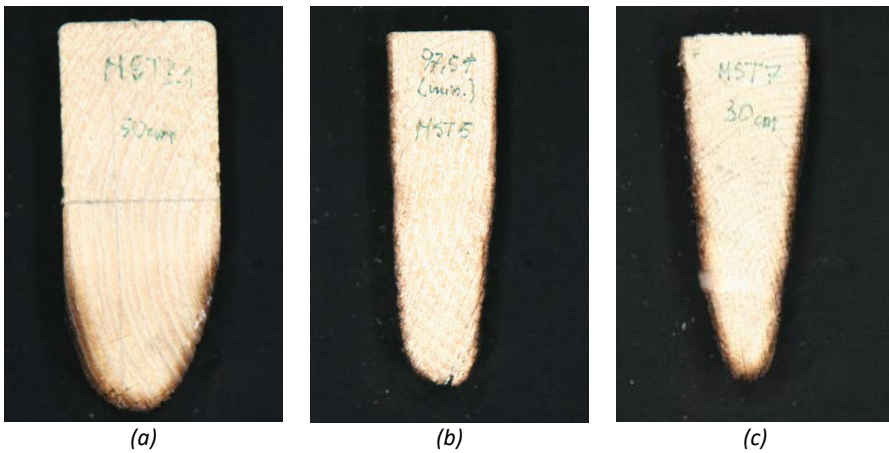


Figure 3-10. Residual cross-section for the timber members from a specimen which was insulated with (a) HTE mineral wool (Test 2), (b) glass wool (Test 8), and (c) cellulose fibre (Test 10).

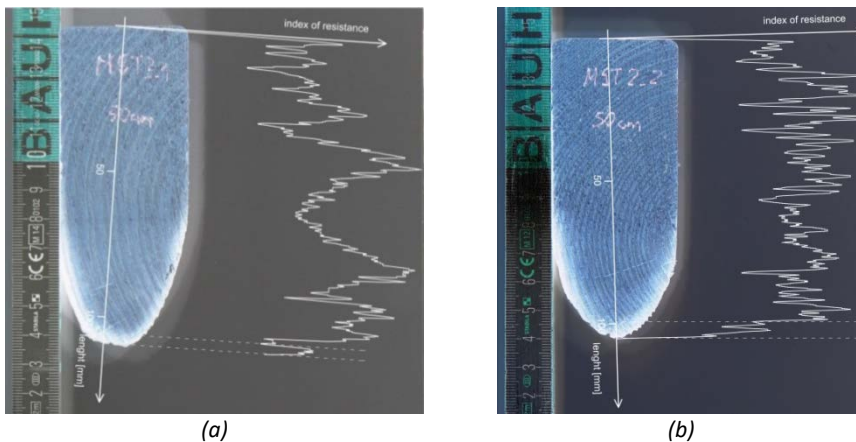


Figure 3-11. Resistance profile in the middle of the timber member.

The profiles obtained were compared to the negative pictures of the residual cross-section. This comparison should show whether there is any decrease in resistance in the pyrolysis zone of the wood. This method was adopted to make it possible to obtain further in-depth information on the properties of the residual cross-section.

The comparison of resistance profiles with the negative pictures of residual cross-section reveals that a resistance exists to penetration in the pyrolysis zone (Figure 3-11). These findings suggest that even the white zone visualised in a negative picture should be considered when the geometrical properties of the residual cross-sections are measured.

For all of the specimens being tested, the following analysis was carried out on the collected residual cross-section:

- residual cross-sections were photographed, including a ruler in the picture as a form of reference;
- pictures of the residual cross-section were post-processed in negative colours;
- pictures in negative colours were imported in AutoCAD (Autodesk, 2011);
- imported pictures were scaled and mass properties of the residual cross-sections were determined using AutoCAD's mass property function.

The charring depth at the position of the 300°C isotherm in the middle of the cross-section (line 2 on Figure 3-2b, which is subsequently referred to as  $d_{300,m}$ ) was obtained from temperatures that were measured by thermocouples, with a linear trend between the measurement points assumed in the same protection phase (Figure 3-12a). In addition, the depth on the wood-insulation interface (line 1 and 3 on Figure 3-2b, which is subsequently referred to as  $d_{300,s}$ ) was evaluated as the position of the 300°C isotherm with a linear trend between the measurement points assumed in the same protection phase (Figure 3-12b).

Variations in the charring depth in the middle of the member ( $d_{300,m}$ ) differed for the most part in the post-protection phase, as shown in Figure 3-12a. Comparisons of  $d_{300,s}$  for specimens with different forms of cavity insulation indicated that two different groups with respect to the speed of recession ( $v_{rec}$ ) could be observed. The speed of recession, as was also defined by Just (2010b), is the rate at which the 300°C isotherm on the wood-insulation interface advances in the post-protection phase. In addition, the test with EPS showed a steep velocity for the  $d_{300,s}$  during the protection phase.

Moments of inertia in the residual cross-sections ( $I_{fi}$ ), divided by the initial moments of inertia ( $I_{20^\circ C}$ ), are plotted against time taken in Figure 3-12a. In the same figure, moments of inertia as a function of the time predicted by design models for TFA with cavities which are filled with stone wool (König and Walleij, 2000) and glass wool (Just, 2010b) are also shown. The moments of inertia are plotted for the cross-sections at the points at which thermocouples were installed and at the point at which the charring depth resulted deepest. From this data, it can be observed that the greatest residual moments of inertia were accomplished in timber members of specimens which had been insulated with stone wool and high temperature-extruded mineral wools. In fact, members in those specimens which had been insulated with SW and HTE products at sixty minutes presented a reduction in the moment of inertia ( $I_{fi}/I_{20^\circ C}$ ) which comprised between 0.2 and 0.4 (Figure 3-12a). Smaller residual moments of inertia were measured in that specimen which had been insulated with cellulose fibre. The reduction of the moment of inertia ( $I_{fi}/I_{20^\circ C}$ ) in the timber member with CF insulation which was evaluated from the test assembly could be comparable to the design model for TFA which was insulated with glass wool (Just, 2010b) at 60 minutes. The test of the

specimen which had been insulated with EPS was interrupted at the same time of the predicted fall-off of the cladding, since the cavity insulation had already disappeared and the combustion of the timber member had begun on three sides. During the post-protection phase, the timber member would have been fully exposed to fire from three sides and a reduction of the moment of inertia would have occurred which was even faster than the one predicted by the design model for TFA which was insulated by glass wool.

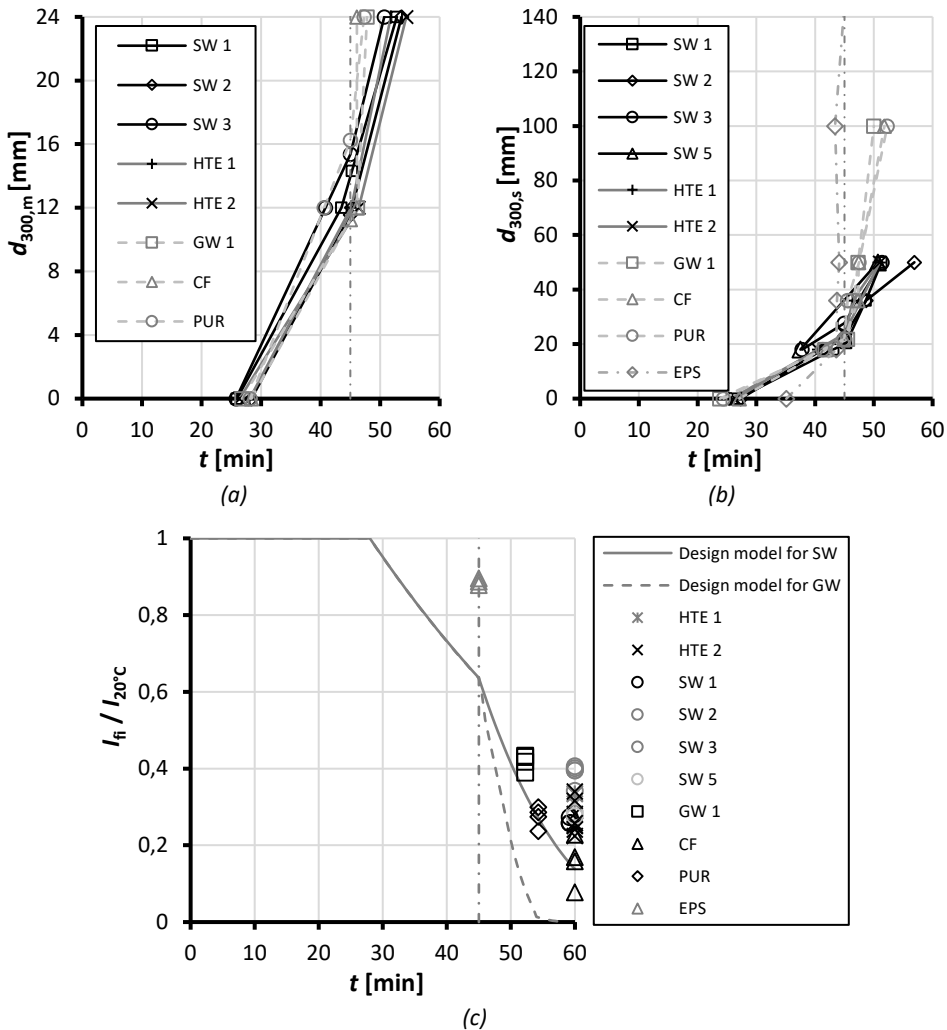


Figure 3-12. (a) charring depth in the middle of the cross-section ( $d_{300,m}$ ); (b) charring depth on the wood-insulation interface ( $d_{300,s}$ ) as a function of time; and (c) residual moments of inertia divided by the initial moments of inertia when compared to the design models for SW and GW.

### 3.3 Protection levels for cavity insulations

The results of this first test programme have indicated that the protection against charring of a timber element which is provided by the various forms of cavity insulation can vary quite noticeably. The resulting residual moments of inertia showed that it is

possible to identify different groups of insulation materials that provide a similar protection against the charring in a timber member. However, within these groups it does not seem possible to correlate the protection against the charring with the source material being used in the cavity insulation. Therefore a new approach is needed when it comes to distinguishing between insulation materials.

The main assumption for this test configuration is that protection against charring that is provided by insulation materials can be viewed as a decrease in the heat flux affecting the sides of the timber member; hence it may be crucial to understand where the protection ends where it is offered by insulation materials.

It can be assumed that the protection against the heat flux affecting the sides ceases where charring occurs on those sides. The 300°C isotherm on the interface between wood and insulation ( $d_{300,s}$ ) is also an indicator of charring on the sides of the member. On the other hand, this can also be seen as an indicator of the loss of protection against charring that is provided by the insulation material. The recession of protection against charring which is provided by insulation also serves to influence the general charring behaviour of the cross-section. As long as the sides are protected against charring, it is possible to simplify the charring behaviour as a form of notional charring from the fire-exposed side only (see the definition of fire-exposed side in Figure 2-8b). When protection against the charring happens to fail, combustion from the lateral sides has to be considered (see the definition of lateral sides in Figure 2-8b).

For any distinction between tested materials in significantly different groups, it is reasonable to consider two-thirds of the member depth as the border for defining the start of charring from the lateral sides, i.e. the position of  $d_{300,s}$  being equal to 100 mm in the case of a 145 mm-deep timber member. A criterion for qualifying the protection provided by different cavity insulations can be based on the fact of whether the recession of any protection exceeds a depth of 100 mm or not.

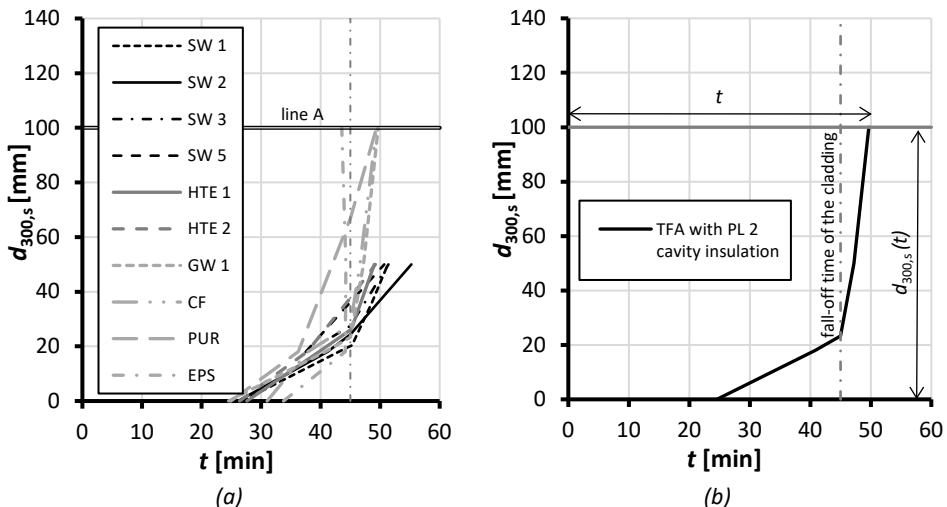


Figure 3-13. (a) Proposal for a qualification methodology for batt-type insulations with respect to the protection against the charring in timber members; (b) definition of the speed of recession of cavity insulation.

Values should be taken as the average of measurements for four sets of thermocouples which have been placed on the lateral sides of the timber member.

According to this proposal (Figure 3-13a), three different groups of cavity insulation can be recognised. The methodology described above is designed for reaching a determination of a level of protection against the charring in the timber member for cavity insulations being used in timber frame assemblies.

### 3.3.1 Criteria for protection levels

When comparing the results for the proposed qualification criterion (Figure 3-13a), with the reduction of the moment of inertia (Figure 3-12c), and charring in the middle of the cross-section (Figure 3-12a), it is possible to suggest that different levels of protection against the charring provided by batt-type insulations may be defined.

These protection levels (PL) against the charring in the timber member for sixty minutes of standard temperature-time fire exposure can be summarised as follows (from stronger to weaker):

- PL 1: insulation materials which allow less than 100 mm of charring depth on the wood-insulation interface during post-protection ( $d_{300,s} < 100$  mm for  $t > 60$  min) at 60 minutes of fire testing;
- PL 2: insulation materials which allow 100 mm of charring depth on the wood-insulation interface during the post-protection phase and before 60 minutes can be reached in fire testing ( $d_{300,s} = 100$  mm for  $45 \text{ min} < t < 60 \text{ min}$ , line A on Figure 3-13a);
- PL 3: insulation materials which allow 100 mm of charring depth on the wood-insulation interface during the protection phase ( $d_{300,s} = 100$  mm for  $t < 45$  min, line A on Figure 3-13a).

According to this proposal, high temperature-extruded mineral wools (HTE) and stone wool products (SW) are qualified as being amongst the stronger level of protection, or PL 1; glass wool (GW), cellulose fibre (CF), and polyurethane board (PUR) qualify in the middle level of protection, or PL 2. Expanded polystyrene (EPS) qualifies in the weaker level of protection, or PL 3. Within these protection levels, different protective performance may be distinguished in terms of insulation materials by the speed at which  $d_{300,s}$  moves during the post- protection phase, which is also defined as the speed of recession ( $v_{rec}$ ). The speed of recession can be evaluated as:

$$v_{rec} = \frac{d_{300,s}(t)}{t - t_f} \quad \text{for} \quad t < t_f \quad (15)$$

where  $d_{300,s}$  is the charring depth on the interface-wood insulation,  $t$  is the time at which  $d_{300,s}$  is considered, and  $t_f$  is the fall-off time of the cladding. An example of the evaluation of the speed of recession is also shown in Figure 3-13b.

By means of Equation (15), it was possible to evaluate the speed of recession for the cavity insulation that was being tested. For example, the value of  $v_{rec}$  which was obtained from Tests 8, 10, and 11 (Table 3-2) are 23.4, 13.4, and 22.7 mm/min respectively for GW 1, CF, and PUR.

The described qualification methodology should help the designer to distinguish between the wide range of forms of cavity insulation that is available for protecting timber members against charring.

### 3.3.2 Earlier fall-off of the cladding

As can be noticed from Table 3-2, Tests 14, 15, and 16 had their cladding fall off in under 45 minutes due to a failure in the fastening system. In particular, in Test 16,

the cladding fell off in 42 minutes, while in Tests 14 and 15 the length of time it took for the cladding to fall off occurred at 33 and 35 minutes respectively. A difference of three minutes' duration in the protection phase for Test 16 when compared to a duration of 45 minutes for most of the tests that were carried out has been considered as not being very significant in terms of a charring-related scenario during the post-protection phase. Therefore the cavity insulation type SW 5 has been included in the data that has been analysed with the majority of forms of cavity insulation that have been tested. Protection phase durations for Tests 14 and 15 have been considered as being unsuitable for a comparison with the rest of the test results, and these test results have been analysed separately. Both Tests 14 and 15 had SW 4 as their form of cavity insulation. The results for  $d_{300,s}$  were evaluated as being average for two sets of thermocouples for SW 4, as shown in Figure 3-14.

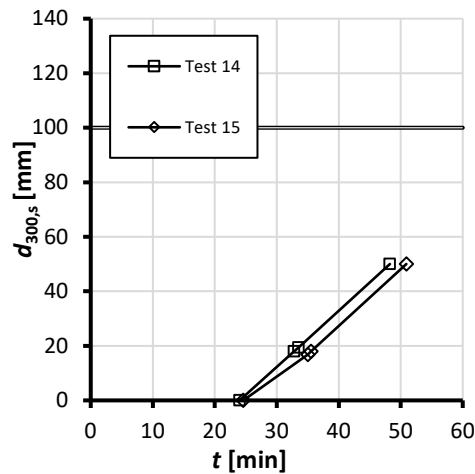


Figure 3-14. Charring depth on the wood-insulation interface ( $d_{300,s}$ ) as a function of time for Test 14 and Test 15.

In general, if the fall-off of the cladding occurs earlier than expected, this results in higher temperatures than expected being experienced in the layers behind this (Just, 2010b; König and Walleij, 2000). Charring depths on the wood-insulation interface for both Test 14 and Test 15 do not reach a depth of 100 mm after 60 minutes of fire tests. Therefore SW 4 can be assigned with protection level 1 (PL 1) as was the case for all of the other stone wool products that were subjected to investigation.

### 3.3.3 Validity of the methodology used for loose-fill cavity insulations

In the first test programme (Table 3-2), only batt-type (slab) cavity insulation was included. More of the two cubic metre furnace tests were also carried out to investigate the behaviour of loose-fill cavity insulations. For this purpose, two loose-fill insulation products were selected: a cellulose fibre (CF 1) and a glass wool (GW 3). The selected loose-fill insulation products were tested in the cubic metre furnace following the methodology described in Section 3.2.

Specimens were prepared which included a section of floor with central timber member (Figure 3-2). In these two specimens, the loose-fill insulation products were insufflated into the cavities. The density of the loose-fill insulation product at the ambient temperature was evaluated by checking the weight of the tested specimens

before and after the installation of the cavity insulation. Considering the volume of a single cavity to be equal to 0.044 m<sup>3</sup>, the densities of the insulation products were equal to 25 kg/m<sup>3</sup> and 35 kg/m<sup>3</sup> respectively for CF 1 and GW 3. In order to prevent the cavity insulation from falling off, a steel net was placed on the assembly following the installation of the cavity insulation. With the two specimens that were prepared, the steel net was affixed with screws at different points: on the specimen using CF 1 this was only on the 1000 mm-long sides, whilst on the specimen that was insulated with GW 3 it was on all of the timber components (Figure 3-15).

*Table 3-3. An overview of cubic metre tests carried out with loose-fill cavity insulations.*

<b>Test number</b>	<b>Cavity insulation</b>	<b>Fall-off time of the cladding [min]</b>	<b>Duration of the test [min]</b>
Test 17	CF 1	45	60
Test 18	GW 3	25.5	32.2



(a)



(b)

*Figure 3-15. Loose-fill insulation and steel net positioned into the wooden frames which were prepared for (a) Test 17 and (b) Test 18.*

After the imposed falling-off of the cladding for Test 17, the steel net presented a noticeable expansion. In this condition it was found that the insulation material did not exactly surround the timber member, which was the same for the batt-type insulations. In fact, the expansion of the steel net created an air gap between the insulation layer and the particle board. In Test 18, the constrained expansion of the steel net caused an earlier fall-off of the cladding by the gypsum plasterboard being pushed out. The methodology being used to test loose-fill insulation products needs improvement.



*Figure 3-16. Bending of the steel net occurred in the specimen that was prepared for Test 17.*

## 4 Improved charring model

In the previous section a methodology was proposed to distinguish between insulation materials based upon their capability to protect timber elements against charring. In this section, a study was conducted of the various parameters which may affect the load-bearing capacity of timber frame assemblies that have been exposed to fire. Charring developments and a reduction of the mechanical properties of uncharred wood were investigated by means of fire tests and also numerical simulations. An extension and improvement of the current design models is proposed for the load-bearing function of TFA where this has been exposed to the standard temperature-time fire exposure.

### 4.1 Unloaded cubic metre furnace tests

An investigation was carried out into the parameters which can affect the charring process in load-bearing timber members that are included in floor assemblies, using the cubic metre furnace. In this test programme (with the following being referred to as the second test programme), a total of eighteen cubic metre furnace tests were carried out involving TFA in the horizontal position (Table 4-1). All eighteen specimens were mounted following the procedure described in Section 3.2.1 and were then exposed to the standard temperature-time fire exposure according to EN 1363-1 (CEN, European Committee for Standardization, 2012). Also for this test programme, the assemblies consisted of a wooden frame (of the external dimensions 800 × 1000 mm) with a timber member placed in the middle which provided two cavities at the member sides as shown in Figure 3-2a. To investigate the influence of the timber member's width on the charring rate at the middle of the cross-section, different widths were chosen. The timber member cross-sections that were tested were 45 × 145 mm, 75 × 145 mm, and 120 × 145 mm.

Cavities insulation which were selected for this test programme were GW 1, HTE 2, and CF. Specimens were prepared with insulation batts oversized by 5 mm with respect to the cavity width and length.

The fire-exposed side of the specimens being tested was protected by 15 mm-thick gypsum plasterboard Type F (GtF), installed in one piece of 800 × 1000 mm and held in place by the metal fastenings described in Section 3.2. In order to investigate the influence of the protection phase duration, the fall-off of the gypsum plasterboard was imposed at different times: 30 min, 45 min. Three specimens (one for each cavity insulation that was involved in this test programme) were tested without any gypsum plasterboard on the fire-exposed side. The absence of the gypsum plasterboard on the fire-exposed side is considered as an imposed fall-off of the cladding at  $t = 0$  min. On the unexposed side of the specimen, a particle board with a depth of 19 mm was applied to all of the specimens being tested.

An additional specimen was tested with HTE 2 as its form of cavity insulation and with a member cross-section of 120 × 145 mm, protected by 20 mm-thick gypsum plasterboard Type F. Two plasterboards with the dimensions 500 × 800 mm were applied to the fire-exposed side of the specimen. The fall-off of the two boards was imposed at different times: 60 and 68 minutes. With this configuration, a 90 minutes fire was targeted.

To be able to monitor the charring scenario taking place, thermocouples Type K were embedded in the timber member at different depths, as shown on Figure 3-2b.

Table 4-1. An overview of cubic metre tests carried out in the second test programme.

Test number	Cavity insulation	Cladding	Member width [mm]	Fall-off time of the cladding [min]	Duration of the test [min]
Test 19	HTE 2	No	45	N/A	60
Test 20	HTE 2	GtF, 15 mm	45	30	60
Test 21	HTE 2	GtF, 15 mm	75	30	60
Test 22	HTE 2	GtF, 15 mm	75	45	60
Test 23	HTE 2	GtF, 15 mm	120	45	60
Test 24	HTE 2	GtF, 20 mm	120	60-68	90
Test 25	GW 1	No	45	N/A	21
Test 26	GW 1	GtF, 15 mm	45	30	41
Test 27	GW 1	GtF, 15 mm	75	30	50
Test 28	GW 1	GtF, 15 mm	75	45	60
Test 29	GW 1	GtF, 15 mm	120	30	60
Test 30	GW 1	GtF, 15 mm	120	45	60
Test 31	CF	No	45	N/A	60
Test 32	CF	GtF, 15 mm	45	30	60
Test 33	CF	GtF, 15 mm	75	30	56.7
Test 34	CF	GtF, 15 mm	75	45	60
Test 35	CF	GtF, 15 mm	120	30	59
Test 36	CF	GtF, 15 mm	120	45	60

KEY: GtF – Gypsum Plasterboard Type F; N/A – not applicable

## 4.2 Determination of the cross-section and corner rounding factors

Following the conclusion of the tests, residual cross-sections were collected from the timber members being investigated, taken at different lengths, and their mass properties were evaluated as with the first test programme. In addition, charring depths were obtained at the position of the 300°C isotherm in the middle of the cross-section ( $d_{300,m}$ ) from temperatures that were measured at the thermocouples. In the following analysis, the results of Tests 2, 5, and 7 are also included since the same cavity insulation products were involved in these tests.

Factors already included in the current design models for TFA were evaluated from the results of the cubic metre furnace tests that were carried out.

### 4.2.1 Cross-section factor

The factor  $k_s$  takes into account an increased charring rate for narrow members. The expression to derive the values of factors  $k_s$  (see Equation 3 in Section 2.5) was derived from fire tests which were carried out on TFA that had been insulated with stone wool and without any cladding having been applied on the fire-exposed side (König and Walleij, 2000). In this study, three specimens were tested which had no cladding on the fire-side, with one test being carried out for each form of cavity insulation that was included in the second test programme (see Table 4-1). The values of factor  $k_s$  were derived as:

$$k_s = \frac{d_{300,m}(t)}{t \beta_0} \quad (16)$$

where  $d_{300,m}(t)$  is the charring depth in the middle of the cross-section at a generic time  $t$ ;  $\beta_0$  is the basic charring rate taken as 0.65 mm/min.

The values for the factor  $k_s$  were taken from Test 25 (with GW 1 as the cavity insulation) and Test 31 (with CF as the cavity insulation), with those values being 1.51 and 1.49 respectively. For Test 19 (with HTE as the cavity insulation) the values  $k_s$  were found to be equal to 1.32. Specimens from Tests 19, 25, and 31 had a timber member that was 45 mm wide. The value for  $k_s$  for a 45 mm-wide member which was evaluated by means of Equation 3, were found to be equal to 1.3, while the value that was evaluated by Equation 4 produced a result that was equal to 1.63 (Just, 2010c; König and Walleij, 2000).

Table 4-2. Cross-section factors,  $k_s$ , which were evaluated for this study.

Test number	Cavity insulation	Cladding	Member width [mm]	Evaluated $k_s$
Test 19	HTE 2	No	45	1.32
Test 25	GW 1	No	45	1.51
Test 31	CF	No	45	1.49

Test results confirm the previous work: according to the qualification methodology that has been proposed, HTE 2 provide a stronger protection against the charring in timber members with respect to CF and GW 1 forms of cavity insulation. The equation for  $k_s$  which was proposed by Just (2010c), is addressed towards TFA with cavity insulation that provides less protection in respect to the stone wool product that was tested by König and Walleji (2000), and provides a higher value for  $k_s$  and therefore deeper charring depths occurs on the fire-exposed side.

#### 4.2.2 Corner rounding factor

The factor  $k_n$  takes into account the effects of corner-rounding. In order to evaluate the factor  $k_n$  for TFA, König and Walleij (2000) have compared the reduction of the moment of inertia ( $I_{fi} / I_{20^\circ\text{C}}$ ) with the ratio of charring depth from the fire-exposed side ( $d_{\text{char,fi}} / h$ ). The ratio for the charring depth on the fire-exposed side was taken as the charring depth as measured in the middle of the residual cross-section ( $d_{\text{char,fi}}$ ), divided by the cross-section depth at ambient temperature ( $h$ ).

On Figure 4-1, lines for different values of  $k_n$  are plotted which can correlate the charring depth ratio with the reduction of the moment of inertia. It is possible to observe that, for those specimens which are insulated with HTE 2, the correlation between  $d_{\text{char,fi}}/h$  and  $I_{fi}/I_{20^\circ\text{C}}$  follows the line of  $k_n = 1.2$ . In the majority of the test results, this correlation for a specimen that has been insulated with GW 1 and CF is accomplished with a higher value of  $k_n$ .

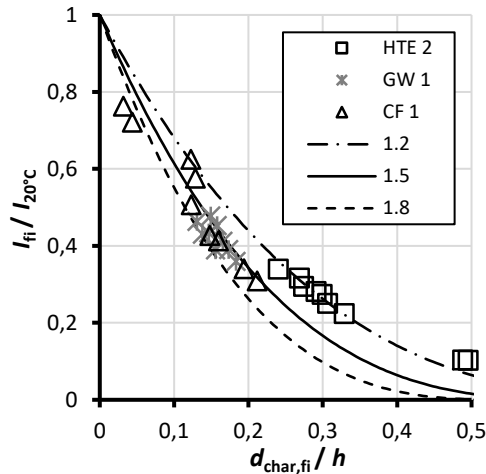


Figure 4-1. The reduction of the moment of inertia versus charring depth ratio.

A correlation between  $d_{char,fi}/h$  and  $I_{fi}/I_{20^\circ C}$  with a value of  $k_n$  which equals a figure of one to indicate that the residual cross-section shape is not affected by corner rounding, while a higher value of  $k_n$  indicates that an important influence on corner rounding or charring has already occurred, with the wood-insulation interface already having been penetrated to a significant depth. For example, the residual cross-section for Test 2 which was insulated with HTE 2 (see Figure 3-10a) supplies a value for  $k_n$  which is equal to 1.21, while residual cross-section for Tests 8 and 10 (in Figure 3-10b and Figure 3-10c) supplies values for  $k_n$  which equal 1.73 and 1.6 respectively.

### 4.3 The charring scenario in the improved design model

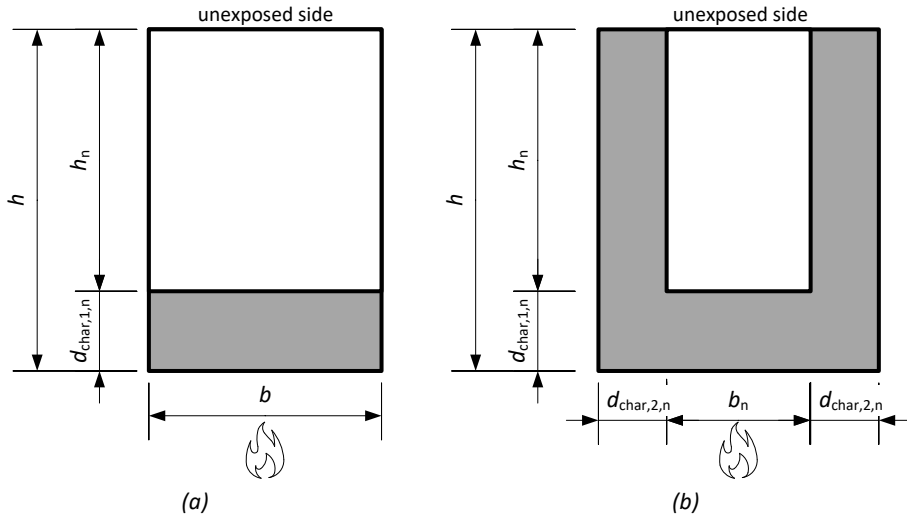
The previous sections have shown that a parameter which could be useful when it comes to evaluating the load-bearing capacity of a member, i.e. the moment of inertia, can be correlated with the process of producing the charring depth on the fire-exposed side of the timber by means of the factor,  $k_n$ . This factor may vary with the performance of the cavity insulation under fire conditions. In addition, the cross-section,  $k_s$  somehow depends upon the behaviour of the cavity insulation. For simplicity in the design model that is proposed below, the influence of the cross-section dimensions and corner rounding are taken into account by means of a unique factor ( $k_{s,n}$ ), which is given as being independent of the cavity insulation. Various charring scenarios are taken into account depending upon the performance of the cavity insulation by means of a notional charring depth on the lateral sides. Definitions of the fire-exposed side and lateral sides of the timber member are shown in Figure 2-8b. The fire-exposed side direction is also indicated in the sub-index as Direction 1, while the lateral side's direction is indicated as Direction 2.

The protection levels described in Section 3.3 have been introduced so that they can provide the basis for an evaluation of the charring depths in the improved design model for timber frame assemblies. The protection levels lead to different design procedures being outputted. The following charring scenarios are proposed:

1. if the cavities are completely filled with cavity insulation which qualified as PL 1, then charring occurs mainly on the fire-exposed side of the timber

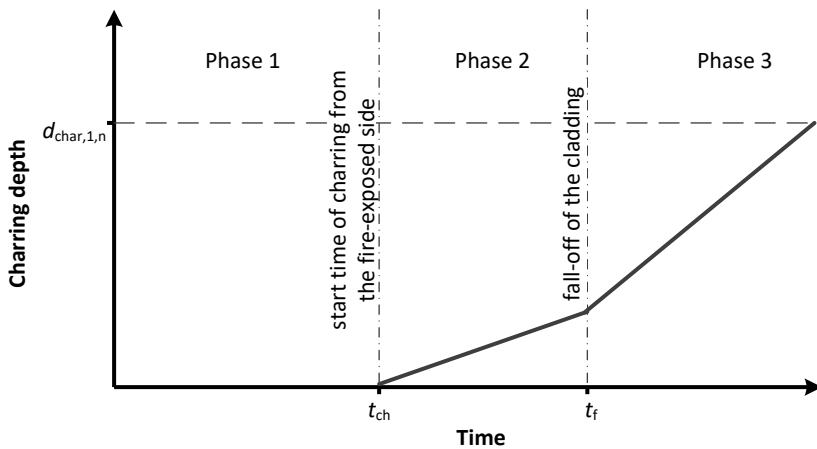
member, while the lateral sides are protected by the cavity insulation (Figure 4-2a);

2. if the cavities are completely filled with cavity insulation qualified as PL 2, then charring is regarded on the fire-exposed side during the protection phase (Figure 4-2a) and on three sides of the timber cross-section during the post-protection phase (Figure 4-2b) due to the recession of the cavity insulation;
3. if the cavities are completely filled with cavity insulation qualified as PL 3, then charring is regarded on three sides of the timber cross-section already during the protection phase (Figure 4-2b).

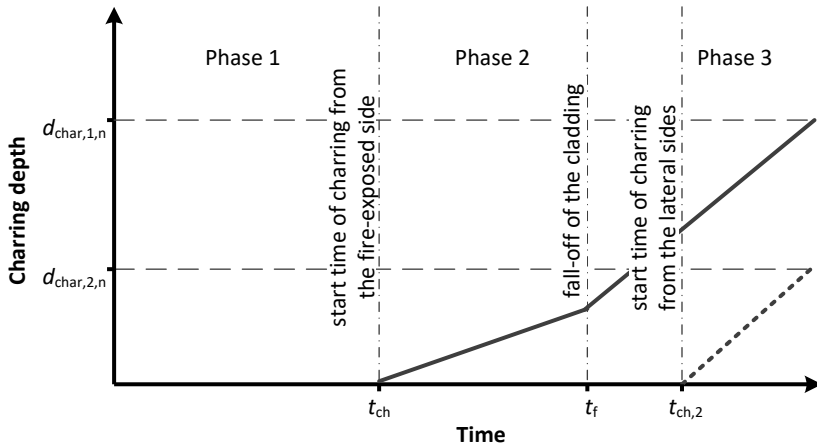


KEY:  $h$  - initial depth of the timber member;  $b$  - initial width of the member;  $h_n$  - notional depth of the member;  $b_n$  - notional width of the member;  $d_{char,1,n}$  - notional charring depth on the fire-exposed side;  $d_{char,2,n}$  - notional charring depth on the lateral sides.

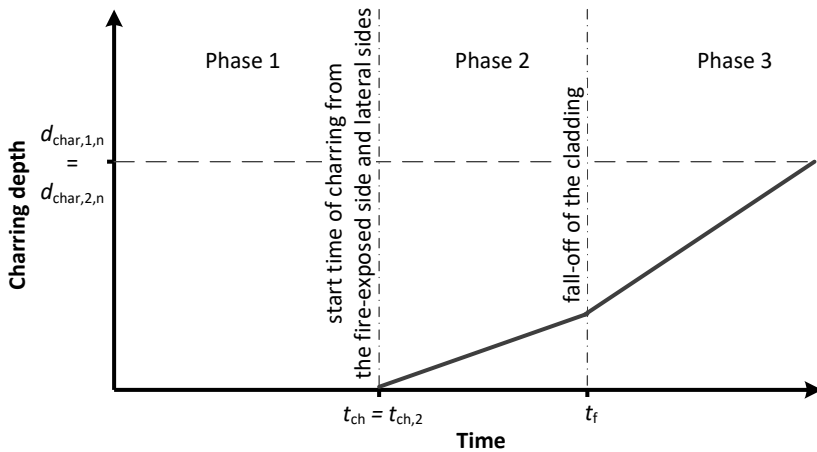
Figure 4-2. Charring scenario in the improved design model for TFA with (a) PL 1, PL 2, and PL 3 cavity insulation before charring has occurred, and (b) after the time at which charring starts on the lateral sides.



(a)



(b)



(c)

KEY:  $t_{ch}$  - start of charring on the fire-exposed side;  $t_f$  - fall-off time of the cladding;  $t_{ch,2}$  - start of charring on the lateral sides.

Figure 4-3. Different charring phases for the improved design model for TFA with (a) PL 1, (b) PL 2, and (c) PL 3 cavity insulation.

In order to calculate the charring depth along the fire-exposed side ( $d_{char,1,n}$ ), the following parameters need to be considered:

- $\beta_0$  is the basic or one-dimensional design charring rate;
- $k_{s,n}$  is the cross-section factor being used to consider the influence of cross-section dimensions on the charring rate;
- different charring rates in different protection phases are described using the protection factors,  $k_2$  and  $k_{3,1}$ . This is similar to the current version of Eurocode 5 Part 1-2. In the improved design model, the sub-index 3,1 for the protection factor indicates the protection factor for the post-protection phase (Phase 3) for the fire-exposed side's direction (or Direction 1).

In order to calculate the charring depth along the lateral sides ( $d_{char,2,n}$ ), the following parameters need to be considered:

- the start time of charring on the lateral sides ( $t_{ch,2}$ );
- the factor  $k_{3,2}$  considers the influence of the recession of cavity insulation on the fire protection of the lateral sides.

The charring depth on the fire-exposed side can be calculated as follows:

$$d_{char,1,n} = \beta_0 k_{s,n} k_2 (t_f - t_{ch}) + \beta_0 k_{s,n} k_{3,1} (t - t_f) \quad (17)$$

where  $d_{char,1,n}$  is the notional charring depth along the fire-exposed side;  $\beta_0$  is the basic design charring rate;  $k_{s,n}$  is the cross-section factor;  $k_2$  and  $k_{3,1}$  are the protection factors for the charring along the fire-exposed side in the protection and post-protection phases respectively;  $t_{ch}$  is the start time of charring on the fire-exposed side;  $t_f$  is the fall-off time of the cladding;  $t$  is the fire exposure time.

The notional charring depth for the fire-exposed side can be evaluated by the sum of two terms as shown in Equation (17): the first term describes the notional charring depth which occurs during the protection phase; the second term describes the notional charring depth during the post-protection phase.

After the start of lateral charring, the charring depth on the lateral sides can be evaluated as:

$$d_{char,2,n} = \beta_0 k_{s,n} k_{3,2} (t - t_{ch,2}) \quad (18)$$

where  $d_{char,2,n}$  is the notional charring depth for the lateral sides,  $k_{3,2}$  is the protection factor for the charring on the lateral sides in the post-protection phase,  $t_{ch,2}$  is the start time of charring on the lateral sides.

The basic charring rate ( $\beta_0$ ) for softwood has to be taken as being equivalent to 0.65 mm/min (Klippel and Schmid, 2017; König, 1999).

The cross-section coefficient  $k_{s,n}$  is given as a function of the member width ( $b$ ) for the charring depth on the fire-exposed side ( $d_{char,1,n}$ ), and as a function of the member depth ( $h$ ) for the charring depth on the lateral sides ( $d_{char,2,n}$ ). The factor  $k_{s,n}$  can be evaluated either for  $d_{char,1,n}$  or  $d_{char,2,n}$  as:

$$k_{s,n} = \begin{cases} 0.00025 b^2 - 0.044 b + 3.41 & \text{for } b \leq 90 \text{ mm} \\ 1.5 & \text{for } b > 90 \text{ mm} \end{cases} \quad (19)$$

$$k_{s,n} = \begin{cases} 0.00025 h^2 - 0.044 h + 3.41 & \text{for } h \leq 90 \text{ mm} \\ 1.5 & \text{for } h > 90 \text{ mm} \end{cases} \quad (20)$$

Equations (19) and (20) for  $k_{s,n}$  are valid for TFA with any type of cavity insulation product. Equation (19) has been derived by multiplying the factor  $k_n$  (which is equal to 1.5) by the expression of  $k_s$  (see Equation (3) in Section 2.5), which was proposed by König and Walleij (2000).

#### 4.4 Protection factors

The protection factor  $k_{pr}$  explains the charring rates in the protection and post-protection phases. The sub-index indicates the number being used for the protection phase:  $k_2$  is the factor for the protection phase (Phase 2), and  $k_3$  is the factor for the post-protection phase (Phase 3). The protection factor  $k_2$  takes into account the influence of cladding on the charring rate. An expression that can be used to calculate

the values for  $k_2$  in relation to gypsum plasterboards has been published in the current Eurocode 5 Part 1-2 (see also Equation 5). For the other cladding products, the value of the factor  $k_2$  can be determined by testing according to EN 13381-7 (CEN, European Committee for Standardization, n.d.).

The post-protection factor  $k_{3,1}$  takes into account the influence of an increased charring rate on the fire-exposed side of the timber member after the cladding has fallen off. This factor is influenced by the form of cavity insulation being used. In this study, values for the factor  $k_{3,1}$  were determined from the results of the second test programme. The values for  $k_{3,1}$  are given as a function of the fall-off time of the cladding ( $t_f$ ) and may vary depending upon the protection level of the insulation.

A determination of values for  $k_{3,1}$  which relates to charring on the fire-exposed side of the cross-section is shown in Figure 4-4 and Equation (21).

$$k_{3,1}(t_f) = \frac{d_2 - d_1}{\beta_0 k_s (t_2 - t_f)} \quad (21)$$

where  $k_s$  is the cross-section factor which has been calculated according to Equation (3),  $\beta_0$  is the basic design charring rate,  $d_2$  is the charring depth in terms of time  $t_2$ , with  $d_1$  being the charring depth in terms of time  $t_f$ , and  $t_f$  is the fall-off time of the cladding.

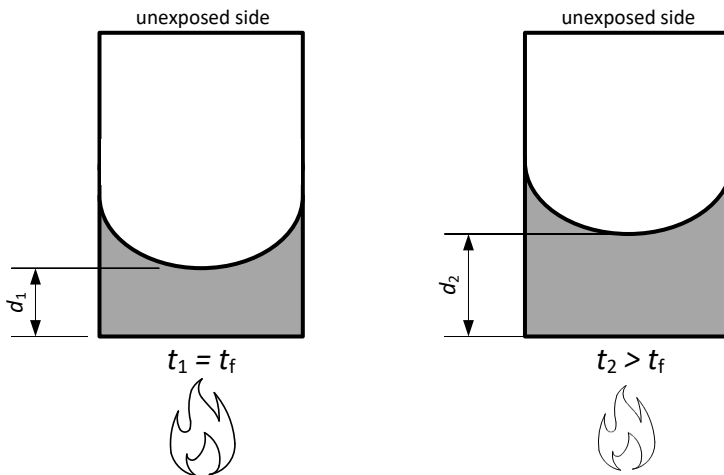


Figure 4-4. Charring depths  $d_1$  and  $d_2$  during the post-protection phase for the evaluation of the factor  $k_{3,1}$ .

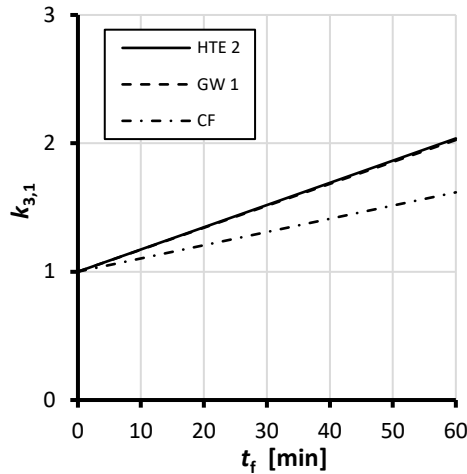


Figure 4-5. Factor  $k_{3,1}$  for the HTE 2, GW 1, and CF being studied.

An expression to determine the values for  $k_{3,1}$  as a function of the fall-off of the cladding ( $t_f$ ) for HTE 2, GW 1, and CF which was obtained from the test results is shown below:

$$k_{3,1} = 0.0173 t_f + 1 \quad \text{for} \quad \text{HTE 2} \quad (22)$$

$$k_{3,1} = 0.0171 t_f + 1 \quad \text{for} \quad \text{GW 1} \quad (23)$$

$$k_{3,1} = 0.0103 t_f + 1 \quad \text{for} \quad \text{CF} \quad (24)$$

#### 4.4.1 Charring on the lateral sides

For TFA with cavity insulations qualified as PL 2, the start time for lateral charring is assumed as the time at which the charring of the lateral side reaches two-thirds of the total depth of the timber member cross-section (Figure 4-6). The assumption of the two-thirds depth is derived from the charring depth of 100 mm on the wood-insulation interface which is taken for 145 mm-deep members to distinguish between the various forms of cavity insulation in terms of their performance under fire conditions (see Section 3.3.1).

In the case of TFA with cavity insulations qualified as PL 2, the time at which charring starts on the lateral sides ( $t_{ch,2}$ ) can be calculated as:

$$t_{ch,2} = t_f + \frac{2}{3} \frac{h}{v_{rec}} \quad (25)$$

where  $t_f$  is the fall-off time of the cladding,  $h$  is the depth of the timber member at ambient temperature and  $v_{rec}$  is the speed of recession for the cavity insulation (see Section 3.3.1).

In the case of TFA with cavity insulation qualified as PL 3, the start time of charring on the lateral sides ( $t_{ch,2}$ ) can be taken as being equal to the start time of charring on the fire-exposed side.

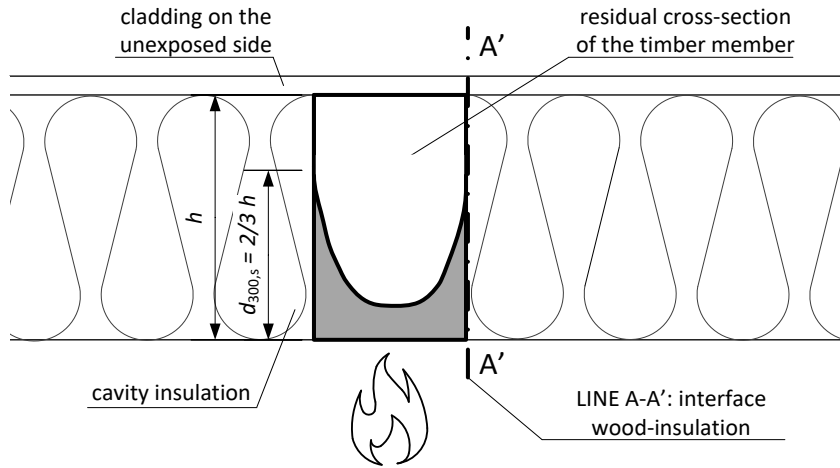


Figure 4-6. Residual cross-section during the post-protection phase at the moment at which the start time of charring on lateral sides is considered.

The post-protection factor,  $k_{3,2}$ , takes into account the charring rate on the lateral sides of the member. The role of the lateral charring rate is to fit the notional charring depth of the lateral sides ( $d_{char,2,n}$ ) on the mass properties of the residual cross-section under fire conditions. The notional charring depth can be fitted on several mass properties: the area ( $A$ ), the section modulus ( $W$ ), or the moment of inertia ( $I$ ). For example, in order to be able to fit on the residual section modulus ( $W_{fi}$ ), the following relationship is considered:

$$\frac{W_{fi}}{W_n} = \frac{b_n}{b} \quad (26)$$

where  $W_{fi}$  is the residual section modulus,  $b_n$  is the notional member width when considering charring from the lateral sides,  $b$  is the original member width,  $W_n$  is the section modulus of the notional rectangular simplified cross-section at the same time when considering only charring on the fire-exposed side as calculated using Equation (27).

$$W_n = \frac{b [h - d_{char,1,n}(t)]^2}{6} \quad (27)$$

where  $d_{char,1,n}$  is the notional charring depth for the fire-exposed side according to Equation (17),  $h$  is the original depth of the member, and  $t$  is the fire-exposure time.

The post-protection factor for the charring on the lateral sides  $k_{3,2}$  is calculated as:

$$k_{3,2} = \left\{ b - \frac{6 W_{fi}}{[h - d_{char,1,n}(t)]^2} \right\} \cdot \frac{1}{2 \beta_0 (t - t_{ch,2})} \quad (28)$$

where  $\beta_0$  is the basic charring rate.

Using the same principle, the factor  $k_{3,2}$  can be derived by fitting on the residual area ( $A_{fi}$ ) or the residual moment of inertia ( $I_{fi}$ ) by considering, respectively, the relationships in Equation (29) and Equation (30):

$$\frac{A_{fi}}{A_n} = \frac{b_n}{b} \quad (29)$$

$$\frac{I_{fi}}{I_n} = \frac{b_n}{b} \quad (30)$$

where  $A_{fi}$  is the residual area,  $b_n$  is the notional member width when considering charring on the lateral sides,  $b$  is the original member width,  $A_n$  is the area of the notional rectangular simplified cross-section,  $I_{fi}$  is the residual modulus of inertia, and  $I_n$  is the modulus of inertia on the notional rectangular simplified cross-section.

For example, values for  $k_{3,2}$  were derived from Test 8: by fitting on the residual section modulus  $k_{3,2}$  which turned out to be equal to 1.11, while by fitting on the residual area and residual moment of inertia the result was figures of 0.83 and 0.96 respectively. By fitting on the residual section modulus, the biggest values were obtained for the factor  $k_{3,2}$ . Therefore the expression to be used to calculate the proposed values for  $k_{3,2}$  were obtained by means of  $k_{3,2}$  values fitted on the residual section modulus.

The expression to calculate the values for the factor  $k_{3,2}$  are given as a function of start time of charring on the lateral sides ( $t_{ch,2}$ ):

$$k_{3,2} = \max \left\{ \begin{array}{l} 0.051 t_{ch,2} \\ 1 \end{array} \right. \quad \text{for} \quad \text{GW 1} \quad (31)$$

$$k_{3,2} = \max \left\{ \begin{array}{l} 0.0361 t_{ch,2} \\ 1 \end{array} \right. \quad \text{for} \quad \text{CF} \quad (32)$$

The values of the factor  $k_{3,2}$  are derived from tests with a timber member that was 145 mm deep (Table 4-1), with an increased charring rate possibly occurring on the lateral sides for a shallower member. For this reason, the factor  $k_{s,n}$  was also included in the Equation (18).

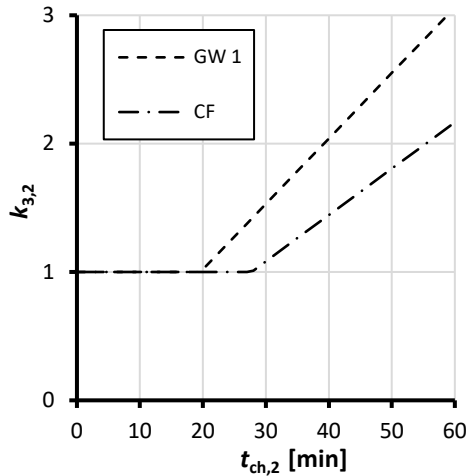


Figure 4-7. Factor  $k_{3,2}$  for the GW 1 and CF that were studied.

#### 4.4.2 Verification of the notional section modulus

In order to verify the proposed charring model, reductions in the notional section modulus ( $W_n/W_{20^\circ C}$ ) were calculated and plotted against the reduction of the section modulus that was evaluated under cubic metre fire tests ( $W_{fi}/W_{20^\circ C}$ ). The results for TFA which had been insulated with HTE 2, GW 1, and CF are shown in Figure 4-8.

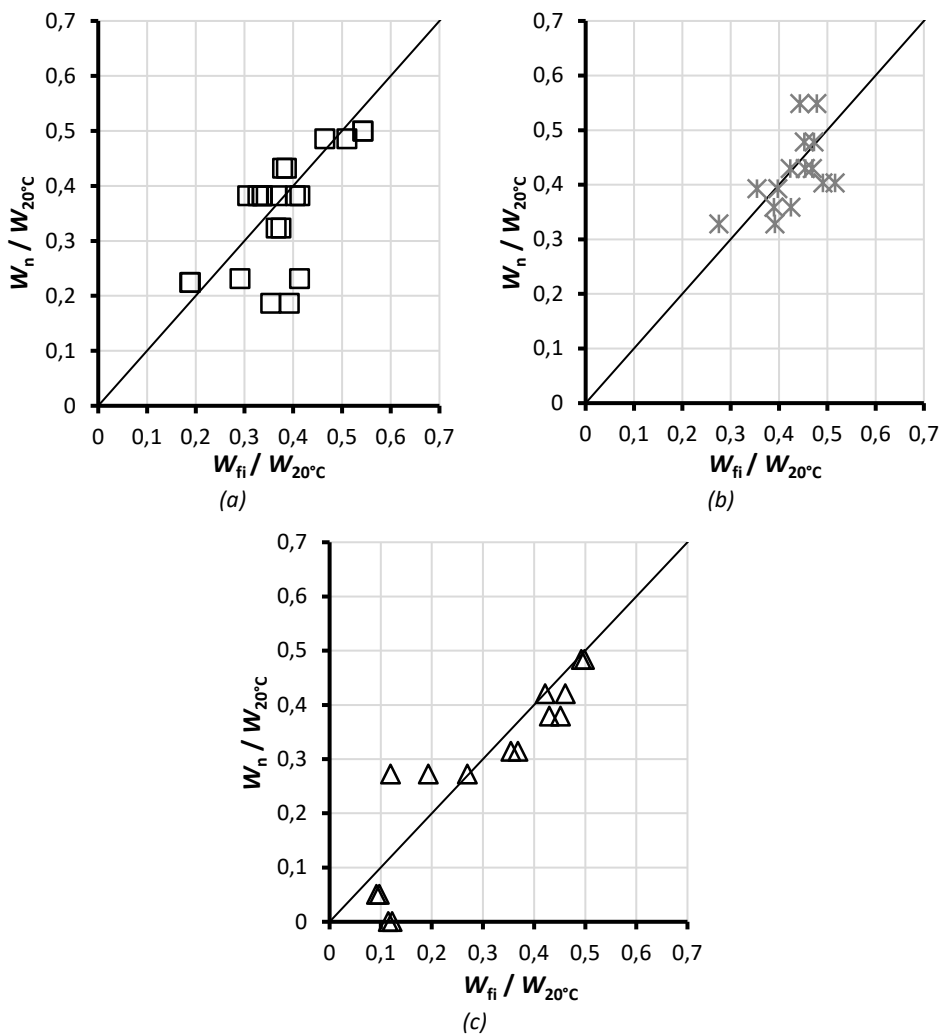


Figure 4-8. Reduction of section modulus as evaluated under fire tests when compared with the prediction by the charring model for assemblies that have been insulated with (a) HTE 2, (b) GW 1, and (c) CF.

#### 4.5 Protection factors evaluated by means of heat-transfer analysis

In order to be able to evaluate the protection factor  $k_{3,1}$  for generic stone wool products, a series of two-dimensional heat-transfer analyses were carried out. The temperature distribution within the cross-section was investigated in two-dimensional models which were implemented via the SAFIR software package (Franssen, 2005) - see Figure 4-9. Thermal exposure was described by means of the ISO 834 standard fire temperature-time curve (ISO International Organization for Standardization, 1999). Heat transfer by convection and radiation to the fire-exposed side of the model was considered using a convection coefficient of  $25 \text{ W}/(\text{m}^2 \text{ K})$  and an emissivity equal to 0.8, as prescribed in Eurocode 1 Part 1-2 (CEN, European Committee for Standardization, 2003).

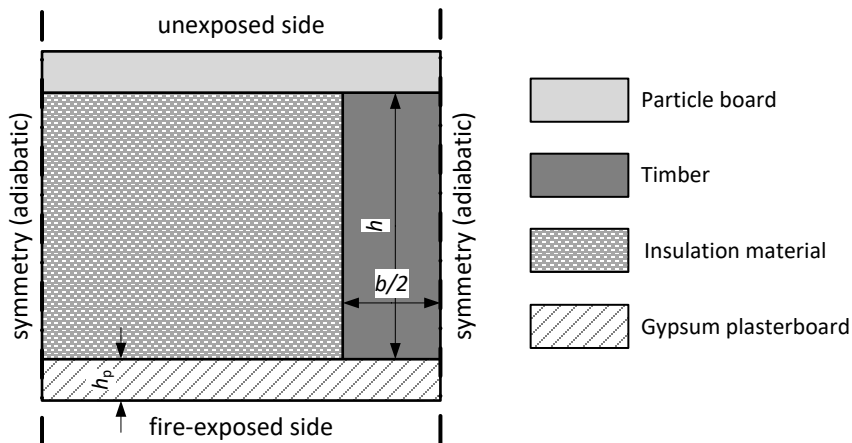


Figure 4-9. Schematics for the heat-transfer simulations.

Heat-transfer through the timber member was modelled using the effective thermal properties of timber as given in Eurocode 5 Part 1-2. Gypsum plasterboards, stone wool, and particle board were described using the effective thermal properties proposed by Schleifer (2009) and given in FSITB (B. Östman et al., 2010). The thermal conductivity of stone wool which was proposed by Schleifer (2009) depends upon its density at ambient temperature ( $\rho_{20^{\circ}\text{C}}$ ). A density at ambient temperature of stone wool equal to  $35 \text{ kg/m}^3$  was considered for this investigation (see also the effective thermal properties that were adopted for this investigation in Figure 5-2).

The same set-ups were simulated which were used to investigate the protection factors by means of cubic metre fire tests. All heat-transfer analyses were carried out on cross-sections with a depth of 145 mm and a 15 mm-thick Type F gypsum plasterboard as cladding. Different cross-section widths and fall-off times of the cladding were both investigated. The simulated set-ups are summarised in Table 4-3.

Table 4-3. Investigated set-ups for the definition of the post-protection coefficient for generic SW products.

Simulation	Cross-section dimensions [mm]	Cladding	Fall-off of cladding [min]	Duration of the fire exposure [min]
1	45 × 145	GtF 15 mm	0	60
2	45 × 145	GtF 15 mm	30	60
3	45 × 145	GtF 15 mm	45	60
4	75 × 145	GtF 15 mm	30	60
5	75 × 145	GtF 15 mm	45	60
6	120 × 145	GtF 15 mm	30	60
7	120 × 145	GtF 15 mm	45	60
8	120 × 145	GtF 15 mm	60	90
9	120 × 145	GtF 15 mm	70	90

KEY: GtF – Gypsum Plasterboard type F

Charring depths in the middle of the timber cross-sections were evaluated as the position of the  $300^{\circ}\text{C}$  isotherm ( $d_{300,\text{m}}$ ) from the output of the heat-transfer analyses. Values for the protection coefficient  $k_{3,1}$  for generic stone wool products were

calculated according to Equation (21). Values for  $k_{3,1}$  which were plotted against the fall-off times of the cladding are shown in Figure 4-10. An expression for  $k_{3,1}$  which was dependent upon the fall-off time of the cladding is proposed as follows:

$$k_{3,1} = 0.022 t_f + 1 \quad \text{for} \quad \text{SW} \quad (33)$$

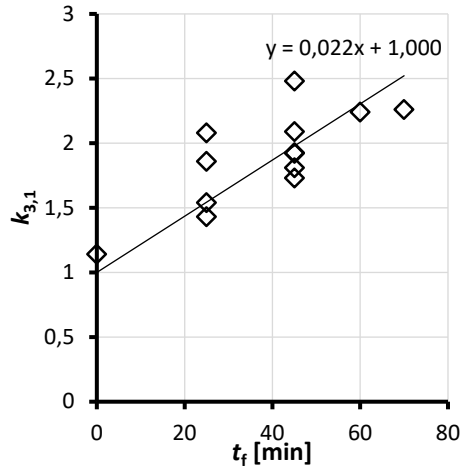


Figure 4-10. Values for  $k_{3,1}$  evaluated by means of heat-transfer analysis.

#### 4.6 Charring of TFA with cavities partially filled

The charring model that is presented is valid only if the cavities are completely filled by an insulation material. Often, timber frame assemblies are constructed with the cavities partially filled. In the following, TFA with cavities that are partially filled are investigated by means of heat-transfer analysis. The positions of the 300°C isotherm on the interface between wood and insulation ( $d_{300,s}$ ) for different configurations are evaluated and compared with the configuration of those cavities that have been completely filled. The design rules are investigated for various configurations of TFA with the cavity being partially filled.

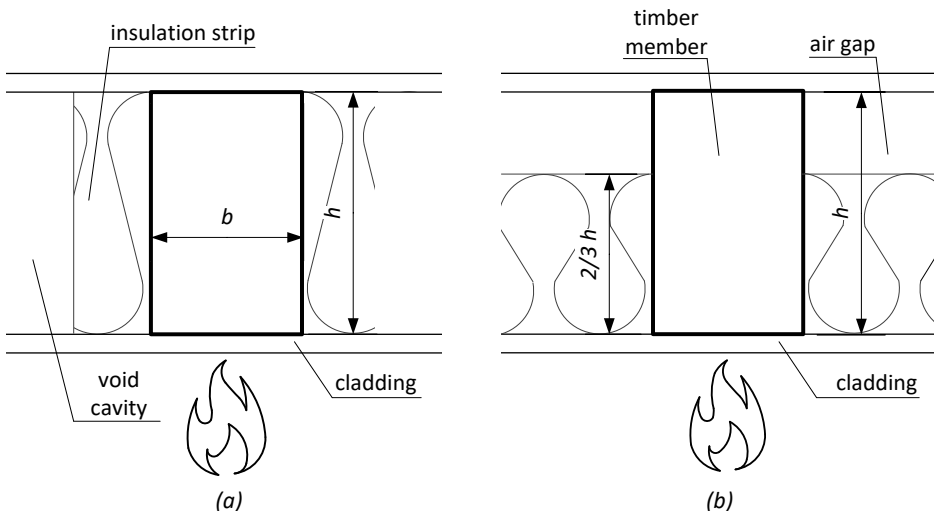


Figure 4-11. Examples of TFA with cavities not completely filled by insulation.

#### 4.6.1 Heat-transfer analysis

Two-dimensional models were implemented in the SAFIR software package (Franssen, 2005). Different configurations of the cavity insulation were investigated: Configuration 1 involved the cavity being completely filled (Figure 4-12a), while Configuration 2 had two-thirds of the cavity depth filled with insulation towards the fire-exposed side (Figure 4-12b), and Configuration 3 (Figure 4-12c) had a strip of insulation placed against the lateral side of the timber member. For Configuration 3, the insulation strip had the same depth as the cavity itself, while four different widths were investigated: 50 mm, 100 mm, 120 mm, and 150 mm. Configuration 1 is representative of the fire test conditions that are necessary when it comes to evaluating the protection levels being offered by an insulation material, as explained in Section 3. In the heat-transfer analysis which was involved for this investigation, HTE 2 was considered as a form of insulation. The effective thermal properties of HTE 2 were calibrated for this study according to the procedure which had been implemented by Mäger (2016). Gypsum plasterboards and particle board were described using the effective thermal properties that were proposed by Schleifer (2009).

Thermal exposure was described by means of the ISO 834 standard fire temperature-time curve (ISO International Organization for Standardization, 1999). Heat-transfer by convection and radiation to the fire-exposed side of the model was considered using a convection coefficient of  $25 \text{ W}/(\text{m}^2 \text{ K})$  and an emissions level of 0.8, as prescribed in Eurocode 1 Part 1-2. Heat-transfer through the timber member was modelled using the effective thermal properties of timber as given in Eurocode 5 Part 1-2. The heat-transfer calculations assumed 60 minutes of fire exposure.

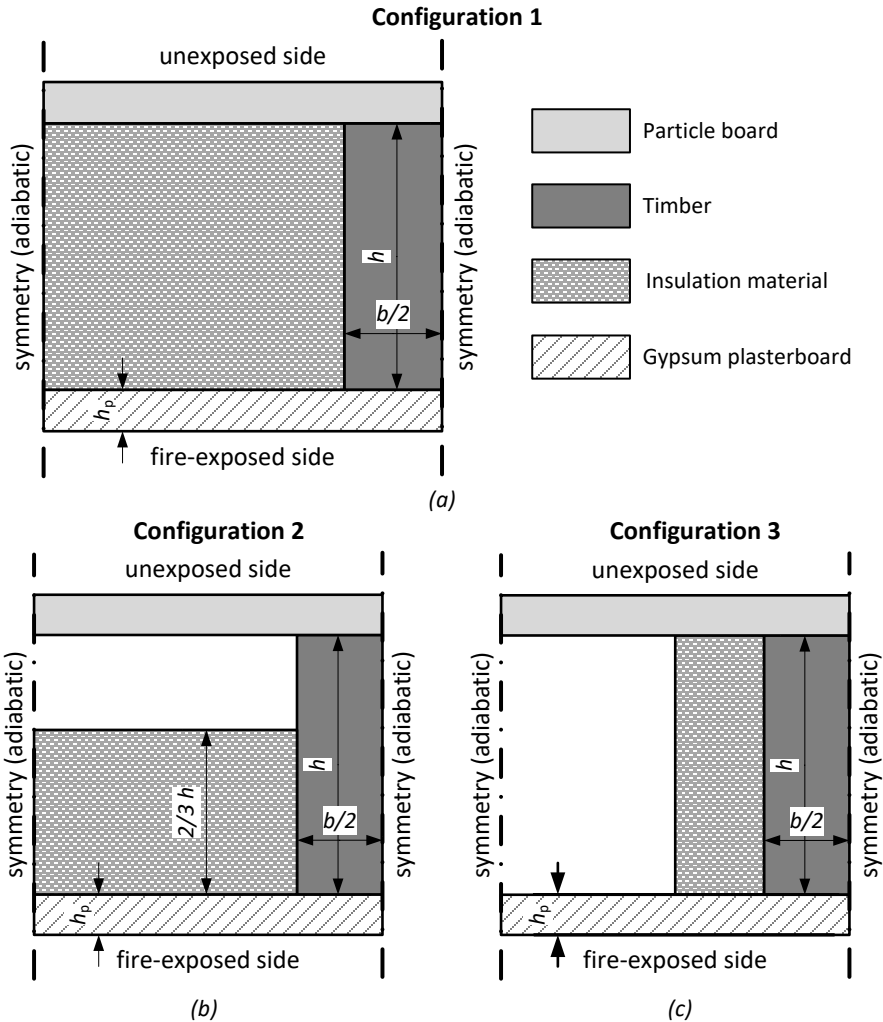


Figure 4-12. Schematics for the heat-transfer analysis with (a) cavity completely filled; (b) two-thirds of the cavity depth filled; and (c) insulation strip applied on the lateral side of the timber member.

Table 4-4. Investigated set-ups for TFA with cavities partially filled by insulation.

Simulation	Configuration	Fall-off of cladding [min]	Insulation material
10	1	45	HTE 2
11	2	45	HTE 2
12	3 – 50 mm wide strip	45	HTE 2
13	3– 100 mm wide strip	45	HTE 2
14	3– 120 mm-wide strip	45	HTE 2
15	3– 150 mm wide strip	45	HTE 2

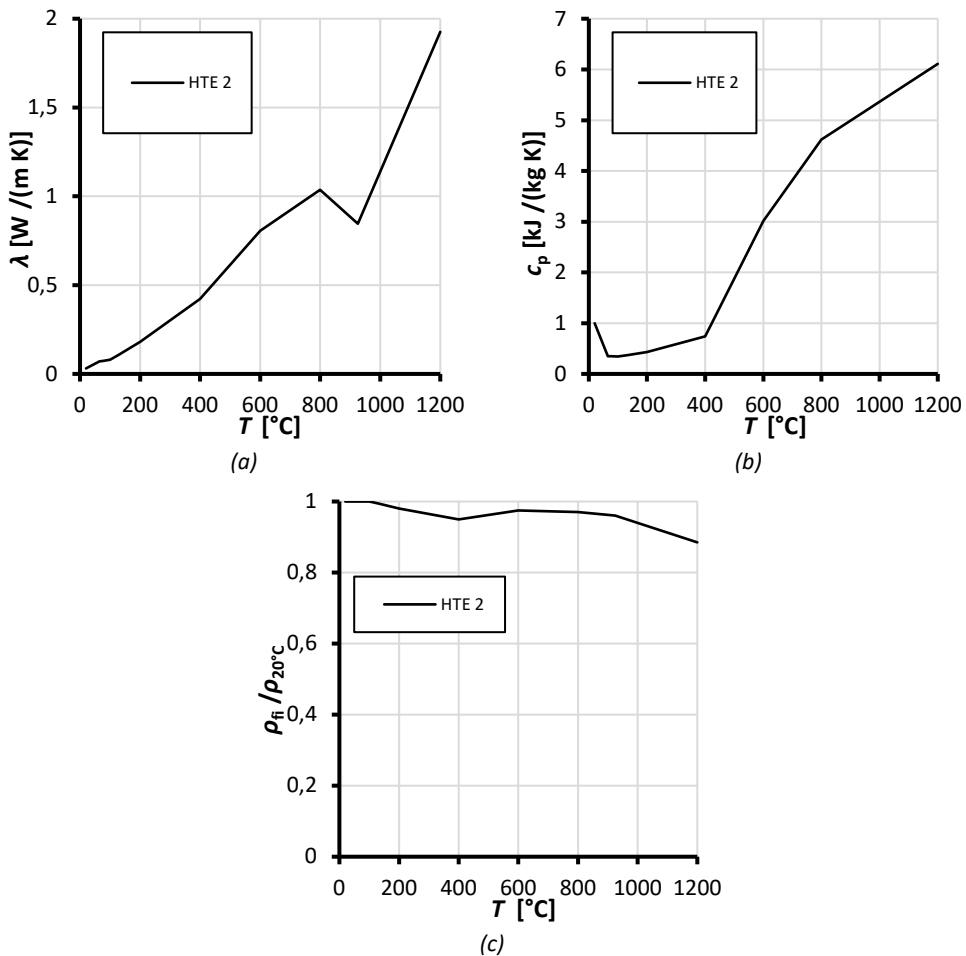


Figure 4-13. Effective thermal properties for HTE 2: (a) conductivity, (b) specific heat, and (c) loss in density as a function of the temperature.

#### 4.6.2 The results of the heat-transfer analysis

The position of the 300°C isotherm on the interface between wood and insulation ( $d_{300,s}$ ) as a function of the time was evaluated for the heat-transfer analysis that was carried out. The results are shown in Figure 4-14. In Configuration 1, the position of  $d_{300,s}$  was less than 100 mm at 60 minutes. In the Configuration 2 and Configuration 3, with a strip of insulation 150 mm wide, the position of  $d_{300,s}$  was less than 100 mm at 60 minutes. In Configuration 3, when the insulation strips are at 50 mm, 100 mm, and 120 mm wide, the 300°C isotherm on the interface between wood and insulation has reached a depth of 100 mm between 45 and 60 minutes.

By applying the criteria to evaluate the protection level being offered by a specific form of insulation in relation to Configuration 2, it is possible to observe that a cavity that has been insulated by two-thirds of its depth, with the insulation towards the fire-exposed side, can guarantee the same protection level for a cavity that has been fully insulated.

Regarding Configuration 3, in order to be able to guarantee PL 1, the insulation strip should be at least 150 mm wide.

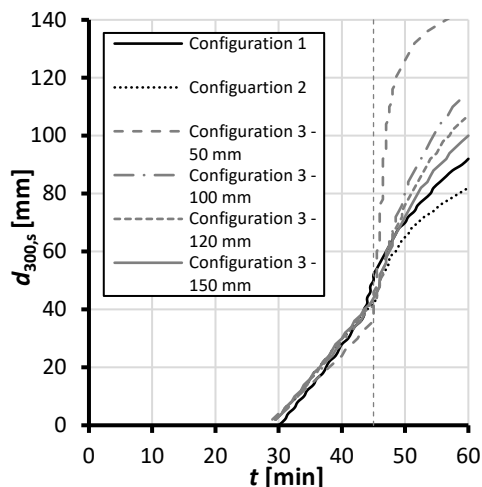


Figure 4-14. Position of the 300°C isotherm on the interface between wood and insulation ( $d_{300,s}$ ) as a function of the time evaluated by means of heat-transfer analysis.

#### 4.6.3 Design prescriptions for TFA with cavities partially filled

Based upon the results from the heat-transfer analyses which were carried out in this investigation, different strategies can be adopted to use the improved design model for TFA when the cavities are partially filled.

Design rules for TFA that is insulated with PL1 cavity insulations can be used when:

- strips of an insulation material qualified as PL 1 with a depth which is the same as the timber members and which are at least 150 mm wide are applied on the sides of the timber members,
- the cavities are filled with an insulation material qualified as PL 1 by two-thirds of the total depth of the cavity and the insulation is placed against cladding that has been exposed to fire.

Design rules for TFA that is insulated with PL 2 cavity insulations can be used when:

- strips of an insulation material qualified as PL 1 with a depth which is the same as the timber members and a width of between 50 and 150 mm are applied on the sides of the timber members.

Once the strips have been applied to the sides of the timber member, the rest of the cavity may be not filled, partially filled, or completely filled with a different form of insulation product.

#### 4.7 Validation of the heat-transfer analysis

In order to verify the heat-transfer analysis, the results in terms of (i) temperature, (ii) charring depths, and (iii) the mass properties of heat-transfer analyses are compared with experimental results.

In order to validate the heat-transfer analysis with TFA which has stone wool as its form of cavity insulation (Table 4-3), the reduction of the moment of inertia ( $I_t/I_{20^\circ\text{C}}$ ) as a function of the time that is evaluated by means of Simulation 3 was compared with cubic metre test results (see Figure 4-15). The reduction of the moment of inertia which was predicted by Simulation 3 is on the safe side with respect to the test results,

thereby determining that the heat-transfer analysis with adopted thermal properties is suitable for defining the factor  $k_{3,1}$ .

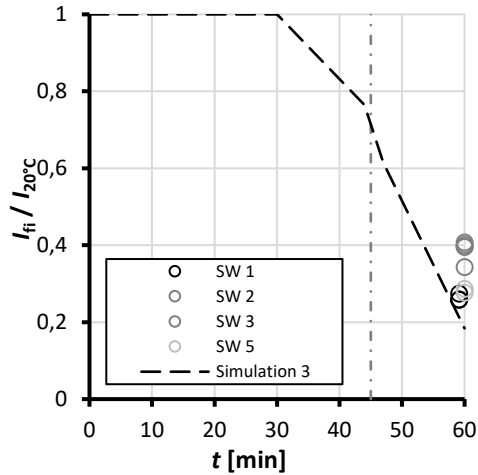
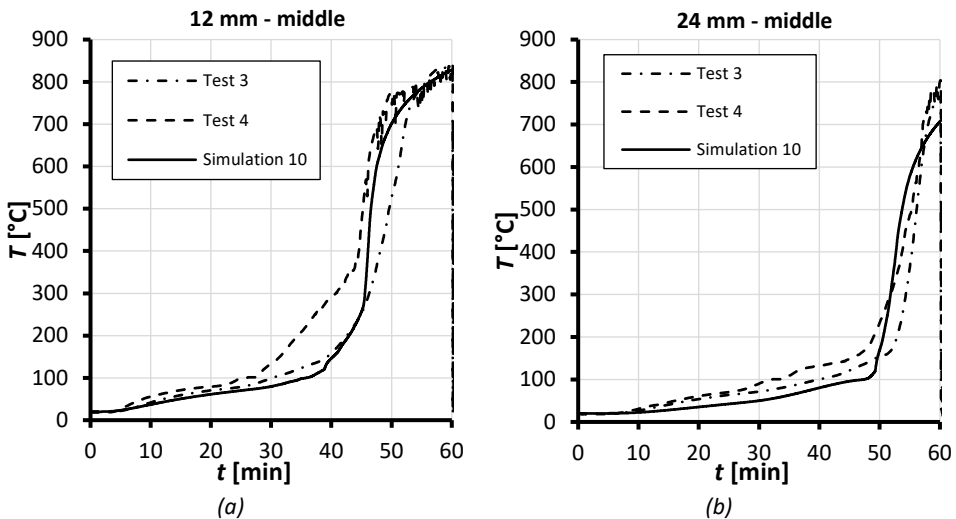


Figure 4-15. (a) Reduction of the moment of inertia as predicted by heat-transfer analysis compared to fire tests results.

In order to be able to validate the effective thermal properties that were calibrated for HTE 2, in Figure 4-16a and Figure 4-16b temperatures as a function of the time which resulted from Simulation 10 are compared to temperatures recorded in the middle of the cross-section (line 2 on Figure 3-2) at depths of 12 mm and 24 mm during Tests 3 and 4 (see test set-ups on Table 3-2). Those temperatures which resulted from the simulation and tests are also compared on the wood-insulation interface (lines 1 and 3 on Figure 3-2) at depths of 50 and 100 mm (Figure 4-16c and Figure 4-16d).



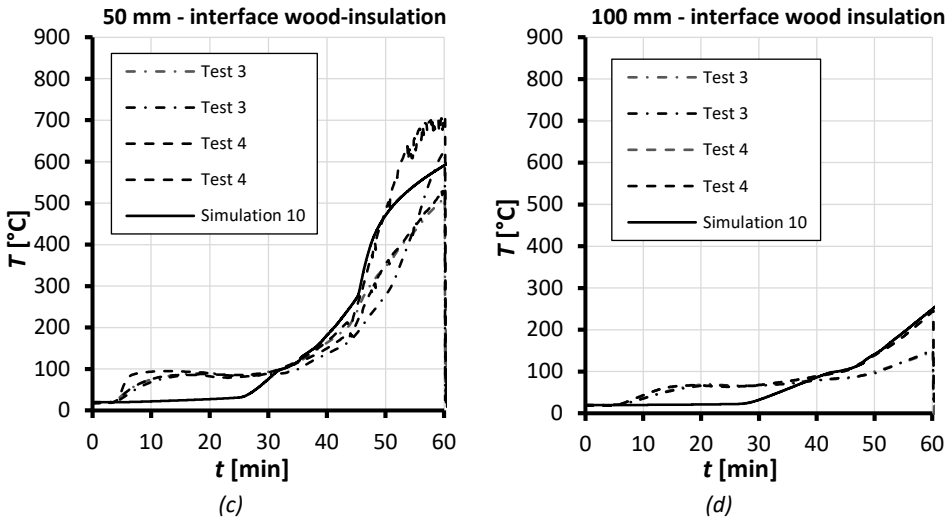


Figure 4-16. Temperatures recorded by thermocouples in comparison to simulation results at (a) a depth of 12 mm, and (b) a depth of 24 mm in the middle of the timber cross-section; at (c) a depth of 50 mm, and (d) a depth of 100 mm on the wood-insulation interface.

In Figure 4-17, the charring depth in the middle of the cross-section which was obtained as the position of the 300°C isotherm ( $d_{300,m}$ ) from thermocouple measurements in Test 3 and Test 4 (the dashed and dot-dash lines in Figure 4-17) is compared to the position of the 300°C isotherm ( $d_{300,m}$ ) which was obtained from the temperature output of Simulation 10 (the continuous line in Figure 4-17). The charring depth in the middle of the cross-section has been also measured from the residual cross-section at the end of the tests: the measurements for Test 3 and 4 are shown as markers in Figure 4-17.

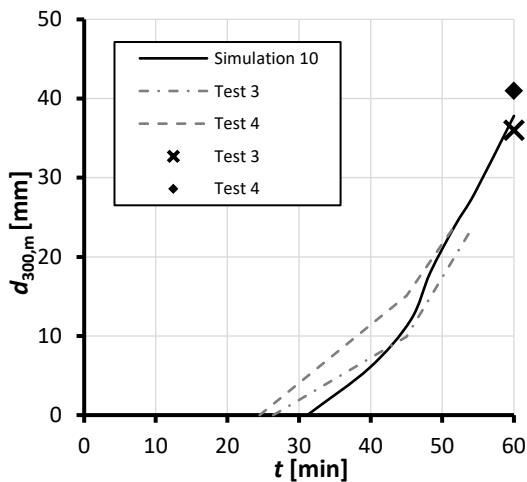


Figure 4-17. Position of the 300°C isotherm in the middle of the cross-section ( $d_{300,m}$ ) as a function of time for Test 3, Test 4, and Simulation 10.

## 5 Improved design model

### 5.1 The mechanical properties of uncharred timber members

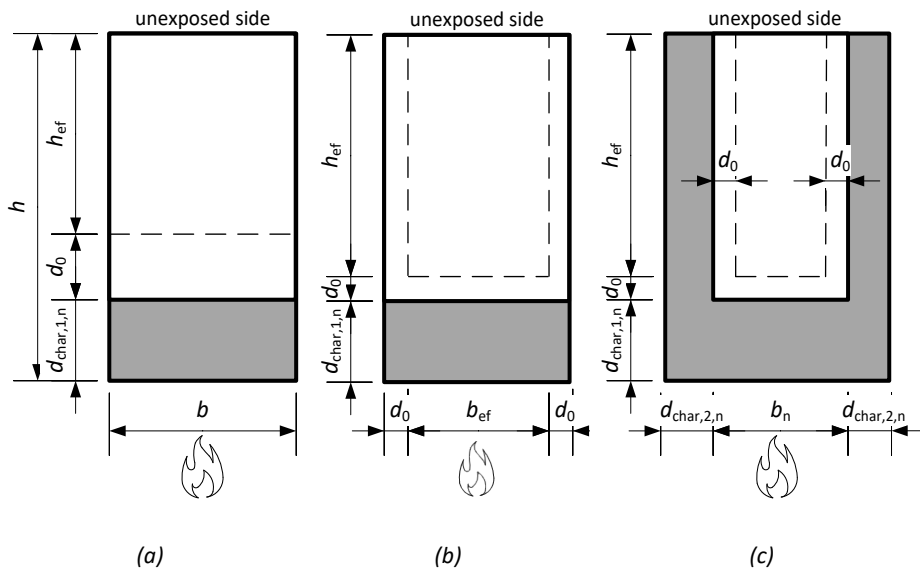
According to the effective cross-section method (ECSM), an effective charring depth can be calculated by increasing the notional charring depth with the addition of a zero-strength layer ( $d_0$ ):

$$d_{ef} = d_{char,n} + d_0 \quad (34)$$

where  $d_{ef}$  is the effective charring depth,  $d_{char,n}$  is the notional charring depth, and  $d_0$  is the zero-strength layer's depth.

The effective cross-section permits the load-bearing capacity of timber members to be predicted when under fire conditions using the strength and stiffness properties at ambient temperature.

In the case of TFA with cavity insulations qualified as PL 1, charring of the timber member is considered on one side. Thus, it is proposed that the zero-strength layer also be applied on the fire-exposed side (see Figure 5-1a) during the total time in which fire exposure is maintained.



KEY:  $h$  - initial depth of the timber member;  $b$  - initial width of the member;  $h_n$  - notional depth of the member;  $b_n$  - notional width of the member;  $h_{ef}$  - effective depth of the member;  $b_{ef}$  - effective width of the member;  $d_{char,1,n}$  - charring from the fire-exposed side;  $d_{char,2,n}$  - charring from the lateral sides;  $d_0$  - zero-strength layer.

Figure 5-1. Zero-strength layers in the improved design model for TFA with (a) PL1 cavity insulation; with PL2 cavity insulation (b) before, and (c) after that start time of charring from lateral sides has occurred.

For TFA with PL 2 cavity insulations, the charring of the timber member is considered on the fire-exposed side during the protection phase whilst, during the post-protection phase, charring on the lateral sides can occur. For the sake of simplicity, zero-strength layers can be subtracted from three sides (as shown in Figure 5-1b Figure 5-1c) during the total time in which fire exposure is maintained.

In order to determine the depths of the zero-strength layer for TFA with different forms of cavity insulation product and for different load conditions, the load-bearing capacities of timber members in TFA were predicted using thermo-mechanical simulations. For this purpose, a two-step process was adopted:

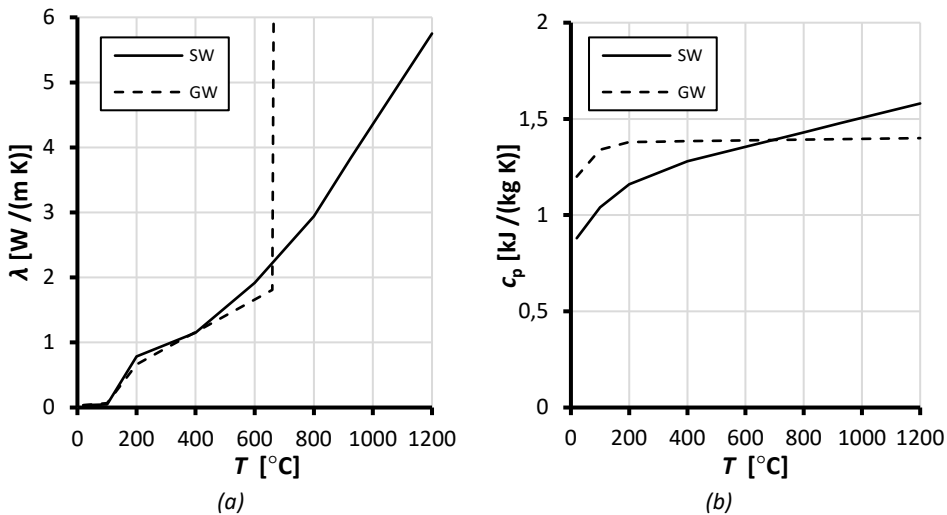
1. Temperature distributions within the cross-section were obtained by means of a two-dimensional heat-transfer analysis which was implemented in SAFIR (Franssen, 2005),
2. The load-bearing capacity with a temperature-dependent reduction in strength and stiffness was calculated with CSTfire (Schmid and König, 2010).

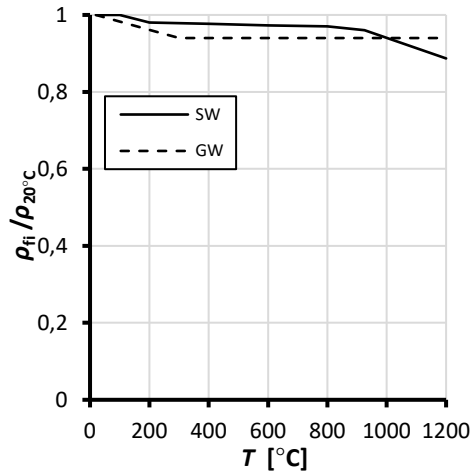
The outputs of the thermo-mechanical simulations were used to calculate the corresponding zero-strength layer depths for different TFA assemblies. The different steps are described in detail below.

### 5.1.1 Heat-transfer analysis

In order to investigate the temperature distribution within the cross-section, two-dimensional models were implemented in the SAFIR software package with the same schematics as described in Figure 4-9.

Three different insulation products were considered for use as cavity insulation: SW, GW, and HTE 2. Thermal exposure, and the thermal properties of timber, gypsum plasterboard, and SW insulations are the same as described in Section 4.5, the while thermal properties of HTE 2 are shown in Figure 4-13. For the GW, the effective thermal properties which were proposed by Schleifer (2009) were adopted. The heat-transfer calculations used 90 minutes as the time for fire exposure.





(c)

Figure 5-2. Effective thermal properties of SW and GW according to Schleifer (2009): (a) conductivity, (b) specific heat, and (c) loss in density as a function of the temperature.

### 5.1.2 Mechanical analysis

For the structural analysis of the timber member, CSTFire was used (Schmid and König, 2010). CSTFire is a Visual Basic macro which is embedded in Excel, having been developed at the RISE Research Institutes of Sweden. This program is capable of calculating the bending moment capacities of timber members that have been exposed to fire. The calculations are carried out by means of an iterative process.

The program (i) takes the temperature distribution of the timber cross-sections from the heat-transfer analysis, (ii) assigns strength and stiffness reductions which are dependent upon temperature, (iii) calculates the geometrical properties of the residual cross-section, (iv) determines the curvatures ( $\kappa_{fi}$ ) and also the related bending moment capacities ( $M_{fi}$ ) over the time at which fire exposure lasts.

The bending moment capacities ( $M_{fi}$ ) are calculated by assuming that plane sections remain plane sections. For a given curvature ( $\kappa_{fi}$ ), the strain distribution is defined within the entire cross-section. Based upon the strain distribution, the stress distribution is calculated using a material model which is represented by a stress-strain relationship. Once the stress distribution is specified, the moment ( $M_{fi}$ ) can be determined by integrating the stresses over the cross-section.

The material behaviour of timber different when it is subjected to compression or tension that is parallel to the grain. To take into account the non-linear material behaviour of timber in compression parallel to the grain, a bilinear elastic-plastic stress-strain relationship (Neely, 1898) (Figure 2-6b) was considered. The reduction of strength and solidity in tension and compression were assumed according to Eurocode 5 Part 1-2 (Figure 2-6a).

### 5.1.3 Simulation programme

Different cross-section dimensions and forms of cladding were investigated. Cross-section dimensions were chosen as the most common dimensions present in the European market. The set-ups are summarised in Table 5-1. The type of cladding that was considered are also given, corresponding to the different cross-section dimensions.

Table 5-1. Cladding on the fire-exposed side of the set-ups being investigated.

		Initial depth of cross-section			
		<i>h</i> = 95 mm	<i>h</i> = 145 mm	<i>h</i> = 195 mm	<i>h</i> = 295 mm
Initial width of cross-section	<i>b</i> = 45 mm	-	GtF 15 mm	GtF 15 mm	GtF 15 mm
	<i>b</i> = 60 mm	GtF 15 mm	GtF 15 mm	GtF 20 mm	GtF 20 mm
	<i>b</i> = 75 mm	-	GtF 15 mm	GtF 20 mm	GtF 20 mm
	<i>b</i> = 90 mm	GtF 15 mm	GtF 15 mm	GtF 20 mm	GtF 20 mm
	<i>b</i> = 120 mm	GtF 15 mm	GtF 15 mm	GtF 20 mm	GtF 20 mm

KEY: GtF – Gypsum Plasterboard Type F

For each set-up, at least two different fall-off times ( $t_f$ ) of the claddings were considered. For 15 mm-thick gypsum plasterboard as the form of cladding, falling off times of 25 and 43 minutes were considered. For 20 mm-thick gypsum plasterboard, falling off times of 26 and 53 minutes were considered. The fall-off times were selected according to the fall-off times for gypsum plasterboards in floor and wall positions which were proposed by Just (2010b) and which were also adopted in the FSITB guideline (B. Östman et al., 2010).

The cross-sections of members which had been subjected to bending are subjected to both compression and tensile stresses. For each investigated set-up, both the fire exposure which affected the tension side and, in a different analysis, the compression side of the cross-section were considered. In the currently available literature (König and Schmid, 2010), the tension side of the cross-section which had been exposed to fire is referred to as ‘tension-side warm’ (TSW), and the compression side of the cross-section that had been exposed to fire is referred to as ‘compression-side warm’ (CSW).

For each form of insulation material, at least 72 different simulations were carried out. In order to further investigate the influence of the cladding on the zero-strength layer, four additional set-ups were simulated with cross-section dimension of 45 × 145 mm and which were insulated with HTE 2. For a falling off time of 43 minutes, gypsum plasterboard as a form of cladding was also investigated at thicknesses of 12.5 mm and 20 mm. Two other additional falling off times were studied at zero minutes and 90 minutes. These two cases correspond to cases involving the post-protection phase alone and protection phase alone, respectively, during the entire fire exposure period.

Table 5-2. Additional set-ups which were investigated for TFA that was insulated with HTE 2.

Cross-section dimensions [mm]	Cavity insulations	Thickness of gypsum plasterboard as cladding [mm]	Fall-off time of cladding [min]
45 × 145	HTE 2	-	0
45 × 145	HTE 2	15	90
45 × 145	HTE 2	12.5	43
45 × 145	HTE 2	20	43

The results for several thermo-mechanical simulations are shown in Figure 5-3.

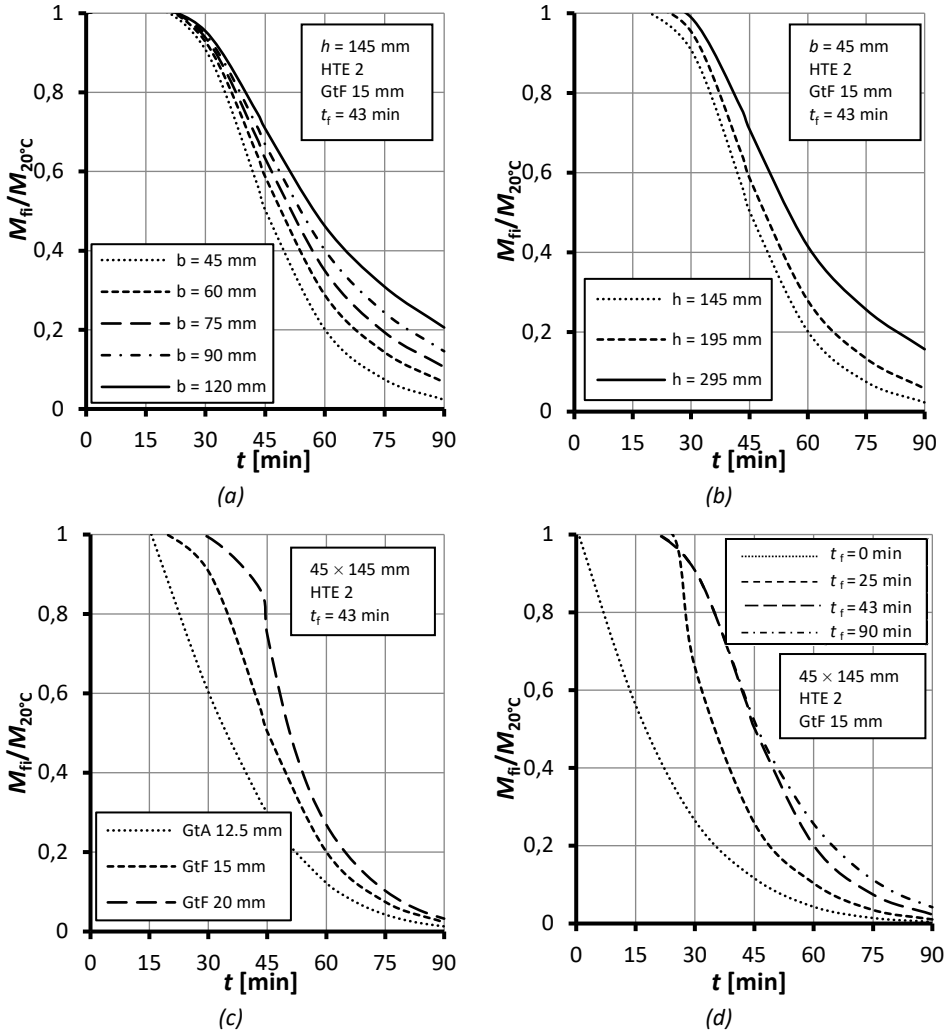


Figure 5-3. Reduction of the bending moment capacity ( $M_{fi}/M_{20^{\circ}\text{C}}$ ) against the time for FFA with HTE 2 as a form of cavity insulation. A comparison of different (a) timber widths, (b) timber depths, (c) cladding types, and (d) fall-off times of the cladding.

#### 5.1.4 Evaluation of zero-strength layer depths for bending members

In order to determine the depth of the zero-strength layer ( $d_0$ ) for a member subjected to bending (e.g. a floor element), the bending capacity of the heated cross-section was taken to be equal to the bending capacity of an effective cross-section with the same strength and stiffness properties that the timber would have at ambient temperature. For TFA which was insulated with a form of cavity insulation qualified as PL1, the bending capacity during a fire is as follows:

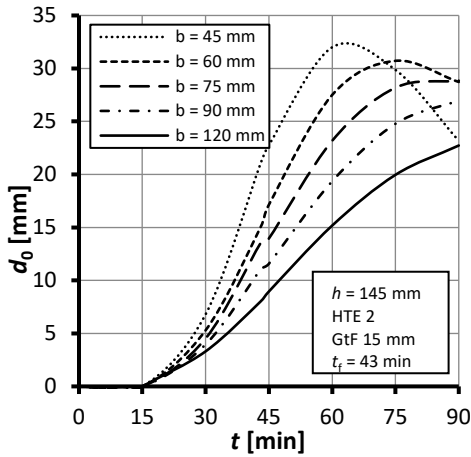
$$M_{fi} = W_{ef} f_{m,20^{\circ}\text{C}} = \frac{(h_n - d_0)^2 b}{6} f_{m,20^{\circ}\text{C}} \quad (35)$$

where:  $W_{ef}$  is the section modulus of the effective cross-section;  $f_{m,20^{\circ}\text{C}}$  is the bending strength at ambient temperature;  $h_n$  is the notional depth of the cross-section; and  $b$  is the initial width of the cross-section.

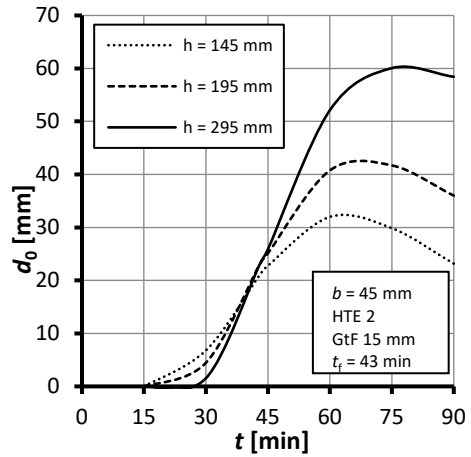
The depth of the zero-strength layer for a timber member which is subjected to bending is derived as:

$$d_0 = h_n - \sqrt{\frac{6 M_{fi}}{b \cdot f_{m,20^\circ\text{C}}}} \quad (36)$$

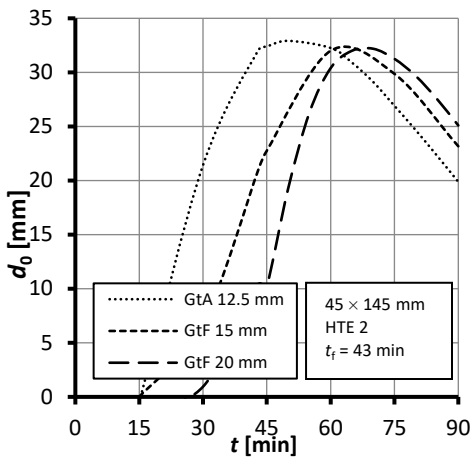
The depths of zero-strength layers have been calculated for each simulation to be carried out. The results are compared for (i) different member widths, (ii) different member depths, (iii) different thicknesses of gypsum plasterboard, (iv) different fall-off times of the cladding and (v) different forms of cavity insulation (Figure 5-4).



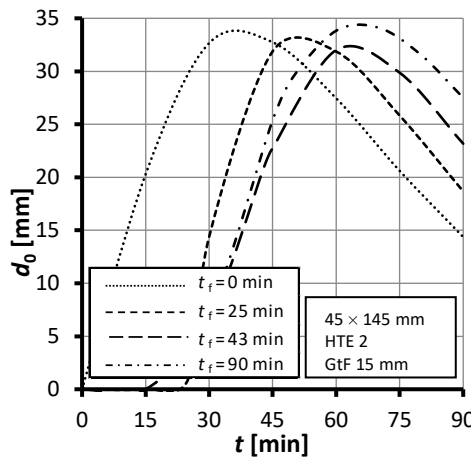
(a)



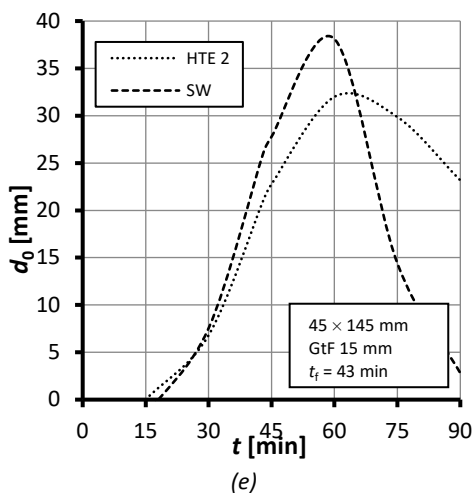
(b)



(c)



(d)



KEY:  $b$  – initial width of the timber member;  $h$  – initial depth of the member; GtA – gypsum plasterboard Type A; GtF – gypsum plasterboard Type F; HTE – high temperature extruded mineral wool; SW – stone wool.

Figure 5-4. Depth of the zero-strength layer for members which are bending for (a) different member width, and (b) depth, (c) different thickness of gypsum plasterboard, (d) different fall-off times of the cladding and (e) different forms of cavity insulation.

It can be seen that the maximum value of  $d_0$  for different member widths and member depths is itself different, because the different curves peak at different values of  $d_0$ . The maximum values of  $d_0$  over the fire exposure time increase for narrow and deeper timber members. The maximum value of  $d_0$  is also different for TFA with different forms of cavity insulation. Vice versa, the comparison shows that there is no significant difference in the maximum value of  $d_0$  for different thicknesses of gypsum plasterboard and fall-off times ( $t_f$ ).

For TFA with PL2 and PL3 cavity insulation, where the zero-strength layer has to be taken into account from three sides, the bending capacity is as follows:

$$M_{fi} = W_{ef} f_{m,20^\circ\text{C}} = \frac{(h_n - d_0)^2 \cdot (b_n - 2 d_0)}{6} f_{m,20^\circ\text{C}} \quad (37)$$

where:  $b_n$  is the notional width of the cross-section.

In this case, the depth of the zero-strength layer is derived by solving Equation (37) by means of an iterative method for non-linear equations.

### 5.1.5 An evaluation of zero-strength layer depths for compression members

Buckling is usually the relevant failure mode for axially-loaded compression members. For timber frame wall assemblies, out-of-plane buckling or in-plane buckling of load-bearing studs may occur. In general, the buckling resistance of a member ( $N_{cr}$ ) under fire conditions is as follows:

$$N_{cr} = \frac{\pi^2 (EI)_{fi}}{l_{cr}^2} \quad (38)$$

where:  $(EI)_{fi}$  is the solidity of a member which is exposed to fire-related conditions, and  $l_{cr}$  is the effective buckling length of a member.

The stiffness of a member under fire conditions can be evaluated from CSTFire as:

$$(EI)_{fi} = \frac{M_{fi}}{\kappa_{fi}} \quad (39)$$

where:  $\kappa_{fi}$  is the curvature of a member under fire conditions.

Zero-strength layers for TFA members which are subject to buckling were evaluated by comparing buckling resistance with an effective cross-section at ambient temperature:

$$N_{cr} = \frac{\pi^2 E_{20^\circ C} I_{ef}}{l_{cr}^2} \quad (40)$$

where:  $E_{20^\circ C}$  is the characteristic modulus of elasticity at ambient temperature;  $I_{ef}$  is the moment of inertia of the effective cross-section.

For TFA which is insulated with a form of cavity insulation qualified as PL1, the moment of inertia for the cross-section for out-of-plane buckling can be calculated as:

$$I_{ef} = \frac{(h_n - d_0)^3 b}{12} \quad (41)$$

And for in-plane buckling as:

$$I_{ef} = \frac{(h_n - d_0) b^3}{12} \quad (42)$$

By combining Equations (38), (40), and (41), it is possible to derive the equation which is required to calculate the zero-strength layer depths for out-of-plane buckling elements:

$$d_0 = h_n \left( 1 - \sqrt[3]{\frac{E_{fi}}{E_{20^\circ C}}} \right) \quad (43)$$

where:  $E_{fi}$  is the modulus of elasticity of the member under fire conditions.

In the same way, when combining Equations (38), (40), and (42), the expression to calculate the zero-strength layer for in-plane buckling is derived:

$$d_0 = h_n \left( 1 - \frac{E_{fi}}{E_{20^\circ C}} \right) \quad (44)$$

In the case of TFA which is insulated with a form of cavity insulation qualified as PL2, the moment of inertia for the cross-section for out-of-plane buckling can be calculated as:

$$I_{ef} = \frac{(h_n - d_0)^3 (b_n - 2 d_0)}{12} \quad (45)$$

And for in-plane buckling as:

$$I_{ef} = \frac{(h_n - d_0) (b_n - 2 d_0)^3}{12} \quad (46)$$

In this case, the depths of the zero-strength layer for out-of-plane and in-plane buckling are calculated by combining Equations (38), (40), and (45) and also Equations (38), (40), and (46) respectively. The resulting non-linear equations are solved by means of an iterative method.

### 5.1.6 A simplified approach to determine zero-strength layer depths

The depths of zero-strength layers in terms of compression and bending were calculated for timber frame assemblies that had been insulated with HTE 2, SW, and GW (see an example in Figure 5-5). In Section 5.1.4, the results of zero-strength layer depths as a function of the time were compared for the different fall-off times of the cladding (Figure 5-4d). The comparison showed that there is no significant difference in the maximum value of  $d_0$  for the different fall-off times, as the different curves peak at

a similar value of  $d_0$ . Furthermore, it was pointed out that the only difference between assemblies that were unprotected ( $t_f = 0$  in Figure 5-4d) and those which were protected for ninety minutes ( $t_f = 90$  in Figure 5-4d) is the time at which the maximum value  $d_0$  occurred.

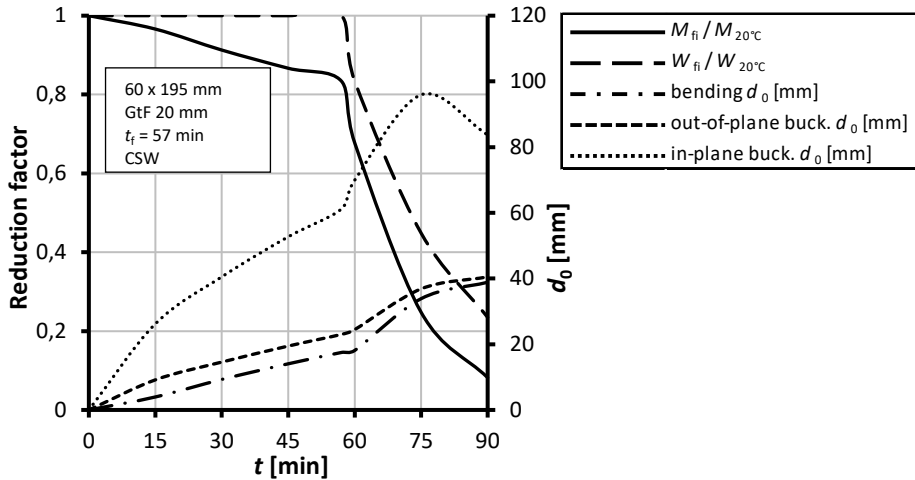


Figure 5-5. Bending moment capacity reduction, section modulus reduction, and the depth of zero-strength layers as a function of the time for an assembly that is insulated with stone wool.

In order to provide a simple approach for the designer, it is reasonable to assume the depth of the zero-strength layer as being independent of time. By means of multi-regression analyses, factors which may serve to influence the zero-strength layers were determined.

For timber frame assemblies which are insulated with stone wool (SW), the following expressions are proposed on the basis of the simulations being presented:

- bending members with the fire-exposed side in tension:

$$d_0 = 9 + 0.25 h - 0.18 b \quad (47)$$

- bending members with the fire-exposed side in compression:

$$d_0 = 27.9 + 0.14 h - 0.26 b \quad (48)$$

- out-of-plane buckling of compression members:

$$d_0 = 29.1 + 0.16 h - 0.26 b \quad (49)$$

- in-plane buckling of compression members:

$$d_0 = 43.6 + 0.43 h - 0.37 b \quad (50)$$

For timber frame assemblies which are insulated with HTE 2, the following expressions are proposed:

- bending members with the fire-exposed side in tension:

$$d_0 = 18.6 + 0.17 h - 0.18 b \quad (51)$$

- bending members with the fire-exposed side in compression:

$$d_0 = 27.9 + 0.14 h - 0.28 b \quad (52)$$

- out-of-plane buckling of compression members:

$$d_0 = 25.5 + 0.17 h - 0.26 b \quad (53)$$

- in-plane buckling of compression members:

$$d_0 = 36.4 + 0.45 h - 0.37 b \quad (54)$$

For assemblies where the cavities are filled with glass wool insulation, the zero-strength layer has to be considered from three sides (see Figure 5-1b and Figure 5-1c), with the following expressions being proposed:

- bending members with the fire-exposed side in tension:

$$d_0 = 2.8 + 0.02 h + 0.01 b \quad (55)$$

- bending members with the fire-exposed side in compression:

$$d_0 = 3.2 + 0.03 h + 0.01 b \quad (56)$$

- out-of-plane buckling of compression members:

$$d_0 = 3.7 + 0.06 h + 0.01 b \quad (57)$$

- in-plane buckling of compression members:

$$d_0 = 3.5 + 0.03 h + 0.01 b \quad (58)$$

Figure 5-6 shows zero-strength layer depths as predicted by the proposed equations being plotted against the peak values which were calculated by means of thermo-mechanical simulations. The comparison shows that the proposed equations provide a good prediction of the peak values for zero-strength layers.

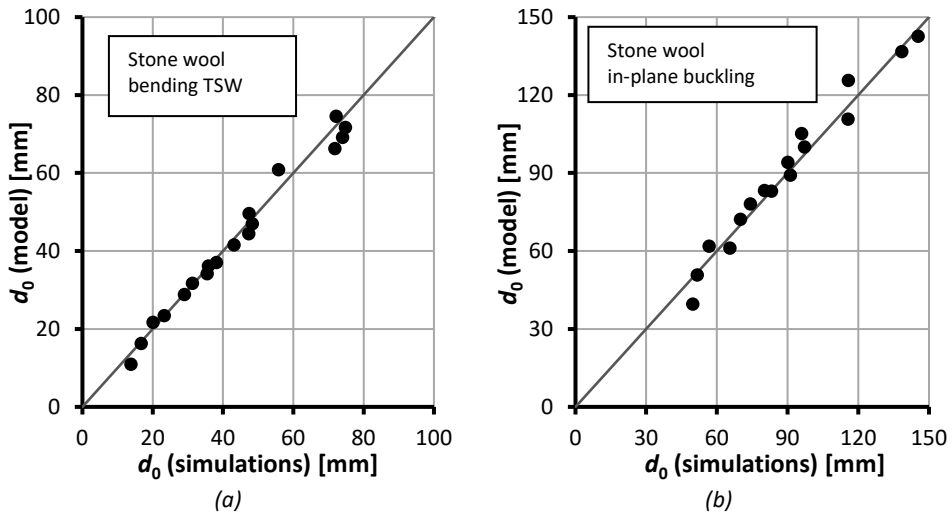


Figure 5-6. Zero-strength layers calculated by means of numerical simulations compared to the models proposed for assemblies that have been insulated with stone wool. A comparison for (a) bending members with the tension side that has been exposed to fire, and (b) compression members with in-plane buckling.

### 5.1.7 Members with an imperfection which are subjected to axial compression and bending

The behaviour of timber members which are subjected to combined axial compression and bending is characterised by a non-linear increase of the deformation due to the increasing eccentricity of the axial load (the P-delta effect), and due to the non-linear

behaviour of the material. Theiler et al. (2013) have assessed the buckling behaviour of timber members which are subjected to combined axial compression and bending at ambient temperature by means of a strain-based model. This model considers the equilibrium between the acting external forces and the resulting internal forces.

The approach proposed by Theiler et al. (2013) is a generalised 2<sup>nd</sup> order structural analysis which is capable of taking into account both the geometric non-linearity and the non-linearity due to the change in member stiffness with an increasing load.

The strain-based model consists of two parts. As a first step the internal force and moment are regarded. For a given cross-section and a given strain distribution, the resulting internal force and moment are calculated, assuming that plane sections remain plane.

In the second step, the deformation of the member is accounted for. The deformation of a member depends upon the curvature and on the distribution of the curvature along the member. The curvature can be calculated as the 2<sup>nd</sup> derivation of the deformation curve. Hence, the maximum deformation due to P-delta effects can be written as:

$$e_{II} = \iint \kappa(x) dx^2 = \kappa \frac{l_{cr}^2}{c} \quad (59)$$

where  $e_{II}$  is the maximum deformation due to the P-delta effects;  $\kappa(x)$  is the curvature along the member;  $\kappa$  is the curvature at the mid-length of the member;  $l_{cr}$  is the effective buckling length, and  $c$  is an integration constant. The integration constant  $c$  depends upon the shape of the deformations. For a simply-supported column with sinusoidal distributed deformations, the constant  $c$  is equal to  $\pi^2$ .

Theiler et al. (2013) derived the external bending moment as being dependant upon the external force  $N_e$  and the curvature  $\kappa$ :

$$M_e = N_e (e_0 + e_1 + e_{II}) = N_e \left( e_0 + e_1 + \kappa \frac{l_{cr}^2}{\pi^2} \right) \quad (60)$$

where  $M_e$  is the acting external bending moment;  $N_e$  is the acting external force (compression);  $e_0$  is the initial deformation of the member;  $e_1$  is the eccentricity of the external force;  $e_{II}$  is the maximum deformation due to the P-delta effects;  $\kappa$  is the curvature at the mid-length of the member; and  $l_{cr}$  is the effective buckling length.

Second order effects upon members were investigated where there was an initial deformation which was subjected to compression and an external moment which corresponded to 10% of the bending moment capacity of the element at ambient temperature. In addition, second order effects upon members were investigated where the members were in compression with only an initial deformation. It was possible to derive the compression force that causes the buckling of a member (with this hereinafter being referred to as  $N_{cr,II}$ ), with an initial deformation and being subjected to bending by solving the following equation:

$$M_{fi} = N_{cr,II} \left( e_0 + \frac{x M_{20^\circ C}}{N_{cr,II}} + \kappa_{fi} \frac{l_{cr}^2}{\pi^2} \right) \quad (61)$$

where  $M_{fi}$  is the bending moment capacity under fire conditions,  $M_{20^\circ C}$  is the bending moment capacity at ambient temperature,  $x$  is the percentage of the ultimate bending moment capacity at the ambient temperature that is applied (0% and 10% were considered),  $\kappa_{fi}$  is the curvature under fire conditions, and  $e_0$  is the initial deformation of the member.

Eurocode 5 Part 1-1 (CEN, European Committee for Standardization, 2004a) provides rules for any consideration of an initial deformation for members in plane frames. When applying these rules to an element of 3000 mm length, the initial deformation which resulted equalled 7.5 mm. The value of  $N_{cr,II}$  against the fire exposure time was calculated for two different set-ups involving TFA with different external bending moments being applied. The results in terms of a reduction of  $N_{cr,II}$  as a function of the fire exposure time are plotted in Figure 5-7. On the same graphs, the corresponding reduction of the load-bearing capacity was plotted for members subjected to out-of-plane buckling that had been evaluated according to the improved design model.

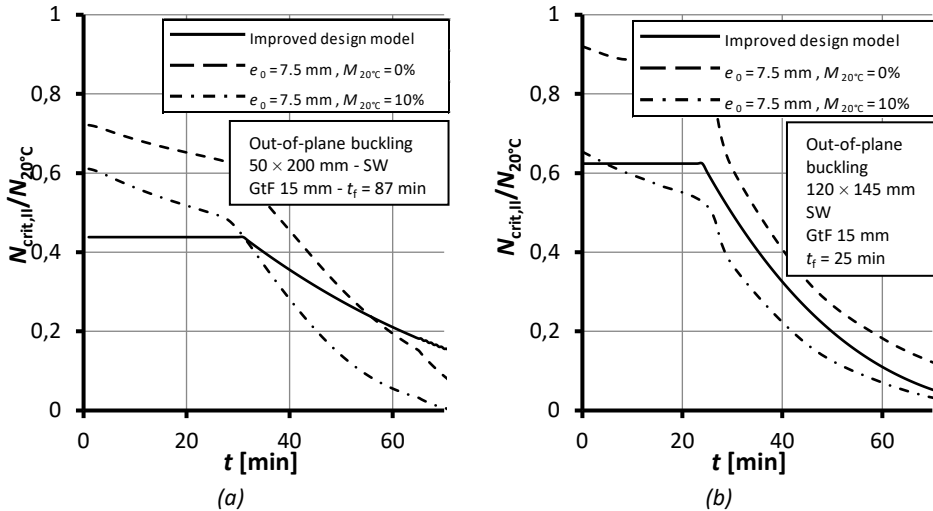


Figure 5-7. Reduction of the load-bearing capacity for out-of-plane buckling ( $N_{crit,II}/N_{20^{\circ}C}$ ) as predicted by the improved design model when compared to the critical normal force of members with an initial deformation that is subjected to combined axial compression and bending.

In both cases, the reduction of  $N_{cr,II}$  for the member that was subjected to compression and an external bending moment (the dot-dash-dot lines in Figure 5-7) falls below the reduction of the load-bearing capacity for out-of-plane buckling as predicted by the improved design model (the continuous lines in Figure 5-7). The reduction of  $N_{cr,II}$  for the member which had an initial deformation and which was subjected to compression only (the dot-dash-dot lines in Figure 5-7) stands above the prediction for the improved design model. Therefore the improved design model can still be used to predict the load-bearing capacity for members with an initial deformation as prescribed in Eurocode 5 Part 1-1. For members with an initial deformation and which are being subjected to compression and an external bending moment, the prediction for out-of-plane buckling according to the improved design model leads to non-conservative results. To provide rules which will allow a consideration of the load-bearing capacity of members which are being subjected to combined axial compression and bending, further studies will have to be carried out.

### 5.1.8 An optimised approach for determining zero-strength layer depths

As can be observed in Figure 5-4, the zero-strength layer's depth increases with the fire exposure time until it reaches a peak and then starts to decrease. The simplified approach for determining the depth of the zero-strength layer can only predict the

peak value. The adoption of the peak value during the entire fire exposure time is a simplified approach; however, it leads to a conservative predation of the load-bearing capacity. To avoid predictions that are too conservative, an approach is proposed which will permit the optimised zero strength layer's depth to be evaluated, as follows.

The time at which the zero-strength layer's depth reaches its peak ( $t_{\text{peak}}$ ) may depend upon the type of cladding being applied on the fire-exposed side, the fall-off time of the cladding, and also on the cross-section dimensions of the timber member (see Figure 5-4). Expressions were determined to evaluate the time at which the zero-strength layer's depth peaks ( $t_{\text{peak}}$ ), for TFA with cavities which are filled with SW, by means of multi-regression analyses:

- bending members with the fire-exposed side in tension:

$$t_{\text{peak}} = 0.06 h + 0.28 b + 0.89 t_{\text{ch}} + 0.36 t_{\text{f}} - 5.1 \quad (62)$$

- bending members with the fire-exposed side in compression:

$$t_{\text{peak}} = 0.09 h + 0.1 b + 1.63 t_{\text{ch}} + 0.11 t_{\text{f}} - 21.4 \quad (63)$$

- out-of-plane buckling of compression members:

$$t_{\text{peak}} = 0.12 h + 0.08 b + 1.51 t_{\text{ch}} + 0.05 t_{\text{f}} - 25.3 \quad (64)$$

- in-plane buckling of compression members:

$$t_{\text{peak}} = 0.13 h + 0.15 b + 0.82 t_{\text{ch}} + 0.23 t_{\text{f}} - 20.5 \quad (65)$$

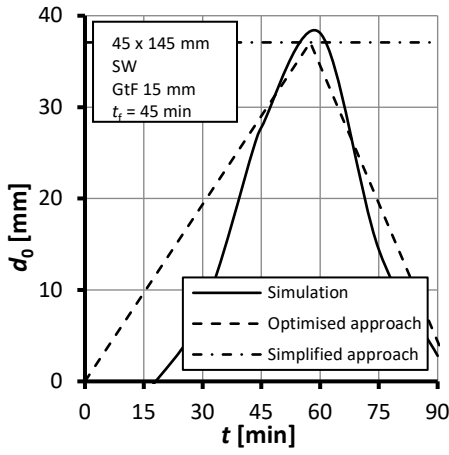
where  $h$  is the initial depth of the timber member as expressed in millimetres,  $b$  is the initial width of the timber member as expressed in millimetres,  $t_{\text{ch}}$  is the start time of charring on the fire-exposed-side as expressed in minutes, and  $t_{\text{f}}$  is the fall-off time of the cladding as expressed in minutes.

It can be assumed that  $d_0$  is equal to 0 millimetres at  $t$  equal to 0 minutes. Then  $d_0$  increases linearly until it reaches the peak value, which is evaluated according to Equations (47), (48), (49), and (50), at  $t_{\text{peak}}$  and with, finally,  $d_0$  decreasing linearly until it again reaches a value that is equal to 0 millimetres. The time at which  $d_0$  is equal to 0 millimetres after it has reached its peak can be assumed as the time at which  $d_{\text{char},1,n}$  is equal to  $h$ . This can be evaluated as:

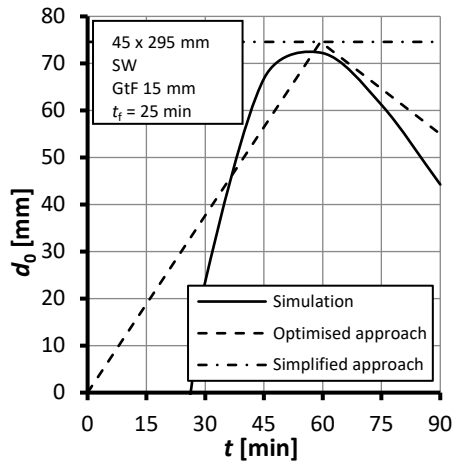
$$t (d_0 = 0) = t (d_{\text{char},1,n} = h) = t_{\text{f}} + \frac{1}{k_{3,1}} \left[ \frac{h}{\beta_0 k_{s,n}} - k_2 (t_{\text{f}} - t_{\text{ch}}) \right] \quad (66)$$

where  $h$  is the initial depth of the timber member;  $\beta_0$  is the basic design charring rate;  $k_{s,n}$  is the cross-section factor;  $k_2$  and  $k_{3,1}$  are the protection factors for the charring along the fire-exposed side in the protection and post-protection phases respectively;  $t_{\text{ch}}$  is the start time of charring on the fire-exposed side; and  $t_{\text{f}}$  is the fall-off time of the cladding.

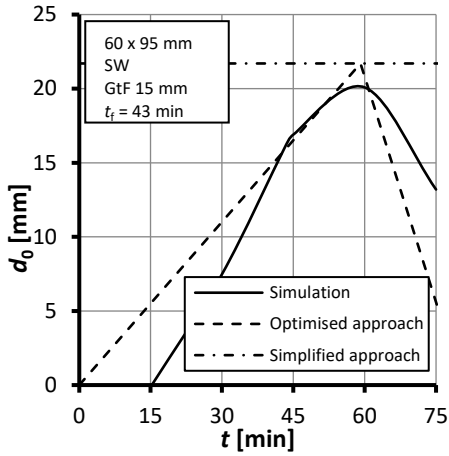
By evaluating the peak value of the zero-strength layer depth, the time at which the peak is reached, and then the time at which the zero-strength layer depth has decreased to a value of zero, it is possible to identify a bi-linear function of  $d_0$  against the time. By using this bi-linear function, it is possible to optimise the prediction of the load-bearing capacity of TFA that has been exposed to fire. An example of the zero-strength layer's depths which have been evaluated by means of thermo-mechanical simulations when compared to the bi-linear function is shown in Figure 5-8.



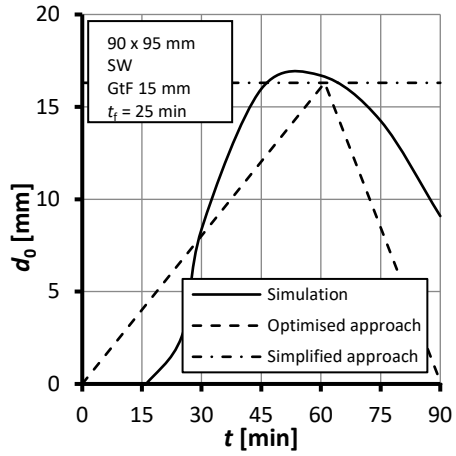
(a)



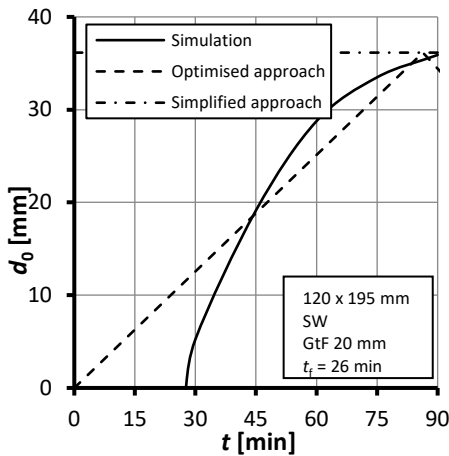
(b)



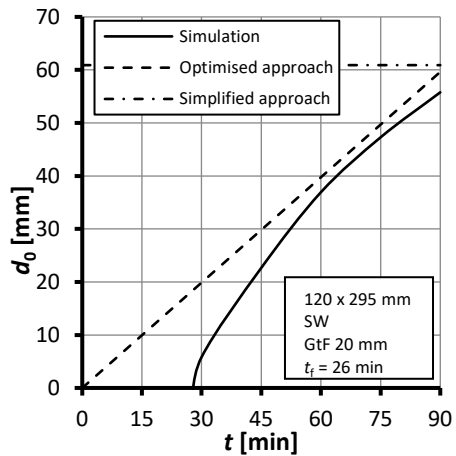
(c)



(d)



(e)



(f)

Figure 5-8. The depth of the zero-strength layer as evaluated by means of thermo-mechanical simulations and being compared to the simplified and optimised approaches.

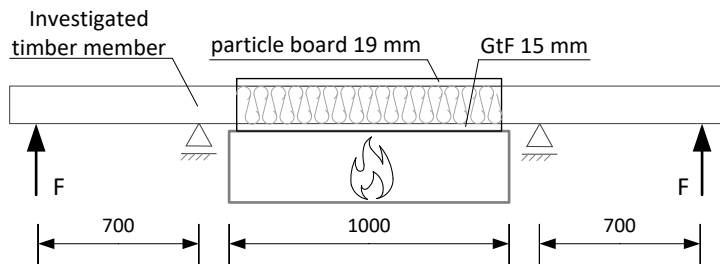
### 5.1.9 Loaded cubic metre furnace tests

Three loaded cubic metre furnace tests were carried out to provide a benchmark for the thermo-mechanical simulations. Specimens as a section of a floor (as shown in Figure 3-2a) were composed of a wooden frame and a load-bearing timber member, with gypsum plasterboard cladding being tested on this assembly. Three different insulation products were inserted into three different specimens: HTE 2, SW 3, and SW 5 (see Table 3-1 for the characteristics of the insulation products). A solid timber member (with cross-section dimensions of 50 × 200 mm) as the load-bearing member was present in the middle of the frame. In addition for these specimens, particle board with a depth of 19 mm was placed on the unexposed side. In order to avoid any increase in the of stiffness of the specimen (the composite effect formed with the load-bearing timber member), the particle board was placed on the unexposed side in 200 mm-wide ribbons. The load-bearing timber member (with cross-section dimensions of 50 × 200 mm) was loaded with four-point bending (see Figure 5-9), with the tension side having been exposed to fire. The exposed side of the assembly was protected by a 15 mm-thick gypsum plasterboard (Type F) which was held in place with screws. Prior to the test, the modulus of elasticity ( $E$ ) and the bending strength at ambient temperature for the load-bearing timber member was assessed by means of high resolution laser scanning and dynamic excitation (Olsson and Oscarsson, 2016). Information concerning the tested load-bearing timber member is shown in Table 5-3.

Table 5-3. Overview of the loaded tests that were carried out.

Test	Cross-section dimensions [mm]	Cavity insulation	Applied $M$ [kNm]	Predicted $E_{20^{\circ}\text{C}}$ [GPa]	Predicted $f_{m,20^{\circ}\text{C}}$ [MPa]
Test 37	50 × 200	HTE 2	5.27	13.2	52.7
Test 38	50 × 200	SW 3	3.86	14.3	57.0
Test 39	50 × 200	SW 5	3.22	12.0	48.2

KEY:  $M$  – bending moment;  $E_{20^{\circ}\text{C}}$  – modulus of elasticity at ambient temperature;  $f_{m,20^{\circ}\text{C}}$  – bending strength



KEY:  $F$  – force applied by the hydraulic jacks; GtF – gypsum plasterboard Type F.

Dimensions in millimetres

Figure 5-9. Longitudinal view of the specimens used in the loaded cubic metre furnace tests.

The specimens were subjected to standard fire exposure conditions in accordance with EN 1363-1 (CEN, European Committee for Standardization, 2012). The bending moments which were applied corresponded to the 20-30% of the bending moment capacity of the timber members at ambient temperature. The results of the cubic

metre furnace tests are also reported in Table 5-4. For Test 37 and Test 39, the gypsum plasterboard fell off in one piece at 34 minutes from the beginning of the test, whilst during Test 38 the gypsum plasterboard fell off at 47 minutes. The end of the test was determined when a rupture of the beam occurred, at 53.3 minutes. After the test, the cross-sections in correspondence of the rupture of the member was collected. The charring depth in the middle width of the ruptured cross-section was evaluated by measuring the depth of the uncharred rupture cross-section and subtracting this value from the original depth of the member.

The zero-strength layer's depths were calculated for each specimen by using Equation (36). The same set-ups that had been tested were also simulated according to the methodology described in Sections 5.1.1 and 5.1.2. The zero strength layers' depths were evaluated from the test results and from simulation results, and were predicted according to Equations (47) and (51), as reported in Table 5-4. From the simulations, the depths of the zero-strength layer were found to be between 1 mm to 4 mm larger than the test results. The general agreement between the experimental and numerical results indicates that the numerical simulations are suitable for predicting the load-bearing capacity of bending beams. The zero-strength layer which was calculated according to Equations (47) and (51) for these set-ups turned out to be equal to 44 mm and 50 mm respectively. The predictions which were reached by using the proposed equations (the simplified approach) gave only the peak values of  $d_0$  during fire exposure. The simplified approach is, as the name suggests, simple but it is also conservative with respect to fire tests and numerical simulations. The zero-strength layer which was predicted by using the optimised approach equals 34 mm for Test 38 and 26 mm for Test 39. In one case (Test 38), the  $d_0$  values which were predicted by the optimised approach is underestimated by an approximate figure of 20%, while in the other case (Test 39) the prediction for the optimised approach is very close to the test result.

*Table 5-4. Results for the loaded cubic metre furnace tests.*

Test	Fall-off of the cladding [min]	Rupture of the timber member [min]	$d_0$ evaluated by test [mm]	$d_0$ evaluated by simulations [mm]	Simplified $d_0$ [mm]	Optimised $d_0$ [mm]
Test 37	34	53.3	36	37	44	N/A
Test 38	47	72.9	41	45	50	34
Test 39	34	87.2	24	28	50	26

Tests 38 and 39 were exposed to fire for a period longer than 60 minutes. Despite these tests, the set-ups do not correspond to the test set-up that was adopted in order to evaluate the PL of an insulation product but, even so, some consideration can anyway be given to the production of the charring depth on the wood-insulation interface ( $d_{300,s}$ ). The results of  $d_{300,s}$  as a function of time are shown in Figure 5-10.

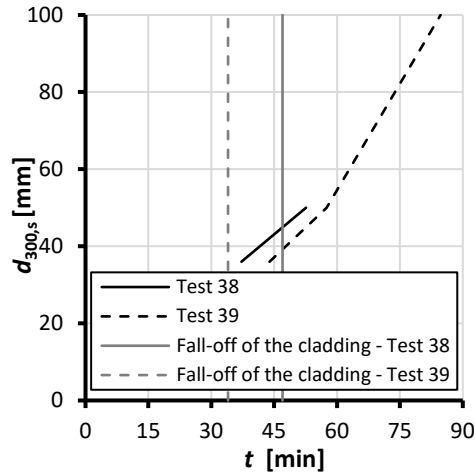


Figure 5-10. Charring depth on the wood-insulation interface ( $d_{300,s}$ ) as a function of time for Test 38 and Test 39.

The cladding falling off for Test 38 occurred at 47 minutes, which shows that the duration of the protection phase is close to the duration of 45 minutes that was suggested in order to evaluate the protection level (see also Section 3.3). In Test 38,  $d_{300,s}$  did not reach a depth of 100 mm after 72.9 minutes of fire exposure. The duration of the protection phase in Test 39 was nine minutes shorter than the duration suggested in order to evaluate the protection level (a total of 36 minutes against 45 minutes), and  $d_{300,s}$  reached 100 mm at 84.7 minutes. This data suggests that the tested stone wool product in Test 39 may guarantee that  $d_{300,s}$  is less than 100 mm for a 90 minutes fire exposure; however, further investigations are necessary.

## 5.2 Validation of the design model by means of full-scale tests

To be able to validate the improved design model, two loaded full-scale tests (involving a wall and a floor respectively) were carried out at RISE Fire Research in Sweden, and test reports have been analysed for seven loaded full-scale tests which were carried out at MPFA Leipzig in Germany.

### 5.2.1 Performed full-scale tests

In order to validate the improved design model, two loaded full-scale tests were carried out. A specimen of a wall (with external dimensions of 3000 × 3000 mm) and a floor (with external dimensions of 3000 × 4800 mm) were exposed to the standard temperature-time curve in accordance with EN 1363-1 (CEN, European Committee for Standardization, 2012).

Both specimens were composed of load-bearing timber members with cross-section dimensions of 50 × 200 mm. The interaxle spacing between the load-bearing members equalled 600 mm. The load-bearing timber elements were classified as C30 according to EN 338 (CEN, European Committee for Standardization, 2009). In both specimens, the fire-exposed side was covered by a 15 mm-thick gypsum plasterboard of Type F and the unexposed side was covered by 19 mm-thick particle board. The gypsum plasterboard was fixed to the timber studs with screws. The screws were 39 mm long and were located every 200 mm. The cavities were filled with SW 3 (see product

characteristics in Table 3-1). Insulation batts were oversized with respect to the width of the cavities by 5 mm. The estimated length of time it would take for the cladding to fall off and thereby expose the cavity insulation during the post-protection phase was hindered by (i) fixing the insulation batts to the unexposed side of the specimens with glue, and (ii) a metal wire being installed onto the fire-exposed side of the cavity.



(a)



(b)

Figure 5-11. Pictures of (a) the wall, and (b) the floor specimens during the mounting process.

The wall was loaded at a compression of 16.7 kN/m (which corresponds to 10 kN for each load-bearing member), and the floor was loaded to 1 kN/m<sup>2</sup> (which corresponds to a maximum bending moment of 1.7 kNm for each load-bearing member).

In both tests, the gypsum plasterboard fell off in large chunks. For the wall test, the first piece of plasterboard detached itself at 87 minutes and the last piece came off at 91 minutes. For the floor test, the first piece fell off at 49 minutes and the last at 58 minutes. The wall test was interrupted at 136 minutes due to a rupture in the load-

bearing elements, while the floor test was interrupted at 100 minutes due to integrity failure.

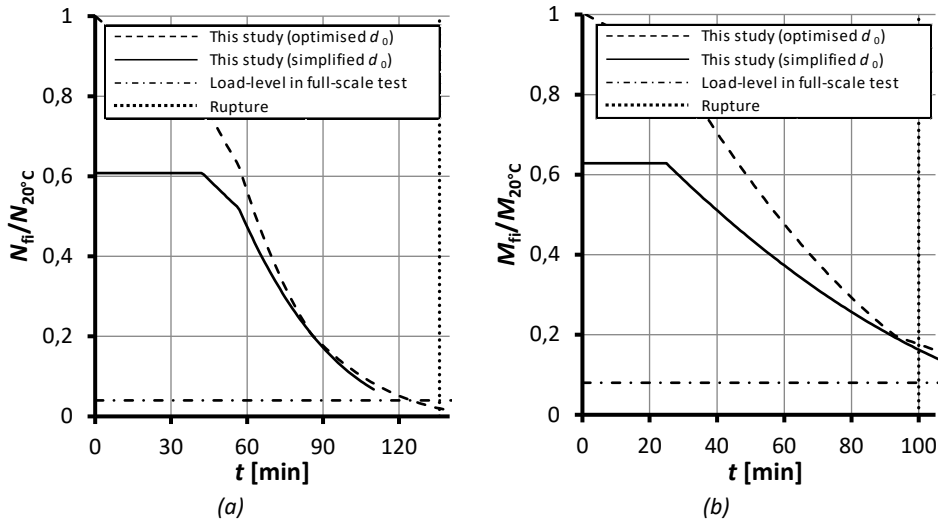


Figure 5-12. Load-bearing reduction as a function of the time predicted by the improved design model when compared to the load applied on (a) the wall specimen and (b) the floor specimen during the full-scale furnace tests

The prediction for the load-bearing capacity of the wall specimen according to the improved design model equalled 92 minutes when the simplified approach was adopted in a determination of  $d_0$  (see Section 5.1.6), and it equalled 103 minutes when adopting the optimised approach to determine  $d_0$  (see Section 5.1.8), while the rupture occurred at 136 minutes. The load-bearing capacity predicted for the floor specimen equalled 77 minutes when adopting the simplified approach in order to determine  $d_0$  (see Section 5.1.6), and equalled 85 minutes when adopting the optimised approach to determine  $d_0$  (see Section 5.1.6). The floor test was interrupted at 100 minutes with no failure of the timber elements. The predicted load-bearing capacity for the wall amounted to 68% of the full-scale test result when adopting the simplified  $d_0$ , and 76% when adopting the optimised  $d_0$ . The rupture time for the floor assembly was less than 77% of the full-scale test result when adopting the simplified  $d_0$ , and less than 85% when adopting the optimised  $d_0$ , since the full-scale test did not get as far as the rupture of the load-bearing members.

The improved design model that was used both with the simplified and optimised approaches for  $d_0$  has predicted conservative results. The predictions (see Figure 5-12) were evaluated by considering the shorter fall-off times than were observed during the tests, which took place at 49 and 87 minutes respectively for the floor and wall specimens.

Other factors which were included in the design model (for example  $k_2$ ) were taken from the available literature. These factors may also have been proposed to provide a conservative prediction. The different predictions for the improved design model when compared to the results of the full-scale tests results may be due to the sum of several factors which were meant as simple approaches but which still provided conservative predictions.

The post-protection factor  $k_{3,1}$  was evaluated according to Equation (21) from the results of the full-scale wall test that was carried out. In Figure 5-13, the values for the factor  $k_{3,1}$  which were evaluated from the test results, are compared to the values that were predicted by means of Equation (33).

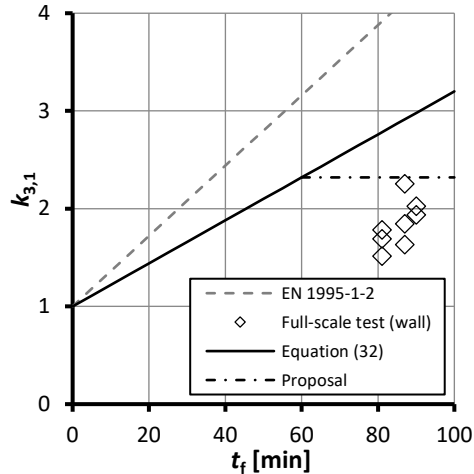


Figure 5-13. Factor  $k_{3,1}$  as a function of the fall-off time ( $t_f$ ) as evaluated from full-scale test results.

For the wall test, the fall-off the cladding occurred after the 80 minute mark. It is possible to observe that the prediction which was reached thanks to Equation (33) is a very conservative one. Therefore it is proposed that the factor  $k_{3,1}$  not be considered as being linearly dependent upon the length of time it takes for the cladding to fall off, when the fall-off exceeds a period of 60 minutes. A new proposal for factor  $k_{3,1}$  in TFA which has been insulated with stone wool products is as follows:

$$\begin{aligned}
 k_{3,1} &= 0.022 t_f + 1 && \text{for } t_f \leq 60 \text{ min} \\
 k_{3,1} &= 2.32 && \text{for } t_f > 60 \text{ min} \quad (67)
 \end{aligned}$$

### 5.2.2 An evaluation of existing test reports

The test reports for seven full-scale tests in the wall position which were carried out at MPFA Leipzig (Peitzmeier, 2017c, 2017d, 2017e, 2017g, 2017a, 2017b, 2017f) were also analysed and compared to the load-bearing capacity that was predicted by the improved design model (see the summary of the analysed full-scale tests in Table 5-5). Various specimens (of external dimensions 3000 × 3000 mm) were exposed to the standard temperature-time curve in accordance with EN 1363-1 (CEN, European Committee for Standardization, 2012). The specimens were composed of load-bearing timber members with an axial distance of 835 mm and different cross-section dimensions. The load-bearing timber members were classified as C24 according to EN 338 (CEN, European Committee for Standardization, 2009). Claddings which comprised two or three layers were applied to the fire-exposed side of the specimens. These layers were composed of different gypsum plasterboard products, Oriented Strand Boards (OSB), or wood fibre (WF) insulation. The cavities of four specimens were filled with a SW insulation product and three specimens were filled with a wood fibre (WF) form of insulation. Two specimens (Wall 1 and Wall 6) presented an air gap of

20 mm between the inner layer of the cladding and the cavity insulation. Schematics for the cross-sections of the specimens are shown in Figure 5-14, while the corresponding materials and depths, cross-section dimensions, and forms of cavity insulation are indicated in Table 5-5.

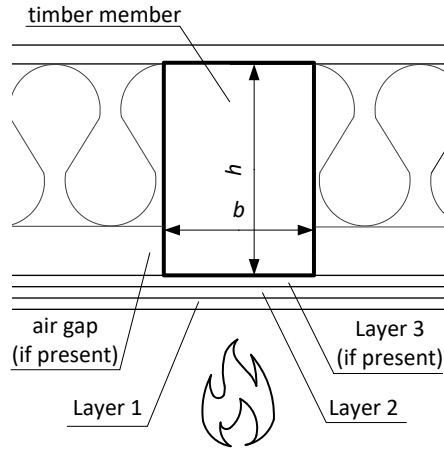


Figure 5-14. Schematics for the cross-section of full-scale wall specimens tested at MPFA Leipzig.

Specimens were loaded in compression with different load levels. Most of the tests were interrupted following a failure of the load-bearing capacity (R-criterion); only in one test did an integrity failure occur (E-criterion). For all of the tests that were reported, the predictions were calculated for the load-bearing capacity according to the improved design model and using the simplified approach for  $d_0$ . In the calculations, the starting times for charring on the fire-exposed side ( $t_{ch}$ ) were taken as the sum of the protection time values ( $t_{prot,i}$ ) which were included in a design model to make it possible to evaluate the insulation (I-criterion) of TFA when exposed to fire as proposed by Schleifer (2009) and which is included in the FSITB guideline (B. Östman et al., 2010). Therefore the starting times for charring were calculated as follows:

$$t_{ch} = \sum t_{prot,i} \quad (68)$$

where  $t_{ch}$  is the start time of charring on the fire-exposed side and  $t_{prot,i}$  is the protection time value for a single layer. The protection time value for a single layer depends upon the material used in the creation of the layer and also its depth. Fall-off times of the cladding ( $t_f$ ) was taken as the fall-off time observed during the tests and which was reported in Table 5-6.

Table 5-5. Overview of the full-scale tests that were analysed.

Test	Cladding			Air gap [mm]	Cavity insulation	Cross-section dimensions [mm]
	Layer 1	Layer 2	Layer 3			
Wall 1	GtA 12.5 mm	OSB 12 mm	no	20	SW	60 × 100
Wall 2	GtF 15 mm	OSB 12 mm	no	no	SW	60 × 100
Wall 3	GtF 18 mm	OSB 12 mm	no	no	SW	60 × 120
Wall 4	GtF 18 mm	OSB 12 mm	no	no	SW	80 × 120
Wall 5	GtF 15 mm	WF 40 mm	OSB 12 mm	no	WF	60 × 180
Wall 6	GtF 15 mm	OSB 12 mm	no	20	WF	60 × 100
Wall 7	GtF 15 mm	OSB 12 mm	no	no	WF	60 × 100

KEY: GtA – gypsum plasterboard Type A; GtF – gypsum plasterboard Type F; OSB –Oriented Strand Board.

The wood fibre (WF) insulation product was not studied in the investigation that was carried out for this thesis; therefore the values for the protection factors and zero-strength layer's depths for the improved design model are not yet available. For this comparison, when the specimens were insulated with WF (Walls 5, 6, and 7), the load-bearing capacities were evaluated by considering the charring scenario as proposed for PL2 insulation products, the values for protection factors proposed for cellulose fibre (CF) products, and the zero-strength layer's depths which were proposed for glass wool (GW) products. The load-bearing capacities which were predicted for the improved design model are reported in Table 5-6; a comparison with the full-scale test results is shown in Figure 5-15.

Table 5-6. The results of the full-scale tests that were analysed.

Test	Load per stud [kN]	Fall-off time of the cladding [min]	Type of failure	Test duration [min]	Evaluated $t_{ch}$ [min]	Evaluated load-bearing capacity [min]
Wall 1	16.7	45-54	R	63	37.3	37
Wall 2	16.7	55	R	66	44.1	44
Wall 3	21.7	45-67	R	97	52.6	60
Wall 4	30.1	67	R	96	52.6	65
Wall 5	30.1	48-74	R	82	43.0	79
Wall 6	16.7	-	R	59	44.1	49
Wall 7	16.7	-	E	67	44.1	49

KEY: R – load-bearing capacity criterion; E – integrity criterion.

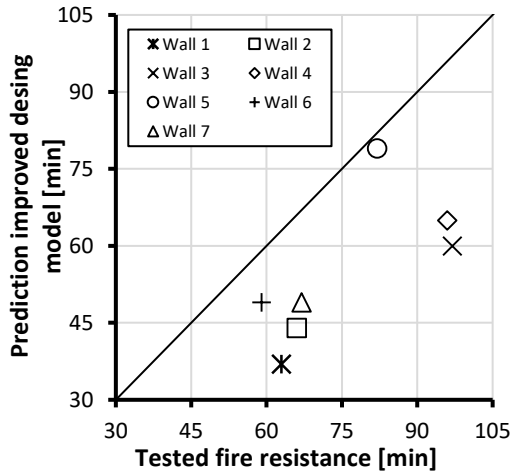
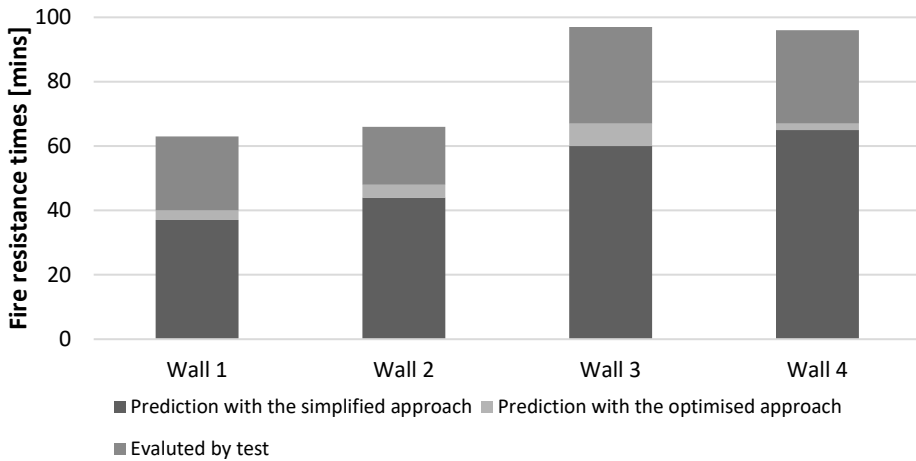
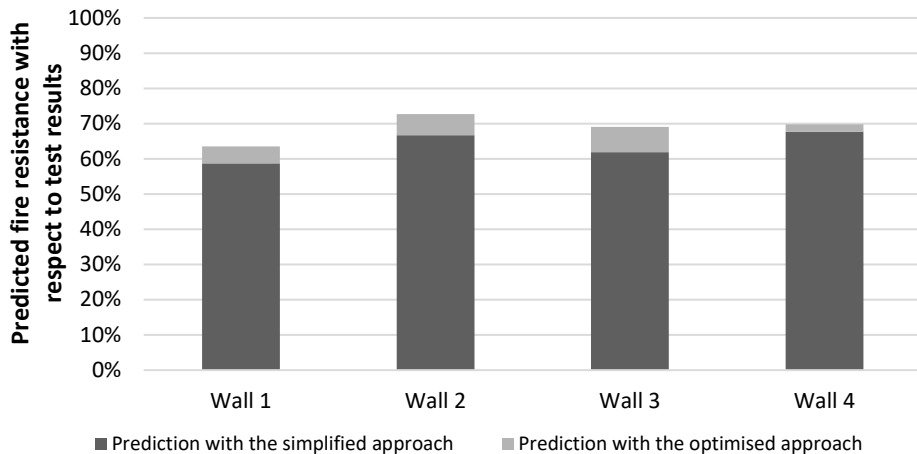


Figure 5-15: Rupture of the load-bearing members as predicted by the improved design model against evaluation by testing.

Also for this comparison, the load-bearing capacities which were predicted by the improved design model are more conservative than the full-scale test results. Later, load-bearing capacities using the optimised approach for  $d_0$  were also evaluated for those walls which had cavities that were being filled with stone wool products (from Wall 1 to Wall 4 on Table 5-6). The results, in terms of predicted fire resistance times and the percentage of the predicted fire resistance times with respect to the tested fire resistance times, are shown in Figure 5-16.



(a)



(b)

Figure 5-16. (a) predicted fire resistance times according to the improved design model, and (b) the percentage of the predicted fire resistance time with respect to the tested fire resistance time

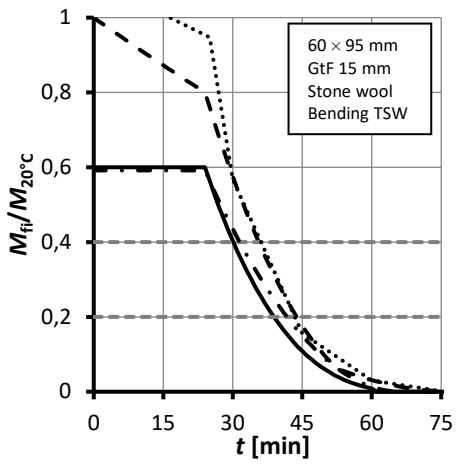
### 5.3 Load-bearing capacity according to EN 1995-1-2:2004 versus improved design model

The design model for TFA with stone wool as a form of cavity insulation which is included in the current Eurocode 5 Part 1-2 is based upon the reduced properties method (RPM) (see Section 2.5 **Error! Reference source not found.**). According to the RPM, the original cross-section has to be reduced by the notional charring depth and, subsequently, the mechanical properties have to be reduced by a modification factor. For example, the modification factor for the strength ( $k_{mod, fm, fi}$ ) is evaluated according to Equation (7).

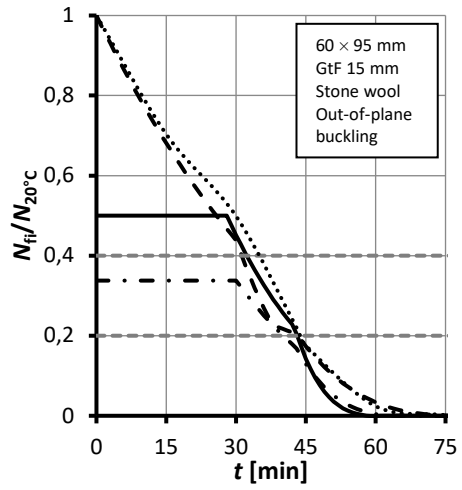
Since  $k_{mod, fm, fi}$  is given as a function of the charring depth, the modification factor implicitly depends upon the fire exposure time. Furthermore, this design model is limited to 60 minutes of fire exposure.

The definition of the charring coefficients and zero-strength layers allows an evaluation also to be made of the load-bearing capacity of TFA with stone wool insulation by means of the improved design model. A comparison of the two design models is therefore made possible. For this comparison, two load configurations are considered: (i) bending with the tension side that has been exposed to fire, and (ii) out-of-plane buckling. In each set-up involving TFA that has been considered for comparison purposes, the load-bearing capacity according to the improved design model has been evaluated according to both the simplified and optimised approach for  $d_0$ . The results of the thermo-mechanical simulations have also been plotted. Comparisons are shown in terms of a reduction of the load-bearing capacity as a function of the time, in Figure 5-17.

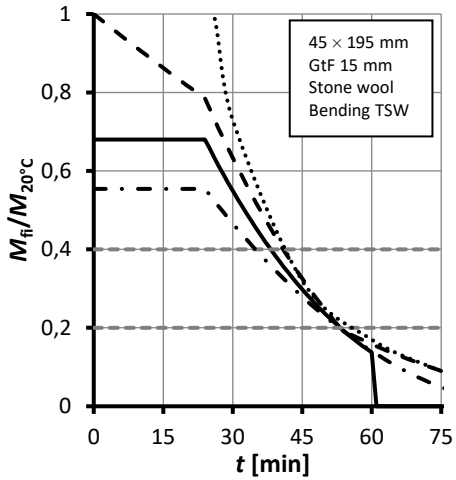
Legend:



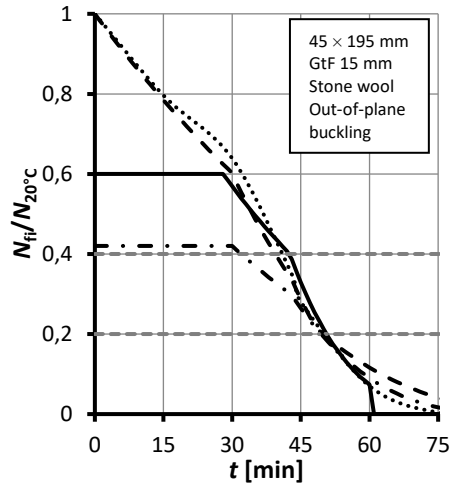
(a)



(b)



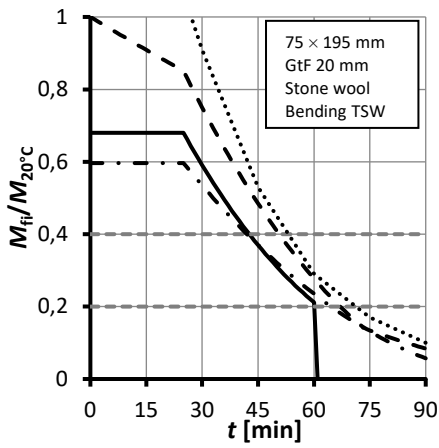
(c)



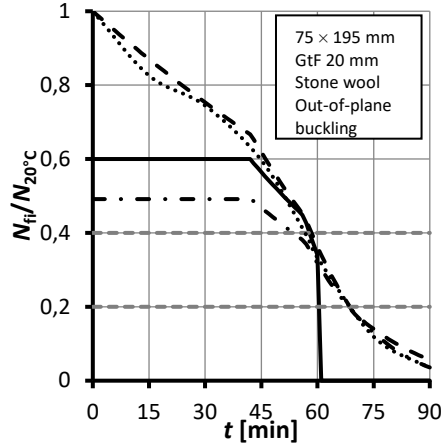
(d)

Legend:

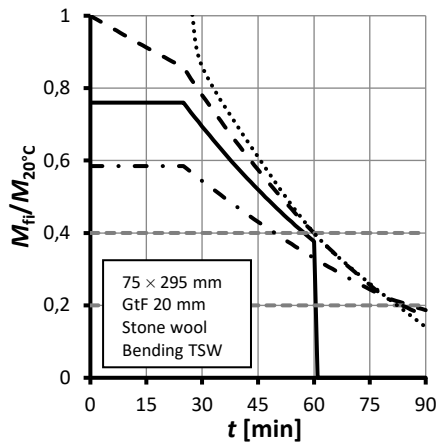
--- This study (optimised  $d_0$ )    -.-.- This study (simplified  $d_0$ )    ..... Simulation    — Eurocode 5 Part 1-2



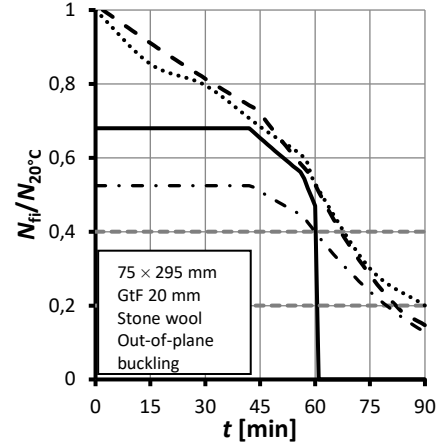
(e)



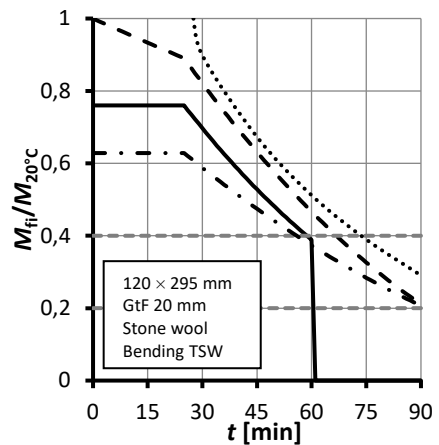
(f)



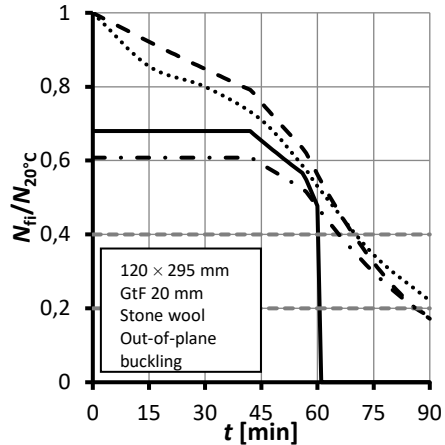
(g)



(h)



(i)



(j)

Figure 5-17. Reduction of the load-bearing capacity against the time for TFA with stone wool as a form of cavity insulation according to Eurocode 5 Part 1-2 and the improved design model.

When comparing the fire resistance level (R-criteria only) as predicted by the improved design model and the Eurocode 5 design model, the improved design model predicts a lower fire resistance level during the first 45 minutes of exposure to fire when the simplified approach for  $d_0$  is applied. This difference is due to the fact that the modification factor  $k_{\text{mod},\text{fm},\text{fi}}$  which is included in the current Eurocode 5 Part 1-2 depends upon the notional charring depth,  $d_{\text{char},\text{n}}$ . This dependence also leads to a more rapid decrease in fire resistance, which is something that is predicted by the Eurocode 5 model. When considering the improved design model to an optimised approach for  $d_0$ , the predicted bending moments are always less conservative than the prediction which is made according to the current Eurocode 5 Part 1-2. In most of the cases, the thermo-mechanical simulations are well predicted by the optimised approach. In the examples, the predictions for the improved design model (both for the simplified and optimised approach) and the Eurocode 5 Part 1-2 design model are similar when the reduction of the load-bearing capacity is comprised between 20% and 40%.

## 6 Cavity insulation remaining in place during fire situations

The improved design model has been developed on the assumption that cavity insulation remains in place after the cladding has fallen off. In the cubic metre furnace tests and in the two full-scale tests which were carried out for this study, a provision was adopted which would avoid the cavity insulation falling off after the cladding has already fallen off.

### 6.1 Prescriptions for the existing design models

The existing design models for TFA with cavities which were filled with stone wool and glass wool products (Just, 2010b; König and Walleij, 2000) are based upon the assumption that the cavity insulation remains in place during the post-protection phase. To ensure this assumption, requirements are given in the European guideline FSITB (B. Östman et al., 2010). These requirements are also summarised in Table 6-1, regarding the minimum depth of the cavity insulation ( $h_{ins}$ ) or whether it is necessary to adopt mechanical installation for the cavity insulation material, or even whether it is possible or not to take into account the protection being provided by the cavity insulation.

Table 6-1. Requirements to prevent fall-off of the cladding during the post-protection phase according to the FSITB guideline.

		Cavity insulation type			
		Stone wool		Glass wool	
		Batt-type	Loose fill	Batt-type	Loose fill
Construction elements	Floors	Mechanical fixing	Protection cannot be taken into account	Mechanical fixing	Protection cannot be taken into account
	Walls	Mechanical fixing for $h_{ins} < 120$ mm	Protection cannot be taken into account	Mechanical fixing for $h_{ins} < 120$ mm	Protection cannot be taken into account

KEY:  $h_{ins}$  – the depth of the cavity insulation.

However, no further information is given regarding the type of mechanical installation that could be adopted. In addition, information is missing regarding the fire resistance levels of installation system for forms of cavity insulation that are present on the market.

### 6.2 An evaluation of the fall-off times of insulation to fall off based upon existing test reports

Fall-off time of cavity insulation ( $t_{f,ins}$ ) has been evaluated based upon test reports for the seven full-scale tests that were carried out at MPFA Leipzig (Peitzmeier, 2017a, 2017b, 2017c, 2017d, 2017e, 2017f, 2017g) as already considered in Section 5.2.2. The set-ups for the specimens are also reported in Table 5-5. These specimens presented an axial distance between the timber members which equalled 835 mm, meaning that the cavity width varies between 755 mm and 775 mm depending upon the timber member's width. The insulation batts which were inserted into the cavities were not as wide as the cavity itself, so a joint was present. The presence of a joint may influence

the length of time it takes for the cavity insulation material to fall off. Thermocouples were inserted between each layer which made up the completed specimen. The fall-off time of the cavity insulation was evaluated by observing the temperature recorded by the thermocouples which had been placed between the cavity insulation and the first layer of the cladding on the unexposed side (see Figure 6-1).

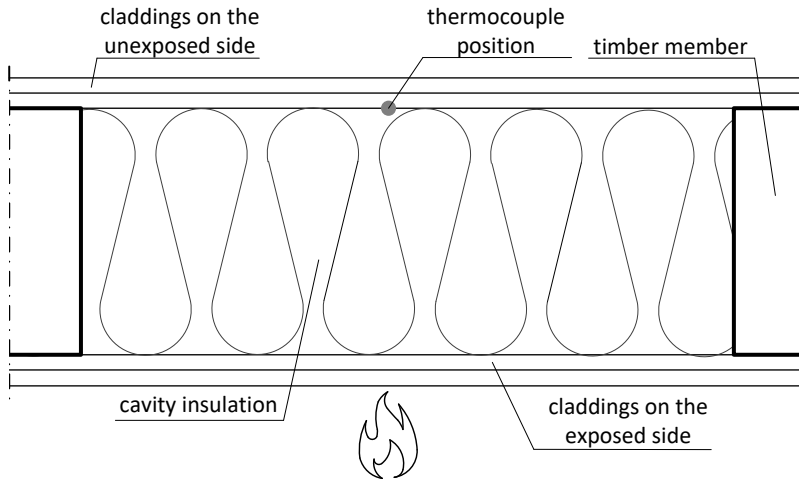
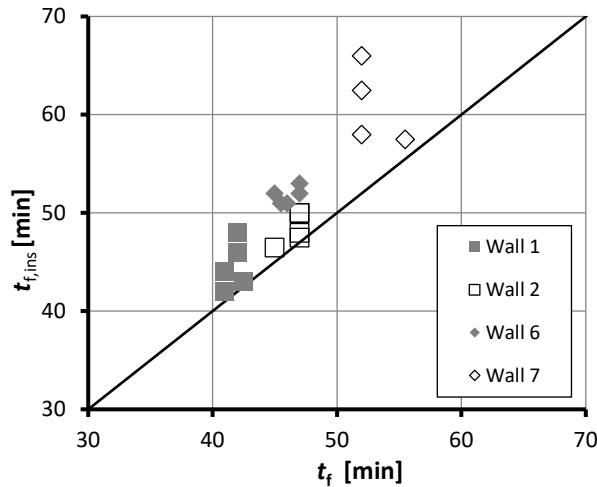


*Figure 6-1. The position of the thermocouples which were considered when it came to evaluating the length of time it takes for the cavity insulation to fall off.*

As fall-off time of an insulation batt, the time was taken at which the temperature increased by at least 100 K in less than one minute. For the tests, on Wall 3, Wall 4, and Wall 5 (see Table 6-1) no insulation falling off was recorded. These tests presented SW as a form of cavity insulation with a depth of at least 120 mm. This finding supports the prescriptions that were given in the FSITB guideline, where no mechanical fixings are deemed to be necessary to prevent any falling-off in stone wool products which have a depth that is greater than 120 mm. In Figure 6-2, the results regarding fall-off times of cavity insulations ( $t_{f,ins}$ ) are compared to the fall-off time ( $t_f$ ) from the inner layer on the side that has been exposed to fire (Layer 2 in Figure 5-14).



KEY:  $t_{f,ins}$  – fall-off time of the cavity insulation;  $t_f$  – fall-off time of the cladding.

Figure 6-2. Fall-off time of the cavity insulation against the length of time it takes for the cladding to fall off.

### 6.3 A survey of the existing fixation systems for cavity insulation in timber frame assemblies

The installation of cavity insulation can play a crucial role in the length of time it takes for that cavity insulation to fall off. In France, for example, rules to install cavity insulation in timber frame floors or attics in accordance with established best practice are given (CSTB, Centre Scientifique et Technique du Bâtiment, 2009), while rules involving installations in wall elements are currently under review. However, these rules are provided only to guarantee thermal and acoustic performance. Some of the installation solutions that have been adopted in practice in order to guarantee thermal or acoustic performance or to facilitate the mounting process may improve the ability of cavity insulation to remain in place during the post-protection phase.

In order to address any future investigation of the role of the fixing systems in terms of the insulation materials being able to remain in place under fire conditions, a survey has been distributed across Europe. The aim of the survey was to collect information regarding the possible systems being used to affix cavity insulations within timber frame assemblies and to test the fire performance levels of the most often-used systems.

Questions which were included in the survey were divided into the following four macro areas:

- insulation slabs (or batt-type) which is applied to floor elements,
- insulation slabs (or batt-type) which is applied to wall elements,
- loose-fill insulation products which is applied to floor elements,
- loose-fill insulation products which is applied to wall elements.

For each macro-area, *ad hoc* questions were prepared so that an investigation could be conducted regarding whether fixation systems for cavity insulations are being used, where this is the case which type of systems are being used, and possible characteristics of the system being used. The survey was distributed in the form of a web link.

The survey was addressed to professional cavity insulation installers, carpenters, and contractors. To be able to reach a wide audience, the survey was prepared in English, and was then translated into German and Italian. The English version of the survey is included in Appendix. The first question in each of the macro areas focussed on the system being used (if one was being used at all) to affix the insulation product into the cavities, while the second question addressed the reasons for the use of a particular system. The remaining questions were dependent upon the fixing system selected, using a system which allowed respondents to skip the unnecessary questions. This was done to limit the number of questions being submitted. An open-end question allowed respondents to indicate the type of fixing system being used if this was not included in the multiple-choice question.

Eighty respondents returned the survey; however not all of the respondents replied to all of the questions. Questionnaires were returned from six different countries. An overview of those countries that were involved in terms of respondents returning their questionnaires - along with the relative percentages - are shown in Figure 6-3.

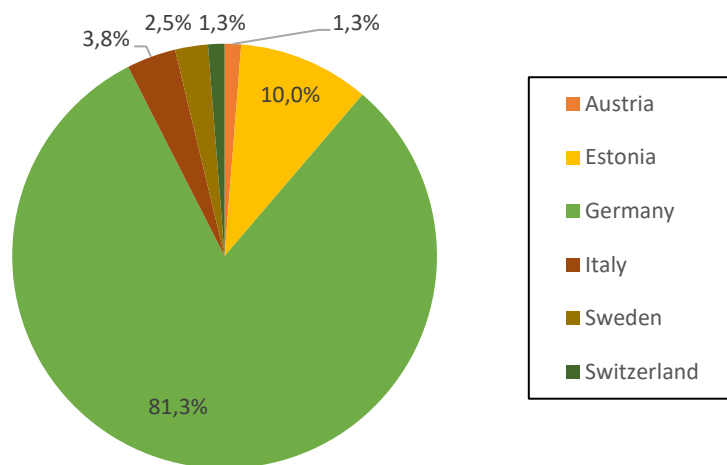


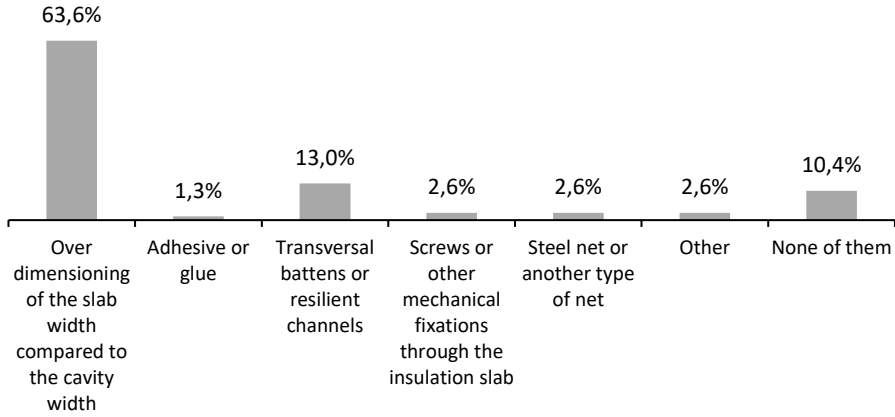
Figure 6-3. Percentage distribution of the countries that returned questionnaires.

Below, the results of the survey are analysed separately for each macro-area that was investigated.

### 6.3.1 Fixing systems used for batt-type insulations being applied to floor elements

In this macro-area, 77 subjects responded to the first answer which was related to the type of fixing system being used. The majority (63.6%) use the over-dimensioning of the insulation width with respect to the cavity width and 57.4% (out of 68 respondents) stated that they used a fixing system because it facilitates the mounting process. Regarding the over-dimension of the insulation slab, 65.3% of the respondents (a total of 49 subjects responded to this question) use insulation slabs which are between 5 mm and 10 mm wider than the cavity itself.

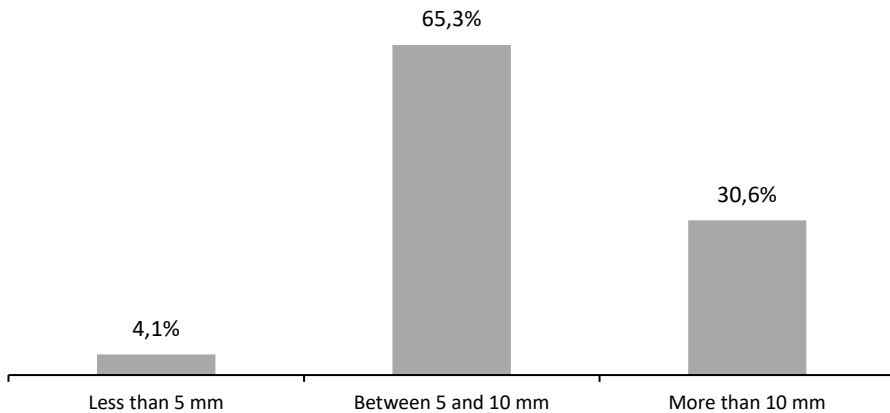
Which method do you normally use to fix the insulation slab in place in the cavities of floor elements?



Respondents: 77

(a)

In the case of the over-dimensioning of the batt width, what is the value of such over-dimensioning?



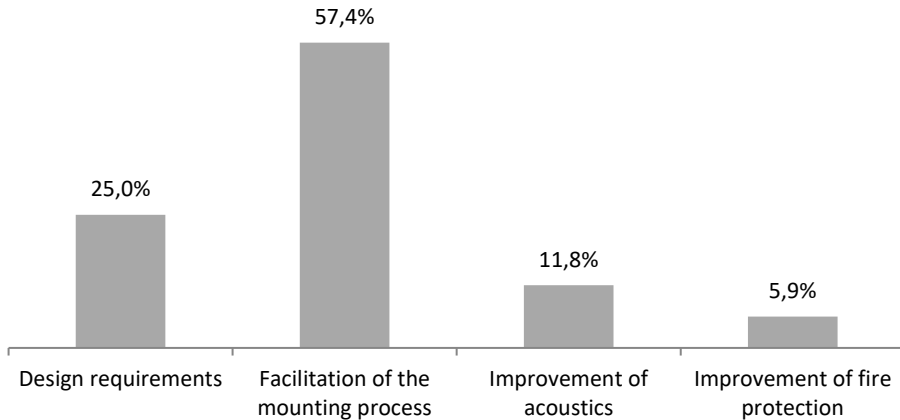
Respondents: 49

(b)

Figure 6-4. The distribution percentage of (a) fixing methods, and (b) over-dimensioning of the batt width for a batt-type insulation in floor elements.

A total of 13% of respondents applied battens or resilient channels, while 10% of respondents were not using any solution which, in the absence of the cladding, may help to avoid the cavity insulation falling off. Only 5.2% of respondents (which corresponds to four individuals in total) were using steel net, screws, or some other form of mechanical fixing.

Which is the reason for the use of the fixing systems?



Respondents: 68

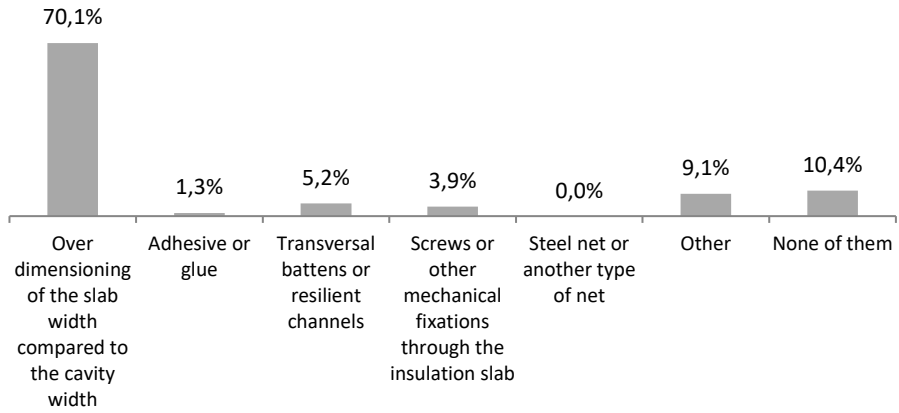
*Figure 6-5. The reasons for using fixations systems for batt-type insulations installed in floor elements.*

Most of the respondents (57.4% of 68 respondents) were using a fixing system for batt-type insulation which was being installed in floor elements because it facilitated the mounting process. The second reason for using a fixation system is because it is required by the designers (covering 25% of respondents).

### **6.3.2 Fixing systems for batt-type insulation which is applied in wall elements**

For batt-insulations which are being installed into wall elements, a total of 77 respondents replied to this part of the survey. The fixation system most often being adopted (covering 70.1% of respondents) is the over-dimensioning of the batt width. A total of 69.2% of 52 respondents were using cavity insulation which was between 5 mm to 10 mm wider than the cavity width. Cavity insulation without any fixation system or over-dimensioning of the width was being installed by 10.4% of the respondents. Despite 9.1% of them using use a fixation system that was not included in the multiple choices supplied, nobody specified the type of fixation system they were normally using.

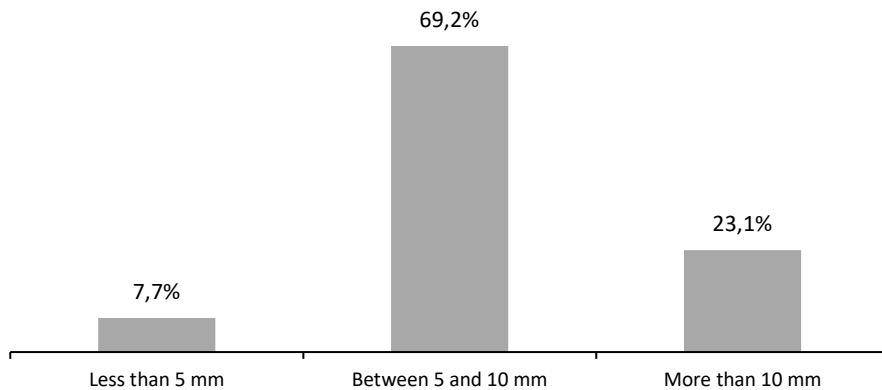
Which method do you normally use to affix the insulation slab in the cavities of wall elements?



Respondents: 77

(a)

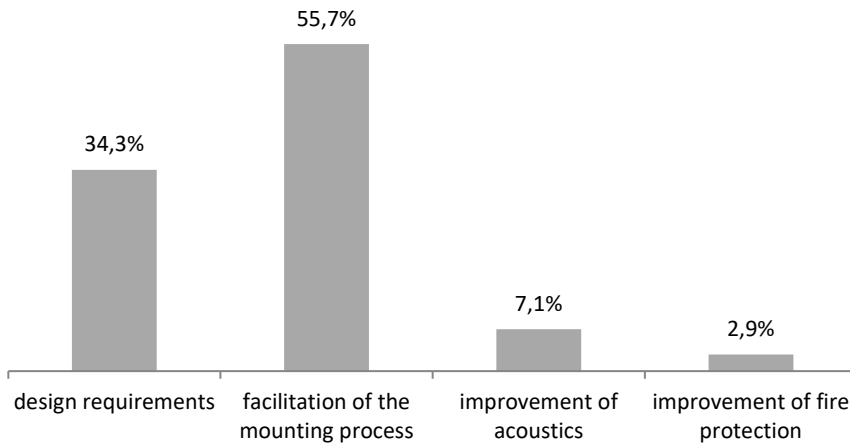
In the case of the over-dimensioning of the slab width, which is the over-dimensioning value being used?



Respondents: 52

(b)

What is the reason for the use of the fixation systems?



Respondents: 70

(c)

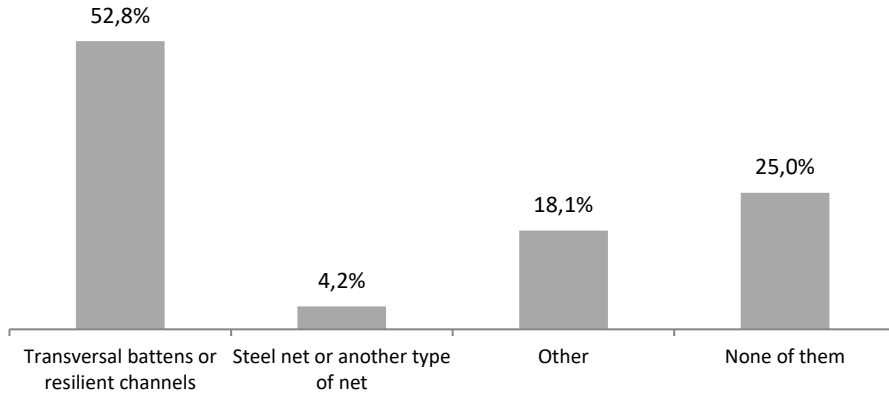
Figure 6-6. The distribution percentage of (a) fixing methods, (b) the over-dimensioning of the batt width, and (c) the reasons for using fixations systems for batt-type insulation in wall elements.

In addition for this macro-area, the improvement given to the mounting process is the main reason for a fixation system being adopted (covering 55.7% of respondents), followed by the design prescription (34.3%).

### 6.3.3 Fixing systems for loose-fill insulation being applied to floor elements

A total of 72 people answered those questions which were related to the loose-fill insulation that was being applied to floor elements. The most frequent systems being used which may help to avoid loose fill insulation from becoming detached from floor elements involves transversal battens or resilient channels (58.2%), while 25% of respondents were not using any system at all. A total of 48.4% were using a system because it facilitated the mounting process. Among those respondents who were using other systems, the most frequent answer given to the linked open-ended question was that they were using a blanket which was installed behind the cladding. In general, the blanket used for installation do not resist under fire conditions.

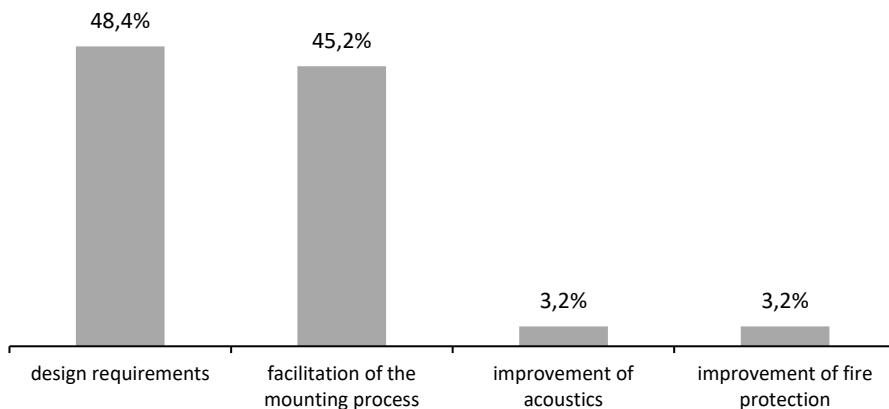
Do you normally use one of the following systems which may hold the insulation in place if the cladding is removed?



Respondents: 72

(a)

What is the reason for the use of the fixation system?



Respondents: 62

(b)

Figure 6-7. The distribution percentage of (a) fixing methods, and (b) the reasons for using fixations systems for loose-fill insulation in floor elements.

### 6.3.4 Fixing systems for loose-fill insulations applied in wall elements

Regarding the type of loose-fill insulation being installed, a total of 71 respondents answered the questions in this macro area. No system which may avoid loose-fill insulation falling off had been installed by 46.5% of the respondents. Instead, the most frequent system being used involves transversal battens or a resilient channel (28.2%).

Do you normally use one of the following systems which may hold the insulation in place if the cladding is removed?

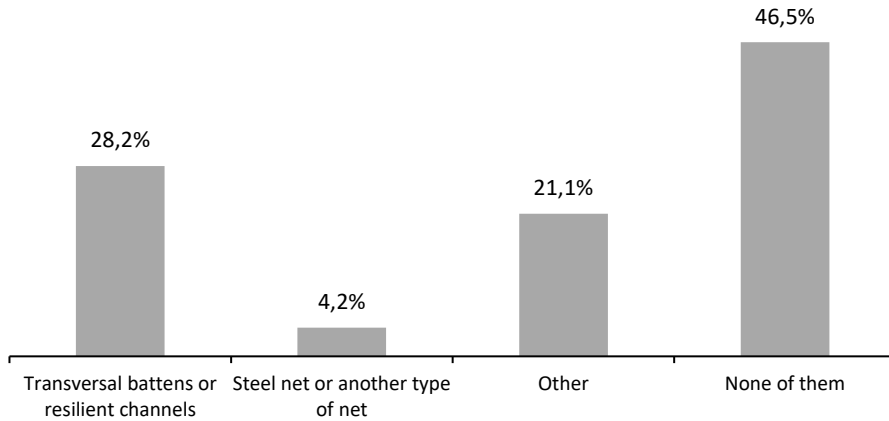


Figure 6-8. The distribution percentage of fixing methods for loose-fill insulation in wall elements.

#### 6.4 Investigation needs to study the fall-off of the cavity insulations

The European FSITB guideline does not required a fixing system in walls if the depth of the cavity insulation exceeds 120 mm (see also Table 6-1). In those test reports that have been analysed as part of this study (see Section 6.2), no falling-off of insulation was found when the cavity insulation was deeper than 120 mm, confirming the validity of the proposals given in the FSITB for wall elements.

However, more investigation is required regarding cavity insulation falling off. The results of the survey showed that a larger proportion of respondents were installing batt-type cavity insulation which was between 5 mm to 10 mm wider than the cavities without any other fixing system being present in both wall and floors elements. Cavity insulation which was installed which was of an oversized width and which was installed in floor elements needs to be investigated by means of full scale tests.

Transversal battens installed behind the cladding can be used to avoid the falling-off of batt-type cavity insulation during the post-protection phase. In this case, the battens should be designed according to the existing rules for timber members that have been exposed to fire.

The contributions which have been provided by loose-fill insulation products during the post-protection phase may not be taken into account if the cavity insulation is not prevented from falling off.

#### 6.5 Limitations of the contribution of insulation materials in the I-criterion

The design model, which is also referred to as the component additive method, and which allows an evaluation to be carried out of the I-criterion of TFA that has been exposed to fire was proposed by Schleifer (2009), and was further improved by other authors (Mäger et al., 2017; Mäger, Just, and Frangi, 2018).

The component additive method makes it possible to evaluate the separating function of TFA which consists of several layers which are made of different materials. The separating function is evaluated by adding the contributions of each layer to the

separating function of the entire assembly. The layer on the side that has not been exposed to fire is considered as being the layer which has an insulating function, while all the other, preceding, layers have a protecting function. Therefore the time at which fire resistance lasts for the I-criterion of the entire assembly is calculated as the time at which the insulation time of the layer which is on the side not exposed to fire, plus the sum of the protection time of the preceding layers. The protection time of a single layer placed under the last layer can be calculated as the basic protection time of the layer corrected by coefficients which take into account its position within the overall assembly and the presence of the joints.

The basic protection time of a single layer depends upon the material being used in the specific layer, plus its depth and density. Basic protection times for solid wood, gypsum board, and mineral wool insulation materials are presented in the European FSITB guideline (B. Östman et al., 2010) which is based upon research that has been carried out by Schleifer (2009).

The claddings have the greatest influence on the total time of fire resistance for I-criterion, the contribution of insulation materials is relatively smaller since it is influenced by factors such as how the insulation layers have been fixed in placed (Mäger et al., 2018). In order to obtain realistic results, the protection time of the insulation must always be less than or equal to the fall-off time of the insulation layer. Limits to the sum of the protection times of the layers preceding the insulation layer and the insulation layer have been proposed by Mäger et al (2018). For insulation material qualified as PL 1, this limit can be calculated as:

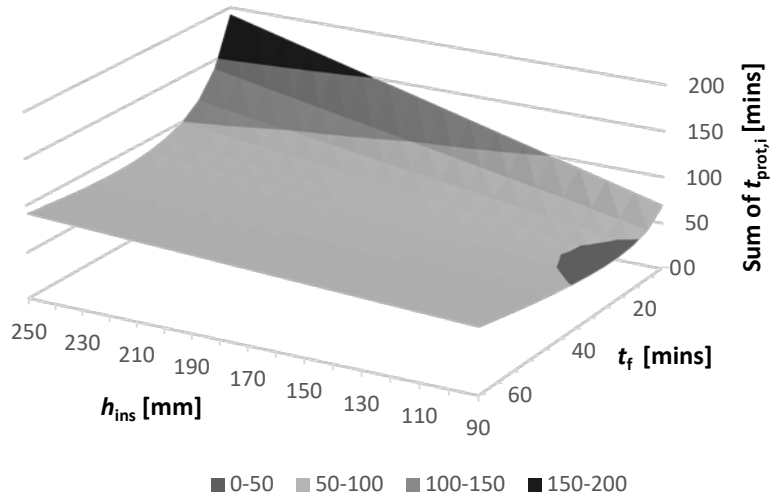
$$\sum_{i=1}^{n-1} t_{\text{prot},i} \leq \frac{h_{\text{ins}}}{0.11t_f + 1.3} + t_f \quad (69)$$

where  $\sum_{i=1}^{n-1} t_{\text{prot},k}$  is the sum of protection times including the insulation layer,  $h_{\text{ins}}$  is the depth of the insulation layer expressed in millimetres, and  $t_f$  is the fall-off time of the cladding expressed in minutes.

For materials qualified as PL 2, the limit to the sum of the protection times for those layers which lie over the insulation layer and the insulation layer can be calculated as:

$$\sum_{i=1}^{n-1} t_{\text{prot},i} \leq \frac{h_{\text{ins}}}{v_{\text{rec}}} + t_f \quad (70)$$

where  $\sum_{i=1}^{n-1} t_{\text{prot},i}$  is the sum of protection times including the insulation layer,  $h_{\text{ins}}$  is the depth of the insulation layer,  $v_{\text{rec}}$  is the speed of recession for the insulation material, and  $t_f$  is the fall-off time of the cladding.



KEY:  $h_{ins}$  – the depth of the insulation layer;  $t_f$  – fall-off time of the cladding;  $t_{prot,i}$  – protection time.  
 Figure 6-9. The limit to the sum of the protection times for the layers preceding the insulation layer and the insulation layer as a function of the insulation layer's depth and fall-off time of the cladding for insulation material qualified as PL 1.

In the absence of any timings for precisely when fall-off times of cavity insulations evaluated by means of full-scale fire tests, the fall-off of the cavity insulation can be taken as the sum of the protection times of the layers preceding the insulation layer and the insulation layer ( $\sum_{i=1}^{n-1} t_{prot,i}$ ), calculated according to Equations (69) and (70) respectively for PL 1 and PL 2 cavity insulations.

## 7 Conclusions and outlook

### 7.1 Conclusions

The aim of this thesis was to investigate the contribution provided by various forms of cavity insulation towards the load-bearing capacity of timber frame assemblies (TFA) where these have been exposed to standard temperature-time fire conditions. A new design approach is presented in this thesis which composed a methodology for the qualification of forms of cavity insulation according to its protection ability and a design model for the load-bearing capacity of TFA that has been exposed to fire.

Twelve batt-type forms of insulation material and two loose-fill types were selected to be investigated in the cubic metre furnace. Cubic metre furnace tests showed that the protection properties inherent in different forms of cavity insulation are themselves different. Test results confirmed the findings of previous studies by proving that the charring process rates for the timber member in the post-protection phase depends upon the form of cavity insulation being used. Test results also showed that the 300°C isotherm on the wood-insulation interface is an indicator of the fire protection being provided by a specific form of cavity insulation. A methodology for the qualification of batt-type insulation materials is described in this thesis, based upon the advancement of the 300°C isotherm. This methodology identifies three different levels of protection, where protection level 1 (PL 1) is the strongest level of protection any form of cavity insulation product can offer and protection level 3 (PL 3) is the weakest. For example, typical stone wool products are normally qualified as PL 1, typical glass wool and cellulose fibre products are qualified as PL 2 and expanded polystyrene products are qualified as PL 3.

The specimens being used to investigate the protection levels were subjected to 60 minutes of standard temperature-time fire exposure. However, two further tests were conducted with a longer fire exposure time, and the results suggested that stone wool products can guarantee protection against charring for the lateral sides also up to 90 minutes of standard temperature-time fire exposure. However, the length of time of the post-protection phase is crucial.

Different charring scenarios for the timber members can be identified in TFA in relation to different forms of cavity insulation with different protection levels. For TFA with cavities that have been completely filled with PL 1 cavity insulation, charring occurs mainly on the fire-exposed side of the member, while the lateral sides are protected by the insulation. For TFA with cavities which have been completely filled with PL 2 and PL 3 cavity insulation, the influence of the rounding of the char line can be noticed and, from a certain point, the timber member also chars from the lateral sides due to the recession of the cavity insulation.

From the selected twelve forms of insulation product, three were chosen for further investigation. A second test programme which was carried out in the cubic metre furnace aimed to investigate the parameters which can affect the charring for load-bearing timber members in framed assemblies. Post-protection factors were evaluated for the charring on the fire-exposed side ( $k_{3,1}$ ) and on the lateral side ( $k_{3,2}$ ). Values were derived for factors which will provide an improved design model for high temperature extruded mineral wool (HTE 2), glass wool (GW 1), and cellulose fibre (CF). It was proposed that the post-protection coefficient for the lateral sides  $k_{3,2}$  depends upon the start of charring on the lateral sides of the beam ( $t_{ch,2}$ ). Despite CF and GW 1 being

qualified at the same protection level, different design values factors have been presented for  $k_{3,1}$  and  $k_{3,2}$ . For reasons of simplicity, the equations which are used to derive the design values of the post protection factors  $k_{3,1}$  and  $k_{3,2}$  can be unified for the protection level, providing one single equation in the same the protection level. Different contributions by specific products which are qualified as being in the same protection level may be characterised by means of the speed of recession they suffer.

Heat-transfer analyses using effective thermal properties were carried out in order to evaluate the factor  $k_{3,1}$  for TFA with cavities that have been insulated with stone wool. The applicability of the improved design model for TFA with cavities that have not been completely filled by the insulation material was also studied by means of heat transfer analysis. Design proposals were proposed that will allow the use of the improved design model as is the case for TFA with cavities that have been completely filled with insulation. The results of the heat-transfer analysis were validated by comparing temperatures and charring depths with the results from the cubic metre furnace tests.

The reduction in the mechanical properties of the residual timber members in the improved design model are compensated through the zero-strength layer  $d_0$ , as is the case with the effective cross-section method. Fire tests can assess  $d_0$  at the time at which rupture occurs, while a thermo-mechanical analysis can provide the depth of the zero-strength layer over the fire exposure time. In this study, an investigation was carried out which looked at the depths of the zero-strength layer of timber members in floor assemblies which have differing set-ups, by means of thermo-mechanical analysis. Variations in the cross-sectional dimensions of the timber members, their depths, fall-off times of the cladding, the forms of cavity insulation product being used, and loading conditions were all considered as part of the simulation programme.

Comparisons between simulation results have shown that the maximum zero-strength layer's depth over the time of the test depends upon cross-section dimensions, the form of cavity insulation being used, and the loading conditions. Conversely, the thickness of the cladding and fall-off time of the cladding do not serve to influence the maximum value of  $d_0$  but only the time at which the peak value is reached.

Two approaches were proposed to derive design values for the depth of the zero-strength layer: a simplified approach in which it is possible to predict the peak value for  $d_0$ , and an optimised approach with a bi-linear function for the fire-exposure time.

Equations were proposed to predict the peak values of zero-strength layers for assemblies in bending and compression with three different cavity insulation materials (two qualified as PL1 and one qualified as PL2). In addition, equations were proposed to predict the time at which the peak value of  $d_0$  is reached for assemblies which have been insulated with stone wool products. This approach was proposed for a maximum of 90 minutes of standard fire exposure.

Three loaded cubic metre furnace tests were carried out to validate the thermo-mechanical simulations. A comparison showed that the thermo-mechanical simulation can be used to investigate  $d_0$  values, while those  $d_0$  values which were predicted by the simplified approach are somewhat conservative.

In order to validate the improved design model, two full-scale furnace tests were carried out. Comparisons have shown that the load-bearing capacity which was predicted by the improved design model is somewhat conservative with respect to the test results. When the simplified approach for  $d_0$  is used, the predicted load-bearing

capacity for the wall was 68% of the full-scale test result, while the rupture time for the floor assembly was less than 77% of the full-scale test result, since the full-scale test did not get as far as rupturing the load-bearing members. When using the optimised approach for  $d_0$ , the predicted load-bearing capacity for the wall and floor was at 76% of the full-scale test results and less than 85% respectively.

Load-bearing capacities which had been predicted according to the improved design model were also compared to the results of full-scale fire tests which had been carried out for commercial purposes. Predictions according to the improved design model were more conservative than those for the full-scale test results, regardless of whether the simplified or optimised approach for  $d_0$  was used.

Furthermore, the fire resistance was compared for TFA with stone wool as its form of cavity insulation, with such fire resistance having been predicted by the design model according to the current Eurocode 5 Part 1-2 and the improved design model. It was shown that the improved design model with its optimised approach for  $d_0$  predicts load-bearing capacities that are always less conservative than the prediction being supplied by the current Eurocode 5 Part 1-2.

All of the investigations which have been outlined above were conducted by following the assumption that the cavity insulation remains in place after the cladding has fallen off. Prescriptive requirements were proposed to guarantee that the form of cavity insulation being used does not fall off during the post-protection phase, as outlined in the European guideline, *Fire Safety in Timber Buildings* (FSITB). However, when mechanical fixing of the cavity insulation is required no further guidance is available on the type of fixing and its fire resistance. An analysis of existing test reports was conducted within this study. This analysis confirmed the prescription given in the FSITB guideline for cavity insulation in wall elements.

Information regarding the systems being used to affix cavity insulation in timber frame assemblies was collected by means of a survey which was distributed to carpenters and installers across Europe. In most cases, it was found that batt-type insulation products are being installed with a width that is between 5 mm and 10 mm wider than the cavities. Inputs are also given for future investigation regarding the falling-off of cavity insulation.

The main finding of this thesis extends the knowledge regarding the fire protection being provided by insulation materials which are applied in TFA. The improved design approach can serve as a form of input for the evolution of design codes.

## 7.2 Outlook

On the basis of this research, the following recommendations for future research can be made:

- The test methodology that was applied to loose-fill cavity insulation showed some drawbacks. These means that when testing loose-fill cavity insulation further improvement is required.
- Fire performance of cavity insulation products were investigated under standard temperature-time fire curve. In future research projects, the protective performance under fire conditions of cavity insulation products should be investigated in natural fire scenarios.
- Further investigation in full-scale fire test is required regarding the falling-off of cavity insulation in floor elements. The most frequent systems used to affix the cavity insulation have to be tested under fire conditions.

## List of Figures

Figure 2-1. Timber frame assembly (TFA) in floor position.....	15
Figure 2-2. Standard temperature-time curve as given in ISO 834, and also adopted in EN 1363-1.....	17
Figure 2-3. (a) thermal conductivity and (b) specific heat of wood as a function of the temperature.....	21
Figure 2-4. (a) thermal conductivity and (b) specific heat of gypsum plasterboard as a function of the temperature.....	22
Figure 2-5. (a) thermal conductivity and (b) specific heat of stone wool (SW) and glass wool (GW) products as a function of the temperature.....	23
Figure 2-6. (a) reduction factors for strength and stiffness properties in compression and tension according to Eurocode 5 Part 1-2 and (b) bilinear elastic–plastic stress–strain relationship (Neely, 1898) with reductions for different temperatures according to Eurocode 5 Part 1-2.....	24
Figure 2-7. Different charring phases for the design model for TFA that has been insulated using stone wool (König and Walleij, 2000).....	25
Figure 2-8. (a) cross-section of a timber frame assembly under fire conditions, (b) schematics for the charring directions used in analytical design models and (c) (d) a definition of charring depths.....	26
Figure 2-9. Charring model for timber frame assemblies which are insulated with stone wool products (CEN, European Committee for Standardization, 2004b; König and Walleij, 2000).....	27
Figure 2-10. Charring phases according to the design model for timber frame assemblies which have been insulated with GW (Just, 2010a, 2010b): (a) protection phase; (b) post-protection phase before the complete recession of GW; (c) the completed recession of GW; and (d) after the complete recession of GW.....	30
Figure 3-1. The most often-used insulation materials grouped according to their chemical or physical structure (Papadopoulos, 2005).....	33
Figure 3-2. Test specimen for a cubic metre furnace: (a) overall plan; and (b) position of thermocouples on the timber member cross-section.....	35
Figure 3-3. Thermocouples positioned (a) on a timber member and (b) on the particle board.....	37
Figure 3-4. Mounting the wooden frame.....	37
Figure 3-5. (a) positioning of the particle board, (c) specimen rotated upside-down and (b) (d) sealing the internal edges with a sodium silicate-based glue.....	38
Figure 3-6. A mineral wool product positioned in a wooden frame.....	38
Figure 3-7. Gypsum plasterboard as fire protection mounted on a specimen.....	39
Figure 3-8. Placing the fastening systems to hold the gypsum plasterboard in place....	39
Figure 3-9. Top view of a specimen.....	39
Figure 3-10. Residual cross-section for the timber members from a specimen which was insulated with (a) HTE mineral wool (Test 2), (b) glass wool (Test 8), and (c) cellulose fibre (Test 10).....	40
Figure 3-11. Resistance profile in the middle of the timber member.....	40
Figure 3-12. (a) charring depth in the middle of the cross-section ( $d_{300,m}$ ); (b) charring depth on the wood-insulation interface ( $d_{300,s}$ ) as a function of time; and (c) residual moments of inertia divided by the initial moments of inertia when compared to the design models for SW and GW.....	42

Figure 3-13. (a) Proposal for a qualification methodology for batt-type insulations with respect to the protection against the charring in timber members; (b) definition of the speed of recession of cavity insulation. ....	43
Figure 3-14. Charring depth on the wood-insulation interface ( $d_{300,s}$ ) as a function of time for Test 14 and Test 15. ....	45
Figure 3-15. Loose-fill insulation and steel net positioned into the wooden frames which were prepared for (a) Test 17 and (b) Test 18. ....	46
Figure 3-16. Bending of the steel net occurred in the specimen that was prepared for Test 17. ....	47
Figure 4-1. The reduction of the moment of inertia versus charring depth ratio.....	51
Figure 4-2. Charring scenario in the improved design model for TFA with (a) PL 1, PL 2, and PL 3 cavity insulation before charring has occurred, and (b) after the time at which charring starts on the lateral sides.....	52
Figure 4-3. Different charring phases for the improved design model for TFA with (a) PL 1, (b) PL 2, and (c) PL 3 cavity insulation. ....	53
Figure 4-4. Charring depths $d_1$ and $d_2$ during the post-protection phase for the evaluation of the factor $k_{3,1}$ . ....	55
Figure 4-5. Factor $k_{3,1}$ for the HTE 2, GW 1, and CF being studied.....	56
Figure 4-6. Residual cross-section during the post-protection phase at the moment at which the start time of charring on lateral sides is considered. ....	57
Figure 4-7. Factor $k_{3,2}$ for the GW 1 and CF that were studied. ....	58
Figure 4-8. Reduction of section modulus as evaluated under fire tests when compared with the prediction by the charring model for assemblies that have been insulated with (a) HTE 2, (b) GW 1, and (c) CF.....	59
Figure 4-9. Schematics for the heat-transfer simulations.....	60
Figure 4-10. Values for $k_{3,1}$ evaluated by means of heat-transfer analysis. ....	61
Figure 4-11. Examples of TFA with cavities not completely filled by insulation. ....	61
Figure 4-12. Schematics for the heat-transfer analysis with (a) cavity completely filled; (b) two-thirds of the cavity depth filled; and (c) insulation strip applied on the lateral side of the timber member. ....	63
Figure 4-13. Effective thermal properties for HTE 2: (a) conductivity, (b) specific heat, and (c) loss in density as a function of the temperature. ....	64
Figure 4-14. Position of the 300°C isotherm on the interface between wood and insulation ( $d_{300,s}$ ) as a function of the time evaluated by means of heat-transfer analysis.....	65
Figure 4-15. (a) Reduction of the moment of inertia as predicted by heat-transfer analysis compared to fire tests results. ....	66
Figure 4-16. Temperatures recorded by thermocouples in comparison to simulation results at (a) a depth of 12 mm, and (b) a depth of 24 mm in the middle of the timber cross-section; at (c) a depth of 50 mm, and (d) a depth of 100 mm on the wood-insulation interface. ....	67
Figure 4-17. Position of the 300°C isotherm in the middle of the cross-section ( $d_{300,m}$ ) as a function of time for Test 3, Test 4, and Simulation 10.....	67
Figure 5-1. Zero-strength layers in the improved design model for TFA with (a) PL1 cavity insulation; with PL2 cavity insulation (b) before, and (c) after that start time of charring from lateral sides has occurred. ....	68
Figure 5-2. Effective thermal properties of SW and GW according to Schleifer (2009): (a) conductivity, (b) specific heat, and (c) loss in density as a function of the temperature...	70

Figure 5-3. Reduction of the bending moment capacity ( $M_{fi}/M_{20^{\circ}C}$ ) against the time for TFA with HTE 2 as a form of cavity insulation. A comparison of different (a) timber widths, (b) timber depths, (c) cladding types, and (d) fall-off times of the cladding.....	72
Figure 5-4. Depth of the zero-strength layer for members which are bending for (a) different member width, and (b) depth, (c) different thickness of gypsum plasterboard, (d) different fall-off times of the cladding and (e) different forms of cavity insulation..	74
Figure 5-5. Bending moment capacity reduction, section modulus reduction, and the depth of zero-strength layers as a function of the time for an assembly that is insulated with stone wool. ....	76
Figure 5-6. Zero-strength layers calculated by means of numerical simulations compared to the models proposed for assemblies that have been insulated with stone wool. A comparison for (a) bending members with the tension side that has been exposed to fire, and (b) compression members with in-plane buckling.....	77
Figure 5-7. Reduction of the load-bearing capacity for out-of-plane buckling ( $N_{crit,II}/N_{20^{\circ}C}$ ) as predicted by the improved design model when compared to the critical normal force of members with an initial deformation that is subjected to combined axial compression and bending.....	79
Figure 5-8. The depth of the zero-strength layer as evaluated by means of thermo-mechanical simulations and being compared to the simplified and optimised approaches.....	81
Figure 5-9. Longitudinal view of the specimens used in the loaded cubic metre furnace tests. ....	82
Figure 5-10. Charring depth on the wood-insulation interface ( $d_{300,s}$ ) as a function of time for Test 38 and Test 39. ....	84
Figure 5-11. Pictures of (a) the wall, and (b) the floor specimens during the mounting process. ....	85
Figure 5-12. Load-bearing reduction as a function of the time predicted by the improved design model when compared to the load applied on (a) the wall specimen and (b) the floor specimen during the full-scale furnace tests .....	86
Figure 5-13. Factor $k_{3,1}$ as a function of the fall-off time ( $t_f$ ) as evaluated from full-scale test results.....	87
Figure 5-14. Schematics for the cross-section of full-scale wall specimens tested at MPFA Leipzig. ....	88
Figure 5-15: Rupture of the load-bearing members as predicted by the improved design model against evaluation by testing. ....	90
Figure 5-16. (a) predicted fire resistance times according to the improved design model, and (b) the percentage of the predicted fire resistance time with respect to the tested fire resistance time .....	91
Figure 5-17. Reduction of the load-bearing capacity against the time for TFA with stone wool as a form of cavity insulation according to Eurocode 5 Part 1-2 and the improved design model.....	93
Figure 6-1. The position of the thermocouples which were considered when it came to evaluating the length of time it takes for the cavity insulation to fall off.....	96
Figure 6-2. Fall-off time of the cavity insulation against the length of time it takes for the cladding to fall off. ....	97
Figure 6-3. Percentage distribution of the countries that returned questionnaires. ....	98
Figure 6-4. The distribution percentage of (a) fixing methods, and (b) over-dimensioning of the batt width for a batt-type insulation in floor elements.....	99

Figure 6-5. The reasons for using fixations systems for batt-type insulations installed in floor elements. ....	100
Figure 6-6. The distribution percentage of (a) fixing methods, (b) the over-dimensioning of the batt width, and (c) the reasons for using fixations systems for batt-type insulation in wall elements. ....	102
Figure 6-7. The distribution percentage of (a) fixing methods, and (b) the reasons for using fixations systems for loose-fill insulation in floor elements. ....	103
Figure 6-8. The distribution percentage of fixing methods for loose-fill insulation in wall elements. ....	104
Figure 6-9. The limit to the sum of the protection times for the layers preceding the insulation layer and the insulation layer as a function of the insulation layer's depth and fall-off time of the cladding for insulation material qualified as PL 1. ....	106

## List of Tables

Table 3-1. Batt-type insulation materials which have been selected for this study. ....	33
Table 3-2. Overview of cubic metre tests carried out in the first test programme. ....	36
Table 3-3. An overview of cubic metre tests carried out with loose-fill cavity insulations. ....	46
Table 4-1. An overview of cubic metre tests carried out in the second test programme... ..	49
Table 4-2. Cross-section factors, $k_s$ , which were evaluated for this study.....	50
Table 4-3. Investigated set-ups for the definition of the post-protection coefficient for generic SW products. ....	60
Table 4-4. Investigated set-ups for TFA with cavities partially filled by insulation. ....	63
Table 5-1. Cladding on the fire-exposed side of the set-ups being investigated. ....	71
Table 5-2. Additional set-ups which were investigated for TFA that was insulated with HTE 2. ....	71
Table 5-3. Overview of the loaded tests that were carried out. ....	82
Table 5-4. Results for the loaded cubic metre furnace tests. ....	83
Table 5-5. Overview of the full-scale tests that were analysed. ....	89
Table 5-6. The results of the full-scale tests that were analysed.....	89
Table 6-1. Requirements to prevent fall-off of the cladding during the post-protection phase according to the FSITB guideline. ....	95

## References

- Andersson, L., and Jansson, B. (1987). Analytical fire design with gypsum—a theoretical and experimental study. *Institute of Fire Safety Design, Lund, Sweden*.
- Ang, C., and Wang, Y. (2009). Effect of moisture transfer on specific heat of gypsum plasterboard at high temperatures. *Construction and Building Materials*, 23(2), 675–686.
- Autodesk. (2011). R11 Reference Manual AutoCAD. *Autodesk, Guildford Sturey*.
- Bénichou, N. (2006). Predicting the structural fire performance of solid wood-framed floor assemblies. In *Proceedings of SiF'06: Fourth International Workshop Structures in Fire* (p. 909).
- Bénichou, N., and Sultan, M. A. (2003). Design considerations for fire resistance performance of lightweight-framed assemblies. In *CSCCE 2003, Annual Conference* (pp. 567–1 – 567–10). Moncton.
- Bénichou, N., and Sultan, M. A. (2004). Fire resistance behavior of lightweight-framed construction. In *Structures in Fire: Proceedings of the 3rd International Workshop* (pp. 119–136). Ottawa.
- Bénichou, N., and Sultan, M. A. (2005a). Behaviour of lightweight-framed timber construction under elevated temperatures. In *APEC Seminar-Fire Performance of Timber Construction, Wellington, NZ* (pp. 1–12).
- Bénichou, N., and Sultan, M. A. (2005b). Thermal properties of lightweight-framed construction components at elevated temperatures. *Fire and Materials*, 29(3), 165–179.
- Bénichou, N., Sultan, M. A., and Kodur, V. R. (2003). Fire Resistance Performance of Lightweight Framed Wall Assemblies: Effects of Various Parameters, Key Design Considerations and Numerical Modeling. In *Proceedings of Fire and Materials 2003 Conference* (p. 9).
- Board, A. B. C. National Construction Code Standards Australia (2015).
- Buchanan, A. H., and Abu, A. K. (2017). *Structural Design for Fire Safety* (2nd ed.). Wiley. Retrieved from <https://www.wiley.com/en-us/Structural+Design+for+Fire+Safety%2C+2nd+Edition-p-9780470972892>
- Bynum, R. T. (2001). *Insulation Handbook*. McGraw-Hill Professional. <https://doi.org/10.1036/0071414614>
- Cachim, P. B., and Franssen, J.-M. (2009). Comparison between the charring rate model and the conductive model of Eurocode 5. *Fire and Materials*, 33(3), 129–143.
- CEN, European Committee for Standardization. Fire resistance tests for load-bearing elements - Part 1: Walls, EN 1365-1:1999 § (1999).
- CEN, European Committee for Standardization. Fire resistance tests for load-bearing elements - Part 2: Floors and roofs, EN 1365-2:2000 § (2000).
- CEN, European Committee for Standardization. Eurocode 1 - General Actions – Part 1-2 - Actions on structures exposed to fire, EN 1991-1-2:2003 § (2003).

- CEN, European Committee for Standardization. Eurocode 5 - Design of timber structures - Part 1-1 - General. Common rules and rules for buildings, EN 1995-1-1:2004 § (2004).
- CEN, European Committee for Standardization. Eurocode 5 - Design of timber structures - Part 1-2 - General: Structural fire design, EN 1995-1-2:2004 § (2004).
- CEN, European Committee for Standardization. Gypsum plasterboards - Definitions, requirements and test methods, EN 520:2004 § (2004).
- CEN, European Committee for Standardization. Fire classification of construction products and building elements. Classification using test data from reaction to fire tests, EN 13501-1:2007 § (2007).
- CEN, European Committee for Standardization. Structural timber - Strength classes, EN 338:2009 § (2009).
- CEN, European Committee for Standardization. Fire resistance tests - Part 1: General Requirements, EN 1363-1:2012 § (2012).
- CEN, European Committee for Standardization. Thermal insulating products for building applications. Determination of thickness, EN 823:2013 § (2013).
- CEN, European Committee for Standardization. Thermal insulation products for buildings - Factory made mineral wool (MW) products - Specification, EN 13162:2013 § (2013).
- CEN, European Committee for Standardization. Test method to determine the contribution to the fire resistance of structural members - Part 7: Applied protection to timber members, EN 13381-7 §.
- Coats, A. W., and Redfern, J. P. (1963). Thermogravimetric analysis. A review. *Analyst*, 88(1053), 906–924. <https://doi.org/10.1039/AN9638800906>
- Collier, P., and Buchanan, A. (2002). Fire resistance of lightweight timber framed walls. *Fire Technology*, 38(2), 125–145.
- CSTB, Centre Scientifique et Technique du Bâtiment. (2009). Isolation thermique des combles: isolation en laine minérale faisant l’objet d’un Avis Technique ou d’un Constat de Traditionalité.
- Dassault Systèmes Simulia. (2012). *Abaqus CAE User’s Manual, Abaqus 6.12*.
- Deutsches Institut für Normung. Brandverhalten von Baustoffen und Bauteilen; Bauteile, Begriffe, Anforderungen und Prüfungen, DIN 4202-2 § (1977).
- Deutsches Institut für Normung. Brandverhalten von Baustoffen und Bauteilen Schmelzpunkt von Mineralfaser-Dämmstoffen Begriffe, Anforderungen, Prüfung.pdf, DIN 4102-17 § (2016).
- Frangi, A. (2001). *Brandverhalten von Holz-Beton-Verbunddecken*. ETH Zurich.
- Frangi, A., Erchinger, C., and Fontana, M. (2008). Charring model for timber frame floor assemblies with void cavities. *Fire Safety Journal*, 43(8), 551–564. <https://doi.org/10.1016/j.firesaf.2007.12.009>

- Frangi, A., and König, J. (2011). Effect of increased charring on the narrow side of rectangular timber cross-sections exposed to fire on three or four sides. *Fire and Materials*, 35(8), 593–605. <https://doi.org/10.1002/fam.1078>
- Franssen, J.-M. (2005). SAFIR: A thermal/structural program for modeling structures under fire. *Engineering Journal-American Institute of Steel Construction Inc*, 42(3), 143–158.
- Fredlund, B. (1988). A model for heat and mass transfer in timber structures during fire: a theoretical, numerical and experimental study.
- Gammon, B. W. (1988). Reliability analysis of wood-frame wall assemblies exposed to fire.
- Gerhards, C. C. (1982). Effect of moisture content and temperature on the mechanical properties of wood: an analysis of immediate effects. *Wood and Fiber Science*, 14(1), 4–36.
- Glos, P., and Henrici, D. (1991). *Festigkeit von Bauholz bei hohen Temperaturen*. Munich: Institut für Holzforschung der Universität München.
- Gustafsson, S. E. (1991). Transient plane source techniques for thermal conductivity and thermal diffusivity measurements of solid materials. *Review of Scientific Instruments*, 62(3), 797–804.
- Hadvig, S. (1981). *Charring of Wood in Building Fires: practice, theory, instrumentation, measurements*. Technical University of Denmark, Laboratory of Heating and Air-conditioning.
- Healy, J., De Groot, J., and Kestin, J. (1976). The theory of the transient hot-wire method for measuring thermal conductivity. *Physica B+ C*, 82(2), 392–408.
- Höhne, G. W. H., Hemminger, W., and Flammersheim, H.-J. (1996). Theoretical fundamentals of differential scanning calorimeters. In *Differential Scanning Calorimetry* (pp. 21–40). Springer.
- Hopkin, D., El-Rimawi, J., Silberschmidt, V., and Lennon, T. (2011). An effective thermal property framework for softwood in parametric design fires: Comparison of the Eurocode 5 parametric charring approach and advanced calculation models. *Construction and Building Materials*, 25(5), 2584–2595.
- Hopkin, D., Lennon, T., El-Rimawi, J., and Silberschmidt, V. (2012). A numerical study of gypsum plasterboard behaviour under standard and natural fire conditions. *Fire and Materials*, 36(2), 107–126.
- ISO International Organization for Standardization. Thermal insulation—determination of steady-state thermal resistance and related properties—guarded hot-plate apparatus, ISO 8302:1991 § (1991).
- ISO International Organization for Standardization. Fire Resistance Tests – Elements of Building Construction – Part 1: General Requirements., ISO 834–1:1999 § (1999).
- Janssens, M. (1994). Thermo-physical properties for wood pyrolysis models. In *Pacific Timber Engineering Conference* (pp. 607–618).

- Just, A. (2010a). Post protection behaviour of wooden wall and floor structures completely filled with glass wool. In *Proceedings of the 6th international conference Structures in Fire: Structures in Fire, East Lansing, USA* (Vol. 2, p. 2010).
- Just, A. (2010b). *Structural fire design of timber frame assemblies insulated by glass wool and covered by gypsum plasterboard*. Tallinn University of Technology, Tallinn, Estonia.
- Just, A. (2010c). *The effect of the insulation on charring of timber frame members* (No. SP report 2010:30). Stockholm: SP Technical research institute of Sweden.
- Just, A., Schmid, J., and König, J. (2012). Post-protection effect of heat-resistant insulations on timber-frame members exposed to fire. *Fire and Materials*, 36(2), 153–163.
- Just, A., Schmid, J., Werther, N., and Frangi, A. (2014). Fire protection of timber members – determination of the fire protection system characteristics for the verification of the load-bearing resistance by means of calculation models (pp. 567–576). Presented at the 8th International Conference on Structures in Fire, Shanghai, China: Guo-Qiang LI, Venkatesh K. R. KODUR, Shou-Chao JIANG, Jian JIANG, Su-Wen CHEN, Guo-Biao LOU (Eds.).
- Keerthan, P., and Mahendran, M. (2012). Numerical studies of gypsum plasterboard panels under standard fire conditions. *Fire Safety Journal*, 53, 105–119.
- Klippel, M. (2014). *Fire safety of bonded structural timber elements* (PhD Thesis). ETH Zurich.
- Klippel, M., and Schmid, J. (2017). Design of Cross-Laminated Timber in Fire. *Structural Engineering International*, 27(2), 224–230. <https://doi.org/10.2749/101686617X14881932436096>
- Kolaitis, D. I., Asimakopoulou, E. K., and Founti, M. A. (2014). Fire protection of light and massive timber elements using gypsum plasterboards and wood based panels: A large-scale compartment fire test. *Construction and Building Materials*, 73, 163–170.
- Kollmann, F. (1951). Über das mechanische Verhalten von Kiefernholz bei Biegung und Temperaturen zwischen 20 und 100 C. *Svenska Träforskningsinstitutet, Trätekniska Avdelningen, Meddelande*, 22.
- König, J. (1995). *Fire resistance of timber joists and load bearing wall frames* (No. I 9412071). Swedish Institute for Wood Technology Research.
- König, J. (1999). *One-dimensional charring of timber exposed to standard and parametric fires in initially unprotected and postprotection situations*.
- König, J. (2005). Structural fire design according to Eurocode 5—design rules and their background. *Fire and Materials*, 29(3), 147–163.
- König, J. (2006). Effective thermal actions and thermal properties of timber members in natural fires. *Fire and Materials*, 30(1), 51–63.
- König, J., Norén, J., Olesen, F. B., and Hansen, F. T. (1997). Timber Frame Assemblies Exposed to Standard and Parametric Fires: Part 1, Fire Tests.

- König, J., and Schmid, J. (2010). Light timber frame construction with solid timber members. In *CIB-W18 Meeting 43*. Nelson, New Zealand.
- König, J., and Walleij, L. (2000). *Timber Frame Assemblies Exposed to Standard and Parametric Fires – Part 2 A design model for standard fire exposure* (No. Rapport 0001001). Stockholm: Institutet för Träteknisk Forskning.
- Kraudok, K. (2015). *Protective effect of gypsum plasterboards for the fire design of timber structures*. Tallinn University of Technology, Tallinn, Estonia.
- Liblik, J., and Just, A. (2017). Design parameters for timber members protected by clay plaster at elevated temperatures. In *International Network on Timber Engineering Research (INTER), Meeting 50* (pp. 375–389). Kyoto, Japan: Ed. Görlacher, R. Karlsruhe: Forschungszentrum Karlsruhe.
- Lie, T. T. (1977). A method for assessing the fire resistance of laminated timber beams and columns. *Canadian Journal of Civil Engineering*, 4(2), 161–169. <https://doi.org/10.1139/l77-021>
- Madenci, E., and Guven, I. (2015). *The finite element method and applications in engineering using ANSYS®*. Springer.
- Mäger, K. N. (2016). *Implementation of new materials to the component additive method for fire design of timber structures*. Tallinn University of Technology, Tallinn, Estonia.
- Mäger, K. N., Just, A., and Frangi, A. (2018). Improvements to the components additive method. In *Proceedings of SiF 2018: 10th International Conference Structures in Fire* (pp. 283–290). Belfast, UK.
- Mäger, K. N., Just, A., Schmid, J., Werther, N., Klippel, M., Brandon, D., and Frangi, A. (2017). Procedure for implementing new materials to the component additive method. *Fire Safety Journal*. <https://doi.org/10.1016/j.firesaf.2017.09.006>
- Mehaffey, J., Cuerrier, P., and Carisse, G. (1994). A model for predicting heat transfer through gypsum-board/wood-stud walls exposed to fire. *Fire and Materials*, 18(5), 297–305.
- Menis, A., Fragiaco, M., and Clemente, I. (2012). Numerical Investigation of the Fire Resistance of Protected Cross-Laminated Timber Floor Panels. *Structural Engineering International*, 22(4), 523–532. <https://doi.org/10.2749/101686612X13363929517659>
- Mikkola, E. (1991). Charring of wood based materials. *Fire Safety Science*, 3, 547–556.
- Moss, P. J., Buchanan, A. H., and Fragiaco, M. (2009). Predicting the behaviour of timber connections subjected to fire. In *Proceedings of the 20th Australasian Conference on the Mechanics of Structures and Materials* (pp. 857–863).
- Neely, S. (1898). Relation of compression-endwise to breaking load of beam. *Progress in Timber Physic: USDA Division of Forestry*, 13–7.
- Olsson, A., and Oscarsson, J. (2016). Strength grading based on high resolution laser scanning – performance of a procedure newly approved for the European market. *European Journal of Wood and Wood Products*, 232–240. <https://doi.org/10.1007/s00107-016-1102-6>

- Östman, B. A.-L. (1985). Wood tensile strength at temperatures and moisture contents simulating fire conditions. *Wood Science and Technology*, 19(2), 103–116.
- Östman, B. A.-L., Mikkola, E., Stein, R., Frangi, A., König, J., Dhima, D., ... Bregulla, J. (2010). *Fire safety in timber buildings: technical guideline for Europe*. Borås, Sweden: SP Technical Research Institute of Sweden.
- Papadopoulos, A. M. (2004). Design and Development of Innovative Stone-wool Products for the Energy Upgrading of Existing and New Buildings. *Project Interim Report, Thessaloniki*.
- Papadopoulos, A. M. (2005). State of the art in thermal insulation materials and aims for future developments. *Energy and Buildings*, 37(1), 77–86.
- Peitzmeier, J. (2017a). *Prüfbericht Nr. PB 3.2/16-001-1* Ä. MFPA Leipzig GmbH.
- Peitzmeier, J. (2017b). *Prüfbericht Nr. PB 3.2/16-001-3* Ä. MFPA Leipzig GmbH.
- Peitzmeier, J. (2017c). *Prüfbericht Nr. PB 3.2/16-001-4* Ä. MFPA Leipzig GmbH.
- Peitzmeier, J. (2017d). *Prüfbericht Nr. PB 3.2/16-001-5* Ä. MFPA Leipzig GmbH.
- Peitzmeier, J. (2017e). *Prüfbericht Nr. PB 3.2/16-001-6*. MFPA Leipzig GmbH.
- Peitzmeier, J. (2017f). *Prüfbericht Nr. PB 3.2/16-001-7* Ä. MFPA Leipzig GmbH.
- Peitzmeier, J. (2017g). *Prüfbericht Nr. PB 3.2/16-001-8* Ä. MFPA Leipzig GmbH.
- Richardson, L., and McPhee, R. (1996). Fire-resistance and Sound-transmission-class Ratings for Wood-frame Walls. *Fire and Materials*, 20(3), 123–131.
- Richardson, L., McPhee, R., and Batista, M. (2000). Sound-transmission-class and fire-resistance ratings for wood-frame floors. *Fire and Materials*, 24(1), 17–27.
- Salmon, D. (2001). Thermal conductivity of insulations using guarded hot plates, including recent developments and sources of reference materials. *Measurement Science and Technology*, 12(12), R89.
- Schaffer, E. L. (1967). *Charring rate of selected woods-transverse to grain*. Forest products lab Madison Wis.
- Schaffer, E. L., Marx, C. M., Bender, D. A., and Woeste, F. E. (1986). *Strength validation and fire endurance of glued-laminated timber beams*. US Department of Agriculture, Forest Service, Forest Products Laboratory.
- Schleifer, V. (2009). *Zum Verhalten von raumabschliessenden mehrschichtigen Holzbauteilen im Brandfall* (PhD Thesis). ETH Zurich.
- Schmid, J., and König, J. (2010). *Cross-laminated timber in fire* (No. 2010:11). SP - Sveriges Tekniska Forskningsinstitut, SP Trä.
- Schmid, J., König, J., and Köhler, J. (2010). Fire-exposed cross-laminated timber-Modelling and tests. In *World Conference on Timber Engineering*.
- Standards New Zealand. *The New Zealand Building Code* (2012).
- Sultan, M. A. (1996). A model for predicting heat transfer through noninsulated unloaded steel-stud gypsum board wall assemblies exposed to fire. *Fire Technology*, 32(3), 239–259.

- Sultan, M. A. (2008). Fire resistance of wood joist floor assemblies. *Fire Technology*, 44(4), 383–417.
- Sultan, M. A., Latour, J., Leroux, P., Monette, R., Seguin, Y., and Henrie, J. (2005). *Results of Fire Resistance Tests on Full-Scale Floor Assemblies-Phase II*.
- Sultan, M. A., and Lougheed, G. D. (2002). *Results of Fire Resistance Tests on Full-Scale Gypsum Board Wall Assemblies*. Retrieved from <http://dx.doi.org/10.4224/20378755>
- Sultan, M. A., Seguin, Y., and Leroux, P. (1998). *Results of Fire Resistance Tests on Full-Scale Floor Assemblies* (No. IR-764). Institute for Research in Construction.
- Takeda, H., and Mehaffey, J. (1998). WALL2D: A model for predicting heat transfer through wood-stud walls exposed to fire. *Fire and Materials*, 22(4), 133–140.
- Theiler, M., Frangi, A., and Steiger, R. (2013). Strain-based calculation model for centrally and eccentrically loaded timber columns. *Engineering Structures*, 56, 1103–1116. <https://doi.org/10.1016/j.engstruct.2013.06.032>
- Thomas, G. C. (2002). Thermal properties of gypsum plasterboard at high temperatures. *Fire and Materials*, 26(1), 37–45.
- Thomas, G. C. (2010). Modelling thermal performance of gypsum plasterboard-lined light timber frame walls using SAFIR and TASEF. *Fire and Materials*, 34(8), 385–406.
- Thomas, G. C., Buchanan, A., Carr, A., Fleischmann, C., and Moss, P. (1995). Light timber-framed walls exposed to compartment fires. *Journal of Fire Protection Engineering*, 7(1), 15–25.
- Wakili, K. G., and Hugi, E. (2009). Four types of gypsum plaster boards and their thermophysical properties under fire condition. *Journal of Fire Sciences*, 27(1), 27–43.
- Walton, W. D., Thomas, P. H., and Ohmiya, Y. (2016). Estimating Temperatures in Compartment Fires. In *SFPE Handbook of Fire Protection Engineering* (pp. 996–1023). Springer, New York, NY. [https://doi.org/10.1007/978-1-4939-2565-0\\_30](https://doi.org/10.1007/978-1-4939-2565-0_30)
- Werther, N. (2016). *Einflussgrößen auf das Abbrandverhalten von Holzbauteilen und deren Berücksichtigung in empirischen und numerischen Beurteilungsverfahren* (Dissertation). Technische Universität München, München.
- Westergaard, M. (2010, February). Energy efficiency in historic buildings - Insulating timber-framed walls. English Heritage. Retrieved from [www.english-heritage.org.uk](http://www.english-heritage.org.uk)
- Wickström, U. (1979). *TASEF-2: A Computer Program for Temperature Analysis of Structures Exposed to Fire*. Lund Institute of Technology, Department of Structural Mechanics.
- Wickström, U. (2016). *Temperature calculation in fire safety engineering*. Springer.
- Winter, S., and Meyn, W. (2009). Advanced Calculation Method for the Fire Resistance of Timber Framed Walls. In *Proceedings of CIB-W 18 meeting 42* (pp. 357–367). Dubendorf, Switzerland.
- Young, W. C., and Budynas, R. G. (2002). *Roark's formulas for stress and strain* (Vol. 7). McGraw-Hill New York.

## Acknowledgements

As much as I can attempt to find the best forms of acknowledgment, I will never cease to be grateful to all of those who have supported this work in any way.

Firstly, I would like to express my deepest gratitude to my supervisor, Professor Alar Just, for being a great teacher and for your endless encouragement. This work would never have been possible without your guidance and motivation.

I would like also to thank Massimo Fragiaco as my co-supervisor.

For your precious collaboration, I am profoundly grateful to Joachim Schmid and Michael Klippel.

My thanks also go to my Estonian colleagues, Johanna Liblik, Katrin Nele Mäger, and Andres Ollino, trustworthy companions of somewhat crazy work experiences and unforgettable moments.

I would like to thank all my colleagues at the RISE Research Institute of Sweden: Birgit Östman, Daniel Brandon, Lazaros Tsantaridis, and Joakim Noren. But a very special thank must go to Magdalena Sterley for always being present when needed.

My sincere thanks also go to the official referees of the work, Andrea Frangi and Norman Werther.

I would like to thank Leif Andersson, Rebecca Bremen, Cristian Ciucasu, Carole Durantet, Andreas Köhler, Nicolas Legendre, Olivier Pons Y Moll, and Torsten Wahls for their support in this project.

I am grateful to the COST Action FP 1404 for contribution to my Short Term Scientific Missions and for fruitful discussions within the Task Group 5 of the Working Group 2.

I am very grateful for the support of Svenska Termoträ, Danish Wood Insulations, the Estonian Research Council (Grant PUT 794), and the Archimedes Foundation.

I am also grateful to Michael Rauch, Florian Schmidt-Hieber, and the Holzbau Deutschland Institut for their help with the survey.

A thank you goes to Flavia Morelli and Anna Predonzani for their contributions to this work with their Master's thesis.

To my friends scattered around Europe, thank you for being there whenever I needed a friend.

For being my very earliest and proudest supporters, and for inspiring me to follow my dreams, grazie mamma e papà. A thank you also goes to my sister, Giada, for her visits, texts, and phone calls.

For her patience in these years in which I have been abroad and in her continuous sustainment of my plans, I owe a lot to Chiara, my better half.

*Mattia Tiso*

August 2018

## Lühikokkuvõte

### Isolatsioonimaterjalide mõju puitkarkass-seinte ja -vahelagede kandevõimele tules

Kasutatavad isolatsioonimaterjalid võivad mõjutada puitkarkasskonstruktsioonide tulepüsivust. Kehtiva Eurokoodeksi 5 osa 1–2 sisaldab mudelit täielikult kivivillaga täidetud tühimikega puitkarkasskonstruktsioonide kandevõime arvutamiseks tulekahju korral. Euroopa tehnilises juhendis *Fire Safety in Timber Buildings* on avaldatud selle mudeli laiendatud versioon, mis käsitleb järelkaitsefaasis klaasvillaga täidetud tühimikega puitkarkasskonstruktsioone. Olemasolevad teadmised teiste isolatsioonimaterjalide tagatava kaitse kohta on aga piiratud. Siinses doktoritöös pakutakse välja uudne projekteerimismeetod, mis võimaldab arvutuslikult hinnata suurema hulga isolatsioonimaterjalide tagatavat potentsiaalset tulekaitset. Meetod hõlmab isolatsioonimaterjalide liigitusmetodoloogiat ja täiustatud projekteerimismudelit.

Töö käigus uuriti ühe kuupmeetri suuruses põletusahjus kokku 14 erinevat isolatsioonimaterjali. Katsetulemused kinnitasid, et 300 °C isotermi kujunemine puitelemendi külgedel näitab, et isolatsioonimaterjal kaitseb puitelementi söestumise eest. Saadud tulemuste põhjal pakutakse välja liigitusmetodoloogia, mis hõlmab isolatsioonimaterjalide kolme tulepüsivuse taset.

Kolme isolatsioonimaterjaliga 14st tehti mudelahjus täiendav katsete seeria. Nende katsete tulemuste põhjal tuletati täiustatud projekteerimismudelisse kasutatavad söestumistegurid. Doktoritöö sisaldab söestumistegurite tuletamiseks kasutatud menetluse üksikasjalikku kirjeldust.

Täiustatud projekteerimismudel järgib efektiivristlõikemeetodi põhimõtteid, mis tähendab, et puitelemendi efektiivristlõike arvutamiseks tulekahju olukorras vähendatakse elemendi algset ristlõiget nominaalse söestumise ja niinimetatud null-tugevusega kihi võrra. Seejärel hinnatakse elemendi kandevõimet, lähtudes selle efektiivristlõikest ja normaaltemperatuurile kohastest mehaanilistest omadustest. Doktoritöös määratakse mitmete termomehaaniliste simulatsioonide alusel erinevaid isolatsioonimaterjale kasutatavate puitkarkasskonstruktsioonide null-tugevusega kihtide väärtused. Esitatakse kaks erinevat lähenemisviisi null-tugevusega kihi väärtuse määramiseks.

Täiustatud projekteerimismeetodi kontrollimiseks tehti kaks täismõõdus katset ja varasemate katsetulemuste analüüs.

Ühtlasi esitatakse doktoritöös projekteerimisjuhised, mis võimaldavad välja töötatud projekteerimismudelit kasutada ka osaliselt isolatsioonimaterjaliga täidetud tühimikega puitkarkasskonstruktsioonide tulepüsivuse prognoosimiseks. Lisaks antakse ülevaade uurimistööst, mis tuleb teha selliste meetmete uurimiseks, millega takistada isolatsioonimaterjalide varisemist tulekahju olukorras.

Dokoritöö laiendab olemasolevaid teadmisi puitkarkasskonstruktsioonide tulepüsivusarvutustest, pakkudes eeskätt välja üldisema meetodi isolatsioonimaterjalide panuse arvutamiseks konstruktsioonide tulepüsivusse.

**Võtmesõnad:** puitkarkasskonstruktsioonid, isolatsioonimaterjalid, tulepüsivus, tulepüsivusarvutus, tulekaitse, puitelemendid, söestumiskiirus, null-tugevusega kiht

## Abstract

### The contribution of cavity insulations to the load-bearing capacity of timber frame assemblies exposed to fire

Insulation materials have the potential to alter the fire resistance of timber frame assemblies (TFA). At present, Eurocode 5 Part 1-2 provides a model for the fire design of the load-bearing function of timber frame assemblies with cavities that are completely filled with stone wool. The extension of this model for TFA with cavities that are filled with glass wool in a post-protection phase was published in the European Technical Guideline, *Fire Safety in Timber Buildings*. However, very little is known about the form of protection which is afforded by other insulation materials. In order to be able to include the potential fire protection being provided by a wider range of cavity insulation products, a new design approach is presented in this thesis. This design approach comprises a qualification methodology for the insulation materials and an improved design model.

Fourteen different insulation materials have been studied by means of a cubic metre furnace. The results showed that the development of the 300°C isotherm on the sides of the timber member is an indicator of the protection being provided by specific forms of cavity insulation against the charring on the timber member. As a result of these findings, the qualification methodology which includes three levels of protection for the fire performance of batt-type insulation materials is proposed.

Three out of fourteen forms of insulation material were selected for a second series of cubic metre furnace tests. Factors involving the charring which were included in the improved design model were derived from the results of the second series of tests. The procedure is explained in the thesis which was followed in order to be able to derive those factors which are involved in the charring.

The improved design model follows the principles of the Effective Cross-Section Method (ECSM), where an effective cross-section of a timber member in fire is calculated by decreasing the original cross-section by a notional charring depth and what is known as a zero-strength layer. Then the load-bearing capacity can be evaluated by applying the mechanical properties at ambient temperature to this effective cross-section. In this thesis, the zero-strength layers for TFA with different forms of cavity insulation product are determined by means of a series of thermal and mechanical simulations. Two approaches are proposed in order to determine the design values of zero-strength layers for TFA with different forms of cavity insulation product. To be able to validate the improved design model, two full-scale tests have been carried out, along with an analysis of existing test reports.

Furthermore, design proposals are provided which also allow the use of the improved design model to predict the fire resistance of TFA with cavities which have partially been filled by insulation materials. Insights are also provided into the investigations required to be able to study measures which will prevent cavity insulation material from falling off under fire conditions.

This thesis extends the existing levels of knowledge regarding the fire design of timber frame assemblies, in particular providing a more generic method to be able to consider the contribution being made to those fire resistance levels which are provided by the insulation materials.

**Keyword:** timber frame assembly, insulation materials, fire resistance, fire design, fire protection, timber elements, charring rate, zero-strength layer

## Abstract

### Il contributo dei materiali isolanti nella capacità portante di costruzioni intelaiate in legno esposte al fuoco

I materiali isolati possono alterare la resistenza al fuoco di costruzioni intelaiate in legno. Un modello analitico per valutare la capacità portante in condizione d'incendio di sistemi a telaio in legno con le cavità riempite di lana di roccia è inserito nell'attuale Eurocodice 5 Parte 1-2. Un'estensione di questo modello per costruzioni intelaiate con cavità riempite di lana di vetro è pubblicato nelle linee guida europee *Fire Safety in Timber Buildings*. Tuttavia, in letteratura non si trovano informazioni riguardanti il contributo offerto da altri materiali isolanti. In questa tesi è presentato un nuovo approccio di progettazione che considera il potenziale contributo anticendio offerto da altri materiali isolanti. Questo approccio è composto da una metodologia di qualificazione per i materiali isolanti e un'evoluzione del modello analitico per la progettazione.

Quattordici diversi tipi di materiale isolante sono stati studiati per mezzo di una fornace con dimensioni interne pari a un metro cubo. I risultati hanno dimostrato che l'andamento dell'isoterma dei 300°C valutata ai lati della trave lignea può essere considerato come un indicatore della protezione contro la carbonizzazione offerta dal materiale isolante. Di conseguenza è stata proposta una metodologia di qualificazione che include tre diversi livelli di protezione per caratterizzare le prestazioni in condizioni d'incendio di un materiale isolante.

Tre materiali isolanti sono stati selezionati tra i primi quattordici per una seconda serie di prove al fuoco. Dai risultati della seconda serie di test sono stati derivati i coefficienti per valutare la carbonizzazione attraverso il modello di progettazione migliorato. I criteri utilizzati per derivare i coefficienti sono inclusi nella tesi.

Il modello di progettazione migliorato segue i principi del metodo della sezione efficace dove la sezione efficace di un elemento in legno in condizioni d'incendio viene calcolata sottraendo dalla sezione originale una profondità di carbonizzazione nozionale e un ulteriore strato per il quale viene considerata una resistenza meccanica nulla (chiamato anche strato a resistenza zero). A questo punto la capacità portante viene calcolata applicando le proprietà meccaniche del legno a temperatura ambiente a questa sezione efficace. In questa tesi sono state valutate, attraverso simulazioni termo-meccaniche, le profondità dello strato a resistenza zero per costruzioni in legno intelaiate con applicati diversi tipi di materiali isolanti. Sono poi proposti due diversi approcci per determinare valori di progetto di strati a resistenza zero per costruzioni in legno intelaiate. Il modello di progettazione migliorato è stato validato per mezzo di due prove in scala reale, appositamente effettuate e un'analisi di rapporti di prove già effettuate in passato.

Sono inoltre forniti criteri di progettazione anticendio per sistemi intelaiati con cavità parzialmente riempite da materiale isolante. Sono proposti anche suggerimenti per una futura investigazione sulla caduta dei materiali isolanti in condizione d'incendio.

Questa tesi estende le conoscenze esistenti riguardo alla progettazione anticendio di costruzioni intelaiate in legno, in particolare fornisce un metodo più generico per considerare il contributo alla resistenza al fuoco offerto dai materiali isolanti.

**Parole chiave:** costruzioni intelaiate in legno, materiali isolanti, resistenza al fuoco, progettazione anticendio, protezione anticendio, elementi in legno, velocità di carbonizzazione, strato a resistenza zero



## Appendix

English version of the survey on the currently used fixation systems for cavity insulation in timber frame assemblies.



Methods of fixing cavity insulation in timber frame assemblies

Insulation slabs installed in floor elements

**The following questions refer to insulation slabs installed in floor elements**

1. Which method do you normally use to fix the insulation slab in the cavities?

Over dimensioning of the slab width compared to the cavity width

Screws or other mechanical fixations through the insulation slab

Adhesive or glue

Steel net or another type of net

Transversal battens or resilient channels

None of them (or other)

1



2. In case of over dimensioning of the slab width, which is the over dimensioning?

- Less than 5 mm
- Between 5 and 10 mm
- More than 10 mm



3. In case of adhesive or glue:

- Applied only to one surface of the slab
- Applied only to two opposite surfaces of the slab (facing a potential fire side and a potential fire un-exposed side)



4. In case of screws or other mechanical fixations, the system was composed of:

- Metallic screws with washer
- Plastic screws with washer/large head
- Other types of fixation

5. In case of screws or other mechanical fixations, the number of fixation elements, in the direction parallel to the load-bearing elements, were:

- 1 per meter
- 2 per meter
- 3 per meter
- More than 3 per meter

6. In case of screws or other mechanical fixations, the number of fixation elements, in the direction perpendicular to the load-bearing elements (number of elements per cavity width), were:

- 1 per cavity width
- 2 per cavity width
- 3 or more per cavity width



7. If you are using a different method, please specify here

8. Which is the reason for the use of the fixation systems?

- Design requirements
- Facilitation of the mounting process
- Improvement of acoustics
- Improvement of fire protection



Insulation slabs installed in wall elements

The following questions refer to insulation slabs installed in wall elements

9. Which method do you normally use to fix the insulation slab in the cavities?

- Over dimensioning of the slab width compared to the cavity width
- Adhesive or glue
- Transversal battens or resilient channels
- Screws or other mechanical fixations through the insulation slab
- Steel net or another type of net
- None of them (or other)



10. In case of over dimensioning of the slab width, which is the over dimensioning?

- Less than 5 mm
- Between 5 and 10 mm
- More than 10 mm



11. In case of adhesive or glue:

- Applied only to one surface of the slab
- Applied only to two opposite surfaces of the slab (facing a potential fire side and a potential fire un-exposed side)



12. In case of screws or other mechanical fixations, the system was composed of:

- Metallic screws with washer
- Plastic screws with washer/large head
- Other types of fixation

13. In case of screws or mechanical fixations, the number of fixation elements, in the direction parallel to the load-bearing elements, were:

- 1 per meter
- 2 per meter
- 3 per meter
- more than 3 per meter

14. In case of screws or other mechanical fixations, the number of fixation elements, in the direction perpendicular to the load-bearing elements (number of elements per cavity width), were:

- 1 per cavity width
- 2 per cavity width
- 3 or more per cavity width



15. If you are using a different method, please specify here

16. Which is the reason for the use of the fixation systems?

- design requirements
- facilitation of the mounting process
- improvement of acoustics
- improvement of fire protection



Loose-fill insulation materials installed in floor elements

**The following questions refer to loose-fill insulations installed in floor elements**

17. Do you normally use one of the following system which might hold the insulation in place if the cladding is removed?

- Transversal battens or resilient channels
- Steel net or another type of net
- None of them (or other)



18. If you are using a different method, please specify here

19. Which is the reason for the use of the fixation system?

- design requirements
- facilitation of the mounting process
- improvement of acoustics
- improvement of fire protection



Loose-fill insulation materials installed in wall elements

**The following questions refer to loose-fill insulations installed in wall elements**

20. Do you normally use one of the following systems which might hold the insulation in place if the cladding is removed?

- Transversal battens or resilient channels
- Steel net or another type of net
- None of them (or other)

21. If you are using a different method, please specify here

22. Which is the reason for the use of the fixation system?

- design requirements
- facilitation of the mounting process
- improvement of acoustics
- improvement of fire protection

# Curriculum vitae

## Personal data

Name: Mattia Tiso

Date of birth: May 4<sup>th</sup>, 1988

Place of birth: Camposampiero, Padua, Italy

Citizenship: Italian

## Contact data

E-mail: [tisomatt@gmail.com](mailto:tisomatt@gmail.com)

## Education

2015 – 2018 Tallinn University of Technology – PhD

2011 – 2014 University of Trieste – MSc

2007 – 2011 University of Padova – BSc

2002 – 2007 Giacinto Girardi High School, Cittadella

## Language competence

English – Fluent

Italian – Native

## Research experiences:

01.2015 – to date. Tallinn University of Technology, Structural Engineering Research Group;

10.2014 – 09.2018. RISE Research Institutes of Sweden;

05.2017 – 07.2017. ETH Zürich, Institute of Structural Engineering;

02.2014 – 04.2014. SP Technical Research Institute of Sweden, Wood Technology.

## Co-supervised master thesis:

Morelli Maria Flavia (Academic Year 2015-16). "Influence of the insulation materials to the timber members at elevated temperatures" University of Catania (Italy).

Predonzani Anna (Academic Year 2015-16) "Modelling the thermo-mechanical behaviour of timber members with insulation material exposed to fire" University of Trieste (Italy).

## Elulookirjeldus

### Isikuandmed

Nimi: Mattia Tiso

Sünniaeg: 4. mai 1988

Sünnikoht: Camposampiero, Padua, Itaalia

Kodakondsus: Itaalia

### Kontaktandmed

E-post: tisomatt@gmail.com

### Hariduskäik

2015 – 2018 Tallinna Tehnikaülikool – PhD

2011 – 2014 Trieste Ülikool – MSc

2007 – 2011 Padua Ülikool – BSc

2002 – 2007 Giacinto Girardi Gümnaasium, Cittadella – Keskkharidus

### Keelteoskus

Inglise keel – Kõrgtase

Itaalia keel – emakeel

### Teadustöö kogemus

01.2015 – Tallinna Tehnikaülikool, ehituskonstruksioonide uurimisrühm;

10.2014 – 09.2018. RISE Research Institutes of Sweden;

05.2017 – 07.2017. ETH Zürich, Institute of Structural Engineering;

02.2014 – 04.2014. SP Technical Research Institute of Sweden, Wood Technology.

### Juhendatud magistritööd:

Maria Flavia Morelli (2015-16). "Isolatsioonimaterjalide mõju puitkonstruktsioonide käitumisele kõrgetel temperatuuridel" Catania Ülikool (Itaalia).

Anna Predonzani (2015-16) "Tulele avatud isolatsioonimaterjalidega puitkonstruktsioonide termo-mehaanilise käitumise modelleerimine" Trieste Ülikool (Itaalia).